Estimating Time of Concentration by Reflecting Flood Inundation Effects and Hazard Mapping

CHONG, Khai Lin

2017

Estimating Time of Concentration by Reflecting Flood Inundation Effects and Hazard Mapping

(氾濫の影響を反映した洪水到達時間の推定とハザードマッピング)

by

CHONG, Khai Lin

A dissertation submitted in partial fulfilment of the
requirements for the Degree of Doctor of Engineering

Department of Civil and Earth Resources Engineering
Kyoto University, Japan

2017

TABLE OF CONTENTS

LIST OF FIGURES

LIST OF TABLES

ABSTRACT

Natural disasters occurred in all over the world cause small or substantial losses and damages depending on the magnitudes or probabilities of the catastrophe and the development of the affected areas. Consequently, economy of the countries, shortages in resources, environment deprivation and zoology unbalance are severely affected by the disasters. One of the most common disasters in the world is floods. Floods are a natural phenomenon and some areas in the world are receiving floods regularly.

Malaysia is one of countries that receives floods on regular basis due to the influence of monsoon climate. One of states which are severely affected by regular flood is Kelantan State. Kelantan usually receives around the end of the year end until the earliest months in the year. One of the main cause of the floods is overflow from Kelantan River.

The Kelantan River, located in the north-east of Peninsular Malaysia, is an important and the only main discharge in Kelantan state. There are many residential areas, business centers, and infrastructures built along the river which are vulnerable to floods. Historical records have shown extensive damages on the human environment caused by floods caused by the river. However, a big flood event occurred in 2014 in Kelantan was the worst floods in the history considering its water depth, inundation extent and also damages on properties and infrastructure. Many villages at the central upstream areas were completely inundated while new zones at downstream areas were added to the flood prone areas. In that particular event, people could no longer stay in their homes as practiced during the previous smaller flood events and thus had to be evacuated. Even more, some homes were washed away just like the soils and vegetation in the headwaters.

Although regular floods are a common feature in the lives of a significant number of Malaysians, the magnitude of damage could be minimized if an early warning system is in place. More to this, since water-related problems have increased due to the increase in flood magnitude and frequency; there is a need to develop a tool to understand the influencing factors of these floods and thus efficiently mitigate the disaster.

A lot of flood hazard studies emphasize on the structural measures than non-structural measures. However, due to the anthropological effects to floods, more accurate calculation is required which to enable engineers applying the flood management measures effectively. As

such, interests in the development of the non-structural methods are increasing in the recent years in supporting decisions in the application of flood management measures. The development of the non-structural methods requires an excellent cooperation among government, community, private sector and NGO's. Public in general do not need the details in the methods of flood control measures, however they need to understand the level of protection and risks that are associated with the flood control measures. The sense of panic in the community and the loss of human lives and properties can be reduced during the flood significantly, if they understand to what extent their living and working places are protected against flood. This study attempted to contribute to research on non-structural flood mitigation measures aiming at building tools for the community to better understand the flood in their region.

This study firstly explains the occurrence of floods in a monsoon catchment and the characteristics of the Kelantan River Basin as a study area. In the first chapters, land use, climate conditions and geological setting of the basin was explained together with meteorological data and GIS layers which were used in the study. The main findings of the study utilize a Rainfall-Runoff-Inundation (RRI) model, a 2D grid cell based hydrodynamic model capable of simulating for both rainfall runoff and flood inundation processes which were set up and calibrated based on observed data. Meteorological data which was used are precipitation and streamflow datasets from during 1970 to 2014. The simulation was using DEM 15 arc-second obtained from HydroSHEDS and 2002 landuse data from Department of Town, Country and Regional Planning (TCPD). The main findings of these research comprise of three important components, namely calculation of time concentration with diffusive wave approximation with consideration of effect of inundation, frequency and trend analysis of rainfall, and hazard maps for Kelantan River Basin.

The study attempted to propose method in determining time of concentration by including diffusive wave assumption and inundation extent. Time of concentration T_c is defined as the wave travel time from the most hydraulically remote point to the point of the study. T_c is an essential element in hydrological studies, especially in drainage system designs and the estimations of flood arrival time. As such it is important to the common approach in the estimation of T_c is based on Kinematic Wave (KW) approximation for both overland flow and river routing. This estimation, however, may be improved for application on a flood plain with inundations by using Diffusive Wave (DW) and inundation extent approximation. The proposed method is demonstrated in the Kelantan River Basin, Malaysia, focusing on a severe flood event in December 2014. This study compares the estimated T_c with other estimations based on RRI

simulation with a simple correlation method between rainfall amount in different durations and peak river discharges. As results, the proposed method with DW approximation with flood inundation showed closer estimations of T_c by the other two methods. These findings are important and can be used for the authorized party such as Department of Drainage and Irrigation (DID) or Kelantan State Government for future development.

The second part of the study attempted to estimate the frequency of occurrence and pattern of the extreme rainfall at the Kelantan River Basin. Frequency analysis of the extreme values was conducted to estimate the return period of the rainfall events using the GEV distributions fitted for extreme values data of each station. The results from frequency analysis can show the average recurrence interval (ARI) of a magnitude of rainfall or return period of a particular precipitation. This research compared the December 2014 Kelantan flood to these return periods and assessed the peculiarity of the rainfall event against historical records. The GEV distribution model for the 1-day, 3-day, 5-day, 7-day and 14-day extreme rainfalls were fitted to its parameters and used to estimate the return periods. The assessment shows that the return period or average recurrence interval (ARIs) of rainfall event in 2014 for most of the stations located at the upstream of the Kelantan River Basin experienced high ARIs rainfall events (ARIs near or over 50-year), compared to stations at the downstream of the river basin (ARIs near or less than 20-year), especially for rainfall periods higher than 3-day. Stations experiencing ARIs near 500 year are stations at GOB (3 and 5-day rainfall) and Brook (5-day rainfall). For the frequency analysis at catchment scale, GEV distribution has been selected. The result shows that the return period or average recurrence interval (ARIs) in the past 44 years at catchment scale are not very rare. The most severe case happened in 2014, where the return period is higher than 50-year in maximum daily and exceed 100-year return periods at maximum 3, 5, 7 and 14-day rainfall.

The second part of this study also analyzed the historical data on precipitation in the Kelantan catchment to understand its trend using the Mann-Kendall non-parametric method and Sen's slope for the magnitude of the trend. The study used two Mann-Kendall methods, the Mann-Kendall 1 (MK1) and Mann-Kendall 3 (MK3). In summary, the calculation using MK1 and MK3 methods gave good agreement in increasing and decreasing trends in almost all stations. Disagreements of results were seen in Kota Bharu Station for Max. 3, 5, 7, and 14-day calculations, in Kg. Jeli Station for max. 1-day and 14-days calculations, and in Ulu Sekor Station for max. 7-day calculation. The trend is increasing at the upstream stations and downstream stations. Station located at upstream (Gunung Gagau, Upper Chiku, Brook, and Blau) tends to bring more precipitation from analysis results. The increasing trend will increase

more surface flow if the land use changes are not well preserved. The increasing of surface flow may trigger more debris flow from upstream to downstream. However, the growing trend of GOB station may not bring many impacts to the catchment as the average annual rainfall was the lowest. Station located at downstream (Ulu Sekor, JPS Machang, Bendang Nyior, Rumah Kastam, and Kg. Durian Daun) show increasing trend for annual, maximum and seasonal precipitation. Downstream station with increase trend tends to cause a severe flood and large flood extent. These can be a high-risk area for future development. Therefore, future concerns need to be considered by the policy maker.

The third part of the study attempted to create hazard maps in Kelantan River Basin simulated in RRI model using ARIs at catchment level from results from the second part of the study. In December 2014 due to extreme rainfall rate, flood event hit almost 90 percent of Kelantan state that caused much difficulty to the residents. It is necessaru to do flood forecasting practically to save lives and property. There is a need to access the flood risk outside the experience because of the uncertainty of the climate change. Flood inundation models allow river discharge upstream to be related directly to flood extent downstream. The development of flood inundation maps is one of a primary non-structural method to understand the impact of floods with certain return periods to the inundation areas of one particular catchment. The inundation maps were developed using different methods and hydrological models, as such it is essential to compare results of the various types of hazard maps using different methods to improve the existing flood management practices. This research uses the GEV frequency analyses and RRI model to visualize the inundated areas of floods with different return periods. This research benefits from the momentum of the unprecedented flood in 2014 in a view to proposing an updated inundation maps.

Finally, findings from this research are hoped to contribute to the current efforts in improving flood management in Kelantan River Catchment. Therefore, comprehensive planning can be made to ensure all the residents can be alerting to make preparation and planning with any possible of flood incident in future.

ACKNOWLEDGEMENTS

First of all, I would like to express my sincere gratitude and special appreciation to my supervisor Prof. Kaoru Takara for the continuous support of my PhD study and related research, for his patience, motivation, and immense knowledge. His guidance helped me in all the time of research and writing of this thesis. I could not have imagined having a better advisor and mentor for my PhD study.

I would like to acknowledge that valuable input of Assoc. Prof. Takahiro Sayama, who has been a tremendous mentor to me and contributed many discussions that helped to shape this research and always willing to help to resolve the most difficult modelling issues. I also would like to give my great appreciate for his encouragement, suggestion, and continuous support for my research.

Besides my supervisor, I would like to express thanks to the other co-supervisor of my thesis committee: Prof. Yasuto Tachikawa and Prof.Tomoharu Hori, for their insightful comments and encouragement, but also for the hard question which incents me to widen my research from various perspectives. I also want to thank you for letting my defence be an enjoyable moment, and for your brilliant comments and suggestions, thanks to you.

I am also eternally grateful to my sponsors who have funded this PhD research; The Ministry of Higher Education and Universiti Utara Malaysia, without which this PhD dream would not be a reality.

I wish to express my higher gratitude to Ms. Sono Inoue and Ms. Kaori Saidera for their unrelenting support of administrative tasks and kindness during my time. This work would not materialise without the technical support by the Drainage and Irrigation Department and Universiti Sains Malaysia. I am grateful to Prof. Ismail Abustan for enlightening me the first glance of research and help me collect research data needed. I also would like to thank Mr. Ahmad Halmi and his team for help me process all the data collected from site.

I thank my fellow lab members for the stimulating discussions, for the sleepless nights we were working together before deadlines, and for all the fun we have had in the last three years. They are Dr. Eliza, Dr. Duan, Dr. Vilasane, Dr. Hu, Dr. Josko, Dr. Hendy, Dr. Xue, Ms. Nga, Mr. Adnan, Mr. Tien, Mr. Toma, Mr. Ha, Mr. Goto, Mr. Takahashi, Mr. Ushiro, Mr. Kobayashi, Mr. Yamamoto, Mr. Sugawara and Mr. Miyake. It was a great pleasure working with them, and I appreciate their ideas, help and good humor. Lovely thanks are also for my dear friends for their companion and assistant of my daily lives in Japan, they are Ms. Eva, Ms. Karlina and Ms. Shi. Also, not to forget Dr. Risyawati, Dr. Faizatul and Ms. Syairah Aimi who companying, encouraging and supporting me to strive towards my goal.

My deepest appreciation belongs to my family for their patience and understanding. Words cannot express how grateful I am to my parents, grandmother, sister and aunties for all of the sacrifices that you've made on my behalf. Your prayer for me was what sustained me thus far. Last but not the least, the highest degrees of appreciations are also to my darling husband Choon Seang for his sacrifices, patience and care towards me during the whole period of my PhD life. Thank you for the love, understanding, humor and most of all for always seeing me at my best even when I am not throughout this entire journey.

CHAPTER 1 INTRODUCTION

1.1 INTRODUCTION

Natural disasters are beyond the control of human beings and cannot be predicted accurately when it occurs. Major natural disasters like floods, earthquake, landslides and droughts when they happen, they result in the threat of human life, loss of property, affect structure, agriculture and environment. The impacts of the disaster are different in intensities and coverage areas. Natural disasters happen every year, and their incidence and frequency seem to have significantly increased in recent decades, mostly because of environmental degradation, such as deforestation, intensified land use and the increasing population.

Flooding is an environmental hazard that can occur almost all around the world. Chow (1956) found that most floods are happen linked to river flood. However, Ang (2015) said in the book “Flood, A Geographical Perspective” written by Roy Ward (1978) stated that the frequency of flood increase was mostly due to the decomposition of the riverside. The book also mentioned that flood is a disaster that can occur in various situation either basin zone or coastal area (Ang, 2015). Flood brings many impacts to the environment and people like physical damages, mentality disturbance, infectious diseases and others.

In general, Geis and Steeves (1980) stated that flooding could be categorised into flash floods, monsoon floods, coastal floods and others. They also mentioned that flood could lead to many problems to human. There are several definitions of the flood had defined by the researchers. Flood is defined as the water of river channel is higher and weaken the river channel capacity, caused the overflow to the dry surface and increased the surface water runoff (Chow, 1956; Junk, 1997; Mays, 2004). Nevertheless, Rostvedt (1968) suggested the definition of the flood should be a water level or discharge that is higher than the flood level or flood discharge. The reason why this definition was made because floods occur due to large amounts of water and water flow that cause the water level exceeds the standard level of the river. In Kelantan, floods usually happened at the stage at where the river channel fully filled with rainfall and overflow to its river bank.

Floods bring many effects to most of the engineering structure such as bridges, embankments, tanks and reservoirs, etc. Therefore, with implementing the structural and non-structural measures in flood protection and mitigation will help to reduce the impacts of floods.

Based on a report by the World Meteorological Organization (WMO), floods found to be the third most common natural disaster contributing to a high number of deaths and loss of properties. Floods occur almost every year in tropical countries, whereas for other basins the frequency of occurrences may vary dramatically. Although floods are an integral part of the dynamics of any river channels, floods have created hazards for human communities for many years (Wohl, 2000). Historical records of floods have shown that the impacts of floods on people's livelihoods are unavoidable (Tapsell et al., 2002; Jonkman and Kelman, 2005; Grothmann and Reusswig, 2006).

Water-related disasters arising from floods, droughts, tropical cyclones, landslides and tsunamis are undoubtedly increased over recent decades and appears to continue to rise, and pose major impediments to achieve human security and sustainable socio-economic development (Milly et al., 2002), as recently witnessed with disasters such as Hurricane Katrina in 2005, the 2011 Tohoku earthquake and tsunami and Thai Floods 2011. Figure 1.1 shows the water-related disasters events increased from 1970 to 2013. Floods and storm events increased drastically from 1970 to 2013, but other types of disaster did not increase significantly during this period. The average of floods from 2001 to 2013 doubled over the average from 1986 to 2000 and storms increased more than 1.5 times.

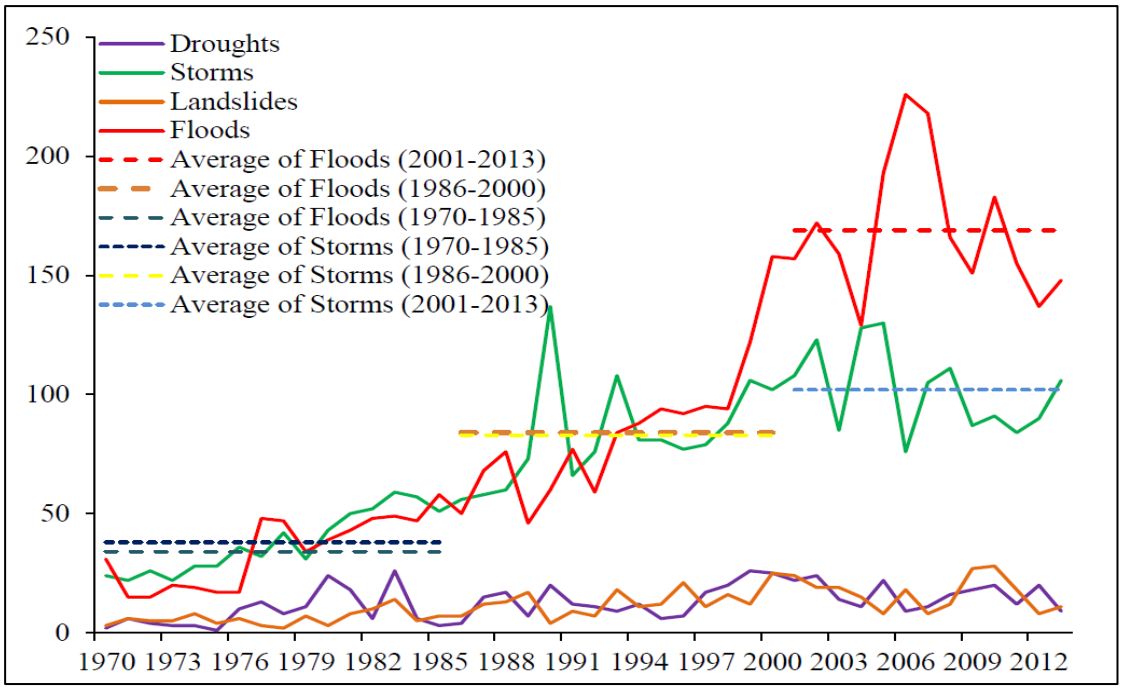

Figure 1.1 Disaster occurrences during 1970-2013.

Floods affect all aspects of life and may have discouraged economic development in highly flood-prone areas (Chan and Parker, 1996). Refer to Table 1.1, flood is a disaster that available and occurred since long time ago. It is not limit to the current conditions but also in the past. Table 1.1 adapted from Wohl (2000) shows historical flood events that occurred in different places of the world from 747 B.C till 1954.

Table 1.1 A partial listing of devastating historical floods.

Location	**Date**	**Cause**	**Damages**
Nile River, Egypt	Ca. 747 B.C	Rainfall	Unspecific
Mississippi River	March 1543	Rainfall	Unspecific
China	1642	Rainfall	300,000 dead
James River, USA	May 1771	Rainfall	City of Richmond, Virginia destroyed, 150 drowned
Connecticut River, USA	May 1874	Reservoir failure	USD 1 million damages, 143 dead
Yangtze River	1911	Rainfall	100,000 dead
Texas, USA	Dec. 1913	Rainfall	USD 9 million damages, 177 dead
Lower Mississippi River basin, USA	March 1927	Rainfall	USD 300 million damages, 313 dead
Yellow River, China	1933	Dike failure	18,000 dead
Kazvin District, Iran	Aug. 1954	Not Stated	2000+ dead

Flood is especially vulnerable to Asia and the Pacific regions. During the year 1998 in China, there is the worst flood affected 223 million people where 3004 people reported dead, and 15 million were homeless. The total economic loss was over USD 23 billion. Cambodia and Vietnam also often faced with the flood. In 2000, Cambodia and Vietnam had reported 428 people dead and estimated economic loss about USD 250 million in a flood event (Ali Khan et al., 2014). Also, flood events that have been recorded in India have killed up to 1,000 people per year and damaged millions of hectares of cropland (De et al., 2005). For the last decade due to the common occurring of floods, thousands of people have been affected due to flood in Asia country, for example, India, Pakistan, Korea, China, and Bangladesh with their agricultural field and resident areas. An effect of floods in less developed countries is more vulnerable compared to developed country. It has many problems with emergency response and early warning preparation. Human involvement in controlling flood disaster by an immense use of different technology can facilitate stakeholder to have an early warning for flood and know what impact are to be caused by a flood (Ali Khan et al., 2014). Furthermore, it can be a major hazard to human health and well-being as well as to the society's infrastructure (Foody et al., 2004).

Another example is the flood in the autumn of 2000, triggered by monsoon rainfall, which caused extensive damage in several South-east Asian (SEA) countries of USD 251 million. Further, four million people were homeless and at risk for diarrhoea, cholera, dengue fever, and malaria. Based on the report from Malaysia's National Register of River Basins Study in the year 2003, about 29,000 km^2 or 9% of the total land area and more than 4.82 million people (22%) in Malaysia are affected by floods annually (Shafiee et al., 2004).

1.2 FLOODS IN A MONSOON CATCHMENT

Floods occur almost every year in tropical countries due to the high magnitude and intensity of rainfall. Based on historical records, virtually all natural rivers are characterised by floods. There are several types of flooding in Asia: extensive basin flooding due to riverbank overflow, inundation basin flooding backwater effects from tidal influence affecting lower reaches, inland flooding. This is caused by poor drainage

from inland flood prone areas and urban flash flooding which is caused by inadequate drainage and storage systems to cater for rapid urbanization (Hamzah, 2005). In Malaysia, there are two major types of flooding seriously impacting human life and the environment, which are flash flooding and monsoon flooding (Chan and Parker, 1996; Shafiee et al., 2004).

Flood events have become more frequent in the 1990s to 2000s due to several factors. Climate change and changes in the land use pattern have been attributed as causes of increases in flood frequency and magnitude as well as changes in hydrological response (Pinter et al., 2006; Guo et al., 2010). Climate change may lead to higher rainfall intensities and prolonged rainfall (Nyarko, 2002), which may cause an increase in flood frequency, magnitude and duration in the affected area (Wilson, 2004) especially for monsoon catchment areas (Zehe et al., 2006). On the other hand, rapid urbanization leads to changes in the land use pattern due to associated activities such as deforestation, agriculture, mining, road construction, reservoir construction (Wohl, 2000; Mustafa et al., 2005) encroachment of settlements into floodplain areas (Kundzewicz and Takeuchi, 1999; Islam and Sado, 2000) and improper management. Such changes have caused disturbance of the natural water flow (Nawaz, 2003) as well as the hydrological response.

In order to deal with the above changes, there is an urgent need for solid modelling of flood events to quantify how these changes affect the hydrologic response as well as the frequency and magnitude of floods (Foody et al., 2004). Much research has been undertaken to mitigate different types of floods, but limited research has been done on monsoon flooding. Hydrological models coupled with a geographical information system (GIS), remote sensing and regional climate models are potentially useful tools for assessing the changes in hydrological response (i.e. peak flow and runoff volume) and flooding.

Malaysia located in a tropical zone and received more than 2500 mm of rainfall in a year. The floods that usually occurs in Malaysia is because of the high amount of rainfall on the upstream of the river basin. The worst flood in Malaysia was recorded in 1926 which have caused the most extensive damage to the environment. Followed major floods were recorded in 1931, 1947, 1954, 1957, 1967 and 1971. Other than major floods, there was some small magnitude flood occurred almost annually in different places.

1.3 RESEARCH PROBLEM AND JUSTIFICATION

Flooding in Malaysia has been reported since the 1800s, with specific attention paid to monsoon flooding and flash floods. The first reported severe flood event took place in 1886 and caused extensive damage in Kelantan, one of the states of Malaysia (Chan & Parker, 1996). In 1926, flooding affected most of Peninsular Malaysia, resulting in extensive damage to property, road systems and agricultural land and crops (Malaysia National Committee, 1976; DID, 2008). In 1967, disastrous floods surged across the Kelantan, Terengganu and Perak river basins, taking 55 lives (Chan, 1995). Again, in 1971, a flood swept across many parts of the country (Chan, 1997; Chan, 2002).

The Kelantan River is important because it is subject to the most severe monsoon flooding in Malaysia (DID, 2004). Further, it is perceived that flooding is increasing along the river, presenting a significant management problem. Flooding appears to be increasing in Kelantan regarding frequency as well as magnitude (Sooryanayana, 1988; DID, 1992; MMD, 2007). For example, intense and prolonged precipitation in 2002 caused flooding of a total area of 1,640 km^2 with an affected population of 714,287. Again, in the year 2004 flooding also occurred, and the frequency increased in 2006 and 2007 when the study area experienced flooding twice per year: in 2006 flooding took place on 12 February and 19 December, and in 2007 flooding took place on 08 January and 13 December. The history of flooding in Kelantan and its impact is shown in Table 1.2. However, little research has been conducted to understand and quantify how these factors contribute to flooding and hydrological response in the Kelantan River catchment.

The Kelantan River is prone to flood disasters, and this is potentially due to meteorological factors (i.e. climate change), rapid changes in land use, and weaknesses in development planning and monitoring. Increases in population, coupled with urbanisation, may contribute to residential and industrial development in the floodplain. Rapid land use changes from the 1970s to 2000s, especially about deforestation (due to logging activities) and conversion to agricultural land (rubber and oil palm) have been reported, especially in the upstream catchment area (Wan Ismail, 1996; Jaafar, 2007). For example, in Kelantan, the rate of urbanisation from the 1970s to 1990s was 7% but slowed in the 2000s to 1.4% (Hassan, 2004) revealing that substantial land use changes have occurred in the area.

Table 1.2 Flood impact in Kelantan from the year 1983 to 2004 with a total number of evacuees, the total amount of damage in Ringgit Malaysia (RM) and in USD.

Year	Total number of evacuees	Total amount of damage (Ringgit Malaysia)	Total amount of damage (in USD)
2004	10,476	14,317,800	3,767,842
2003	2,228	5,554,400	1,461,684
2002	No record	1,420,000	373,684
2001	5,800	8,462,700	2,227,026
2000	506	4,940,620	1,300,163
1999	No record	1,924,440	506,432
1998	136	1,628,455	428,541
1997	No record	922,020	242,637
1996	No evacuation	735,795	193,630
1995	1,172	1,485,095	390,814
1994	441	2,413,922	635,243
1993	13,587	1,512,816	398,110
1992	743	329,256	86,646
1991	No record	1,427,872	375,756
1990	4,581	1,036,100	272,658
1989	No record	-	-
1988	41,059	-	-
1987	402	3,336,589	878,576
1986	7,968	6,092,454	1,603,277
1985	No record	-	-
1984	7,177	1,998,268	525,860
1983	33,816	-	-

Furthermore, human activities such as unplanned rapid settlement development, uncontrolled construction of buildings and problems about drainage management are factors, which may cause increases in runoff (Pradhan, 2009). These changes may lead to higher peak flow and runoff volume when coupled with heavy rainfall in the monsoon season (October to March) as normally experienced in the study area. However, currently no study has been performed to quantify the effects of land use changes (e.g., deforestation, urbanization) and precipitation changes on increased runoff and flooding in the Kelantan River catchment, and this uncertainty currently hampers land use planning and water resource management activities.

Land use change due to human activities may influence hydrological processes such as evapotranspiration and infiltration (Wooldridge et al., 2001). Deforestation may cause

increases in overland and river flow due to lower evapotranspiration capacity (Niehoff et al., 2002). In contrast, urbanization may lead to a greater impervious surface area (e.g., pavements, roads, car parks and buildings) and may cause infiltration excess to occur when poor infiltration conditions are coupled with high rainfall intensities (Chahinian et al., 2005). Several studies have found that changes in land use from forest to other land use (e.g., built-up, agricultural or bare land) may cause increases in runoff volume, frequency of flooding and peak discharge (Zhang et al., 2007; Wang et al., 2008).

In December 2014, two waves of extreme monsoon rainfall hit the catchment. As a result, one of the upstream rain gauges, Gunung Gagau had received 1765 mm of rainfall in a week. The total amount rainfall fall at Gunung Gagau rain gauge is about 50% of the catchment. The water level at Kuala Krai which has a danger level of 5 meters, reached 7.03 meters and Sungai Kelantan which have a danger level of 25 meters, reached 34.17 meters. The overtopped river flow and prolonged rainfall in the catchment have caused almost 90% of the Kelantan state under inundation. The damage was devastating with 25 deaths and RM 2.81 billion loss.

It is important to quantify these supposed changes in precipitation and flooding. Further, it is important to quantify the extent of changes in precipitation (which themselves may be caused by global climate change), to know the future trend and impacts. The answer will determine future flood inundation extent with the correlation of precipitation trend in the area, as well as flood management policy and decisions. Thus, the Kelantan River was chosen as a site of some environmental importance.

1.4 OBJECTIVES OF THE STUDY

This study focuses to increase the efficiency of flood early warning system and reduce the effect of flood to the community and economy. Also understanding the past and future hydrological responses, which have led or may lead to flooding in a monsoon catchment (i.e. the River Kelantan catchment). In 2014, the estimated flood arrival time is shorter than the actual flood time. Therefore, hypothesis for improving method of estimation flood arrival time is made. The specific objectives of the study are as follows:

- To propose an equation for calculating the time of concentration, T_c with a diffusive

wave, *DW* approximation for river channel with considering the effect of inundation extent. The new equation may help to increase the accuracy of estimation of flood arrival time.

- To understand the long-term trend of rainfall and frequency analysis of rainfall to predict future trends.
- To develop the flood hazard map for different return periods and different rainfall intensities for evacuation centre relocation and to identify high risk and low-risk area.

CHAPTER 2 STUDY AREA AND DATA

2.1 INTRODUCTION

This chapter introduces the location and physiography of the study area. Kelantan is a state located on the north-eastern corner of Peninsular Malaysia. Kelantan is annually affected by monsoon flooding, especially in the months of October to March. The description of the dataset used in the research is also presented.

2.2 STUDY AREA

Kelantan is one of the largest states in Peninsular Malaysia occupied 4.4% of the Malaysia with total area 15,105 km^2. It is bordered by one country boundary and three state boundaries where northern part is Narathiwat Province of Thailand; southeast is Terengganu state, west part is Perak state, the southern part is Pahang state and on the east side is the South China Sea (Figure 2.1). It consists of ten districts namely Bachok, Gua Musang, Jeli, Kuala Krai, Machang, Pasir Mas, Pasir Puteh, Tanah Merah, Tumpat and Kota Bharu which has become the state capital.

Based on Department of Statistics in 2015, Kelantan with a total population of 1.76 million. About 68.5% of the population lives in the Kelantan River Catchment. The others are found in the Golok and Kemubu River Basins and the northern coastal plain of the catchment. The major economic activities in Kelantan are agriculture, mainly cultivation of paddy rice, rubber, palm oil and tobacco. Beside plantation, fishing and livestock farming are also main economic activities. Although two-thirds of the Kelantan is covered by rich tropical forest but in recent year palm oil, rubber and tobacco are cultivated extensively in large land development schemes.

In this study, the Kelantan River was chosen to simulate the effect of diffusion wave and inundation map for several return periods. Also, Kelantan River was selected to perform the time series analysis. Kelantan River situated in northeast Peninsular Malaysia and it is also one of the major rivers in Malaysia which frequently affected by monsoon flood events (Awadalla and Noor, 1991; Chan, 1995; Chan, 2002; DID, 2004).

Kelantan River is the main river in Kelantan. The Kelantan River Catchment is located at the north-eastern part of Peninsular Malaysia between the latitudes 4° 40' and 6° 12' North, and longitudes 101° 20' and 102° 20' East. Its catchment area is about 13,100 km^2 occupying almost 85% of the state (Syed Hussain & Ismail, 2013). The origin inlet point of Kelantan River is from Ulu Sepat Mountain, and the discharge point is South China Sea. The length of the river is about 284 km long where the main tributaries are Lebir River (2,500 km^2) and Galas River (8,000 km^2) (Ibbitt et al., 2002).

The Kelantan River system flows northward passing through major towns as Kuala Krai, Tanah Merah, Pasir Mas and Kota Bharu and finally discharging into the South China Sea (Figure 2.2). The average width of the Kelantan River is between 50 to 150 m. Upstream and downstream of Sungai Kelantan show significant changes in slope gradient. Upstream slope gradient from 90/10000 to 70/10000, while the downstream area is a widespread lowland area which the slope gradient is about 1/10000. From the total catchment area, approximately 95% is dominated by steep mountain (mostly covered with virgin jungle) with the height of 2,174 meters while the remainder is urban used land.

Historical records have shown that extensive flood damage on the human environment are unavoidable (Tapsell et al., 2002; Jonkman and Kelman, 2005; Grothmann and Reusswig, 2006). In December 2014, two waves of extreme monsoon rainfall hit the catchment. Thus, one of the upstream rain gauges, Gunung Gagau had received 1765 mm of rainfall in a week. The total amount rainfall fall at Gunung Gagau rain gauge is about 50% of the catchment average. The water level at Kuala Krai which has a danger level of 5 meters, reached 7.03 meters and Kelantan River which has a danger level of 25 meters, reached 34.17 meters. The overtopped river flow and prolonged rainfall in the catchment have caused almost 90% of the Kelantan state under inundation. The damage was devastating with 25 deaths and Ringgit Malaysia (RM) 2.81 billion loss.

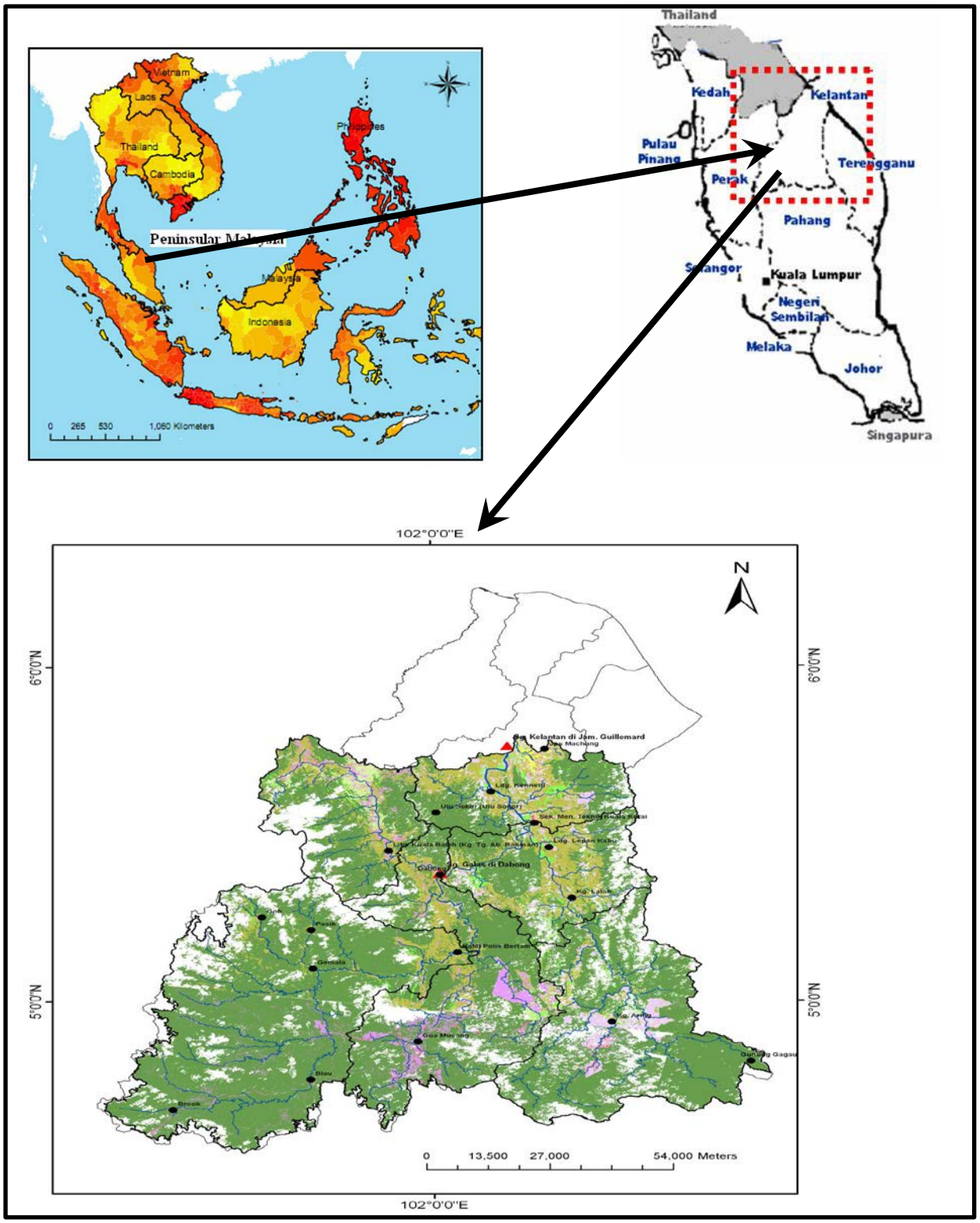

Figure 2.1 (Upper left) Malaysia location, (Upper right) Malaysian states and (Lower left) Kelantan Map.

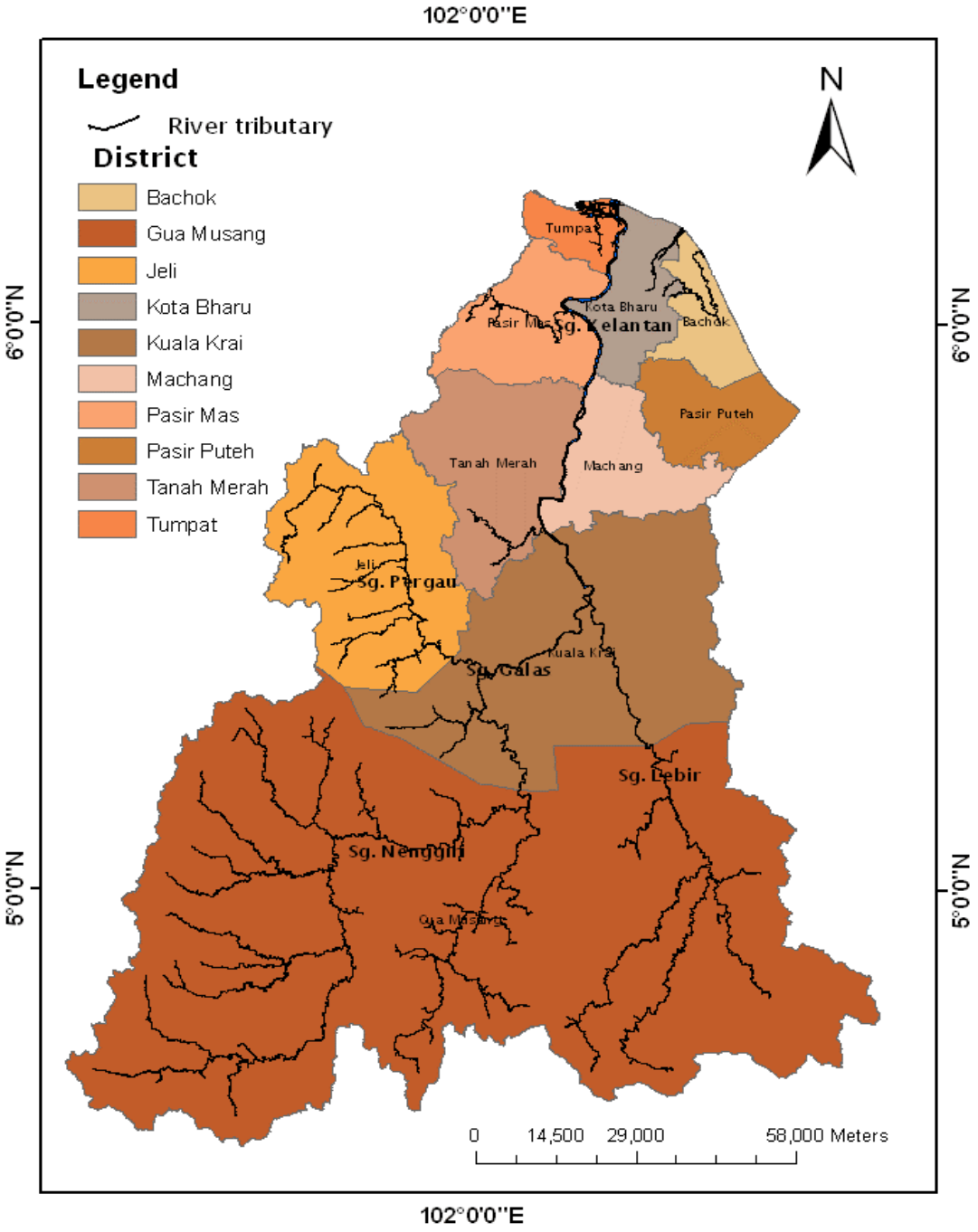

Figure 2.2 Kelantan River tributaries and Kelantan district map.

2.2.1 Land use

Kelantan land use has been dominated by forest reserves which cover an area of 1,078.4 km^2 (71.8% of Kelantan total land area) mainly located in the upstream area or Gua Musang province. It is followed by agriculture which covers an area of 309.28 km^2 (20.6%). Paddy cultivation covers 71.13 km^2 (4.7%), while built-up areas only cover 22.15

km^2 (1.5%) of which 28% is located in the district of Kota Bharu. The distribution of land use by the district in Kelantan for the year 2002 is shown in Table 2.1. Land use change regarding urban growth has been changing progressively from the 1970s to 1990s with 7% growth, and after the 1990s there were very slow developments in the area with only 1.4% growth (Hassan, 2004).

Table 2.1 Present land use by Kelantan district in the year of 2002 (in km^2).

District	Land Use Categories (km^2)				Total Land Area (km^2)
	Built Up	Agriculture	Forest Reserve & Water Body	Others	
Kota Bharu	62.884	327.434	8.54	0.54	399.398
Tumpat	26.303	128.693	20.65	5.58	181.226
Pasir Mas	25.469	446.260	102.063	1.414	575.206
Machang	8.618	254.723	255.253	10.96	529.554
Pasir Puteh	3.081	299.017	115.358	5.338	422.794
Bachok	41.250	196.914	29.606	7.63	275.40
Gua Musang	15.060	829.214	7,306.631	12.61	8,163.52
Jeli	6.615	185.004	1,140.972	0.726	1,333.32
Kuala Krai	9.883	593.506	1,653.931	4.13	2,661.45
Tanah Merah	22.300	542.028	295.932	11.27	871.53
Total	**221.463**	**3,802.793**	**10,928.94**	**60.198**	**15,013.39**

Source: Adapted from Technical Report of RSN Kelantan, 2003-2020

Based on forecasted growth of the population and future needs for other sectors, the projection of land requirements for development in Kelantan for the period 2000-2020 is as shown in Table 2.2.

Table 2.2 Projected development land requirement by category, Kelantan, 2000-2020.

Category		2000 - 2010		2010-2020		Total	
		km^2	%	km^2	%	km^2	%
1.	Residential	127.6	76.9	111.0	82.1	238.6	78.4
2.	Commercial	0.8	0.5	2.1	1.6	2.9	1.0
3.	Industrial	37.6	22.6	22.1	16.3	59.7	19.6
Total		**166.0**	**100.0**	**135.2**	**100.0**	**304.2**	**100.0**

Source: RSN Kelantan, 2003 – 2020

Overall, the projected land requirement for development involves residential, industrial and commercial, with a total required a land area of 304.2 km^2 for the period 2000-2020. The residential development area required is 238.6 km^2.

2.2.2 Climate

Malaysia located entirely in the equatorial zone. The climate is governed by the regime of the northeast (NE) and south-west (SW) monsoons. According to Tangang (2007), October-November-December (OND) represents the early and January-February-March (JFM) represents the late stages of the winter monsoon in Malaysia, also known as the NE monsoon. The April-May-June (AMJ) and July-August-September (JAS) seasons represent the early and late stages of the summer monsoon, respectively, also known as the SW monsoon. The NE monsoon is responsible for the heavy rains which hit the east coast of the peninsula and frequently cause widespread flooding. The SW monsoon is a drier period for the whole country.

The period between these two monsoons is marked by heavy precipitation which are in December to February. Precipitation patterns in the Kelantan River Catchment have been divided into two regions known as the coastal rainfall‖ region and inlands rainfall region. Coastal rainfall region is located in the downstream catchment area and the inlands rainfall‖ region dominates the upstream catchment area. Annual precipitation over the area varies between 0 mm to 200 mm in the dry season to 2000 - 4000 mm in the wet or monsoon season. The estimated runoff for the Kelantan River Catchment is 500 m^3/s during 1950 to 1990. Due to the NE monsoon, which brings along heavy rainfall, the Kelantan River often overflows in the period, causing an almost annual recurrence of flood to the State between the ends of November till early January.

The average temperature throughout the year is very stable (26°C), and the mean annual rainfall varies as described earlier. Regional variations in temperature and rainfall are mainly due to relief. For example, the east part of Peninsular Malaysia has a mean temperature of 18°C and an annual rainfall of over 2500 mm, compared to West part of Peninsular Malaysia of 27°C and 2400 mm. The humidity is high (80%) due to the high evaporation rate in the dry season. The total surface runoff is 566 km^3, and about 64 km^3yr^{-1} (7 % of the total annual rainfall) contribute to groundwater recharge (Zakaria,

1975; Awaldalla and Nor, 1991). However, about 80% of the groundwater flow returns to the rivers and is, therefore, not considered an additional resource. The total internal water resources of Malaysia are estimated at 580 km^3yr^{-1} (Zakaria, 1975; Awaldalla and Nor, 1991).

The Kelantan River Catchment is characterized by relative humidity, mild wind and heavy monsoonal rainfall in the NE monsoon season when the high velocity NE winds bring heavy rain to this area. About 40% of annual rainfall is received in the Kelantan state during the NE monsoon. On a macro scale the Kelantan catchment can be divided into two climate regions according to its land elevation surface and effect of rainfall. The first is North region climate and secondly, Middle Highland region. The North region climate is normally associated with relatively warm weather and stable climate conditions (i.e. dry and wet conditions through the year). Meanwhile, the Middle Highland region is associated with relatively cool climate and less rainfall than experienced in the North region (Figure 2.3).

Precipitation in the Kelantan River Catchment is not uniformly distributed throughout the year. Two weather conditions are experienced in this area which are the wet period and dry period. As described earlier, wet conditions coincide with the NE monsoon. In the extreme NE monsoon season, rainfall has been recorded of about 100 to 300 mm per day (DID, 2004). The dry period normally is characterized by weak winds or usually by calm atmospheric conditions. In 2014, the mean annual rainfall for Kelantan River Catchment was recorded as 3242 mm, with maximum rainfall received of 1267.5 mm in December (during NE monsoon) and minimum rainfall of 5.5 mm and 121.7 mm in February and March. The temperature, precipitation and evaporation for the period of 1952 to 1997 of Kota Bharu observation stations are represented in Table 2.3.

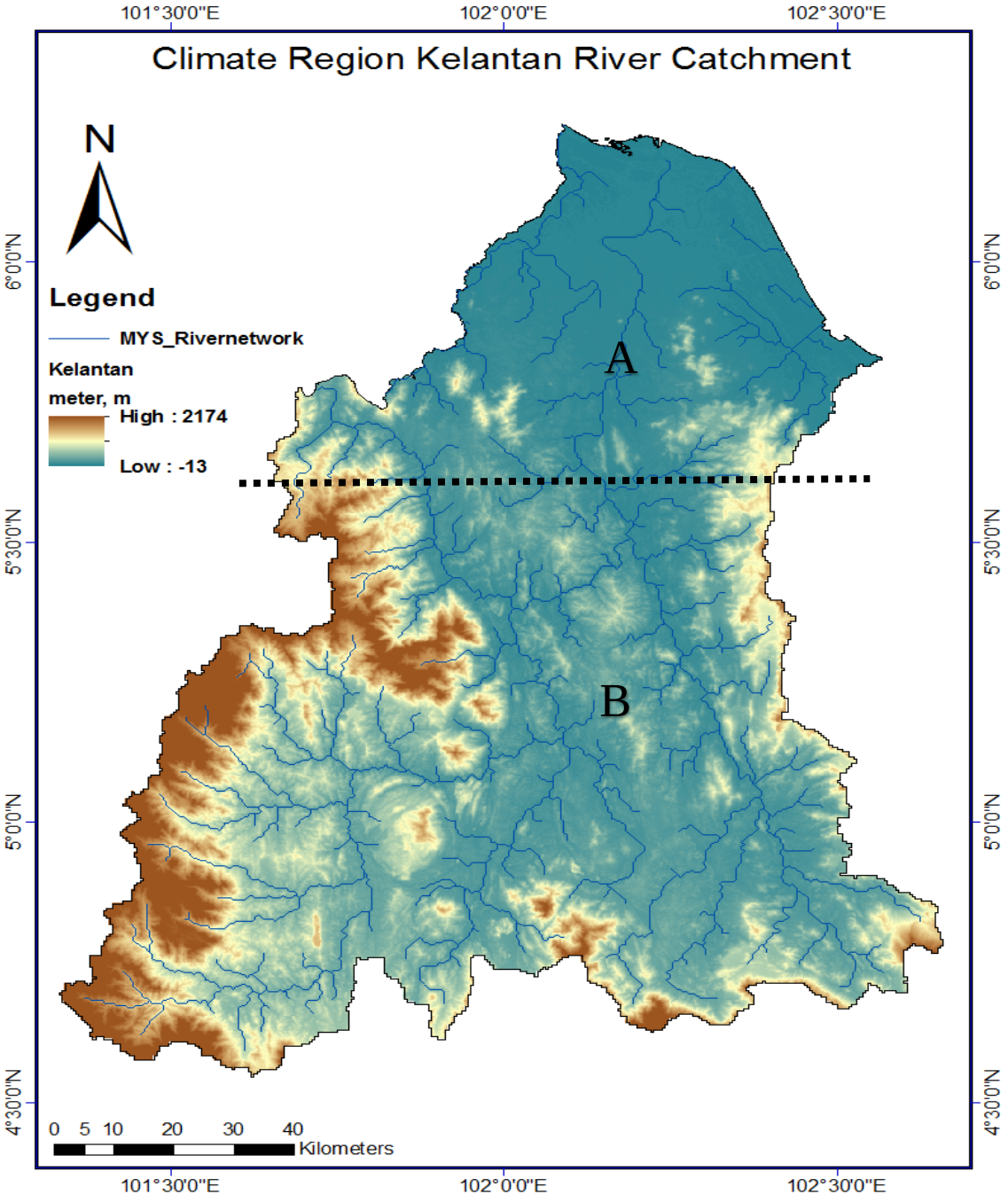

Figure 2.3 Two climate region sub-divisions (approximately) representing by dash line (----) for Kelantan River Catchment of (A) North region climate and (B) Middle highland region climate overlaid with elevation map of Kelantan area.

Table 2.3 The monthly mean temperature and precipitation of Kota Bharu station for the period of 1952-1997.

Month	Temperature (°C)	Precipitation (mm)
Jan	25.7	169
Feb	26.2	74
Mar	27.9	87
Apr	28.1	83
May	27.7	178
June	27.2	187
July	27.0	212
Aug	26.8	257
Sept	26.7	280
Oct	26.0	302
Nov	25.8	640
Dec	26.8	618
Annual	26.8	3087

2.2.3 Geology Formation and Soil Characteristics

Geologic structure in the Kelantan River Catchment is comprised of about 25% granite and intermediate intrusive rocks (Zakaria, 1975). The remaining geology are sedimentary rocks (i.e. argillaceous, arenaceous, rudaceous and calcareous) as shown in Figure 2.4. The granite and intermediate intrusive rocks are located with a steep gradient while the other rocks are situated with a gentle gradient. In the lower gradient of the main river tributaries of Nenggiri, Galas, Lebir and Pergau, extensive floodplains and low river terraces are formed.

Most of the northern area of the Kelantan River Catchment is covered by Quarternary alluvium (i.e. gravel, sand, silt and clay) and topographically is dominated by the coastal plain with elevation less than 75 m above mean sea level. While the eastern and western granitic masses consist of various types of rock (i.e. shales, sandstones, conglomerate, quartzite, limestone, siltstone and mudstone) and metamorphic rocks of the Palaeozoic

age (Awaldalla and Nor, 1991), its depth seldom exceeds a few metres. In the steep land area, particularly in the mountainous area, acid igneous rock formations exist and soils such as alluvium, clay-loam-sand soil which support the growth of thick tropical forest in this area. The soil cover is a metre or so deep but depths of more than 18 m may be encountered in localized areas. The southern parts of the Kelantan state consist of Silurian-Ordovician formations (i.e. schists, phyllite, slate and calcium carbonate, sand and volcanic rocks). The remaining portion, comprising almost one-third of the catchment, is cloaked by a variable soil cover that varies in depth from a few metres to more than 9 m (Zakaria, 1975; Awaldalla and Nor, 1991).

According to DID (2004), the upstream area until the Kota Bharu streamflow gauge station consists of soil from lithosil types on high slopes area. Meanwhile, the low slope areas are dominated by podzol red-yellow mixed with podzol yellow-grey soil (i.e. from granite rock formation) and sediment rocks and laterite soil. These rocks have low baseflow level. However, during heavy rainfall baseflow increases and causes river velocities to change rapidly. Subsequently, flooding can happen due to changing water level conditions (KFD, 2006).

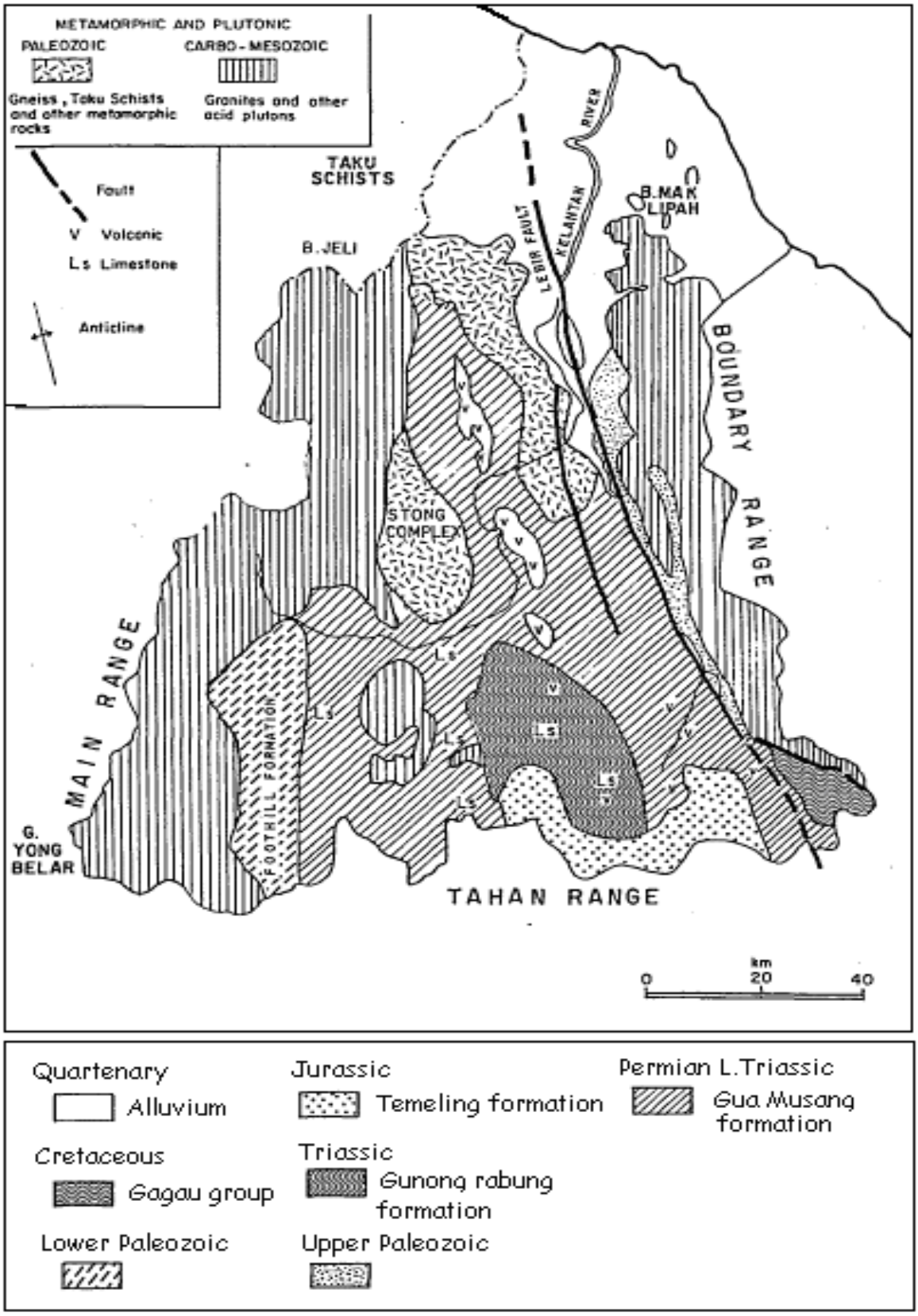

Figure 2.4 Geological map of Kelantan (adapted from Awaldalla and Nor, 1991).

2.3 DATA

2.3.1 Meteorological Data

The hydrological data used in the study comprises precipitation and stream flow records for a period of 1970 to 2014 years. The historical data were extracted from the hydrological data network of the Malaysian Department of Irrigation and Drainage (DID). The data were divided into annual, seasonal and monthly time-series for precipitation for the whole Kelantan River Catchment. For seasonal trend analysis, the year was divided into two main seasons: wet season (October to March) and dry season (April to September). Total precipitation was calculated for every six-month period and trends fitted to these data for each rain gauge station. The data provided good continuity and were chosen based on having few missing data records. A brief description of each gauge is presented in Table 2.4. Overall, approximately 19% of the data were missing from the time-series.

Unavoidably, data of some stations have abnormal values due to some reasons. For abnormal data processing, we used two principles in this study. If the abnormal data have more than15 continuous days or totally 20 days in one year, we consider the error rate is too large for one year (> 4% continuously or > 5% totally) and cancel the analysis of this year.

Table 2.4 Locations and periods of 17 River Kelantan rain gauge stations

Station ID	Station Name	Latitude	Longitude	Period of Records
4614001	Brook	4.6764	101.4847	1982 – 2014
4717001	Blau	4.7667	101.7569	1982 – 2014
4721001	Upper Chiku	4.7653	102.1736	1983 – 2014
4726001	Gunung Gagau	4.7569	102.6556	1981 – 2014
4819027	Gua Musang	4.8792	101.9694	1971 – 2014
4923001	Kg. Aring	4.9375	102.3528	1974 – 2014
5120025	Balai Polis Bertam	5.1458	102.0486	1970 – 2014
5216001	Gob	5.2514	101.6625	1980 – 2014
5320038	Dabong	5.3778	102.0153	1971 – 2014
5322044	Kg. Laloh	5.3083	102.2750	1971 – 2014
5520001	Ulu Sekor	5.5639	102.0083	1978 – 2014
5718033	Kg. Jeli	5.7014	101.8389	1971 – 2014
5719001	Kg. Durian Daun	5.7806	101.9681	1979 – 2014
5722057	JPS Machang	5.7875	102.2194	1970 – 2014
5820006	Bendang Nyior	5.8444	102.4153	1980 – 2014
6019004	Rumah Kastam	6.0236	101.9792	1970 – 2014
6122064	Kota Bharu	6.1083	102.2569	1970 – 2014

Table 2.5 Spatial and temporal information of two streamflow stations comprised of latitude, longitude, and period of records.

Station ID	Station Name	Latitude	Longitude	Period of Records
5222452	Lebir River	5.2750	102. 2667	1986 – 2014
5721442	Kelantan River	5.7625	102.1500	1986 – 2014

Only two streamflow gauges were used, one for upstream (Lebir River) and another one located downstream (Kelantan River) (Figure 2.5). Brief information on the two streamflow gauges is given in Table 2.5. There are only 17 stations were used due to data completeness, with the record length ranging from 1970 to 2014 (Table 2.4).

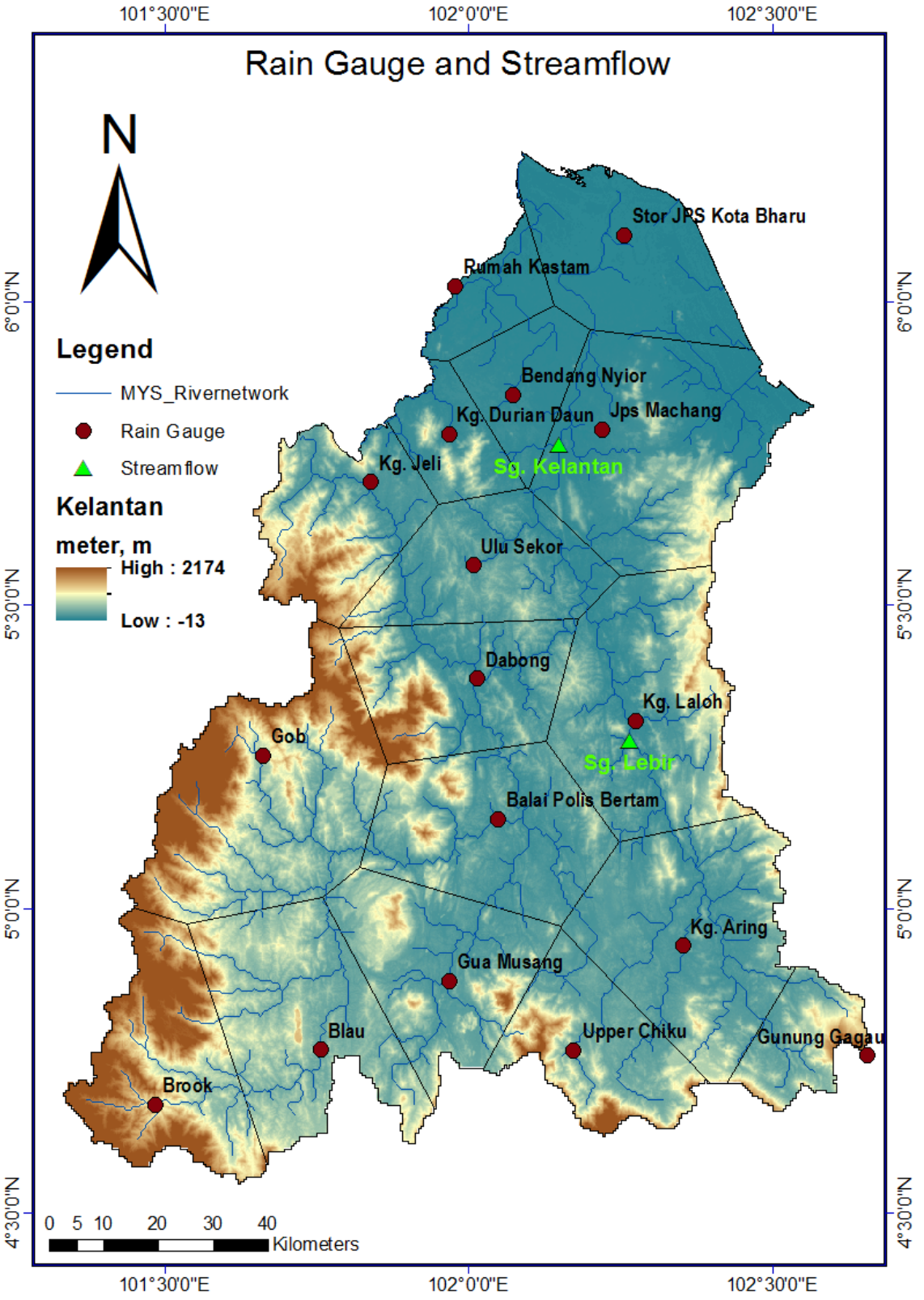

Figure 2.5 GIS layers consisting of 500 m DEM, streamflow gauge stations, rain gauge stations and Kelantan River network.

2.3.2 GIS Layers

A Digital Elevation Map (DEM) that representing the Kelantan catchment were obtained from HydroSHEDS 15 arc-second. The layers comprise of a grid data structure of digital elevation model (DEM) with 500 m spatial resolution, flow direction and flow accumulation. A digital land use map of 2002 provided by the Department of Town, Country and Regional Planning (TCPD) was used to aid the land use classification. Additionally, GIS layer of river network was obtained from DID, Malaysia (Figure 2.5).

The most crucial data for catchment delineation is a DEM. A DEM consists of a matrix of square grid cells with the mean cell elevation stored in a 2-D array of numbers representing the spatial distribution or topography of elevations above some arbitrary datum in a landscape (Garbrecht and Martz, 2000). DEMs have become important data to derive drainage network structures based on automatic procedures such as provided by the RRI tool (Sayama, 2012) as is used in this research.

CHAPTER 3 HYDROLOGICAL MODELLING WITH RAINFALL-RUNOFF-INUNDATION MODEL

3.1 INTRODUCTION

This chapter introduces the method and flow of the study. Hydrological basic knowledge and the theoretical assumptions on modelling will be introduce in this chapter.

3.2 RAINFALL-RUNOFF-INUNDATION SIMULATION

3.2.1 Model Structure Overview

The RRI model is a 2D grid cell based hydrodynamic model capable of simulating for both rainfall runoff and flood inundation processes (Figure 3.1). All model grid cells receive rainfall, and the model tracks the flow based on 2D diffusive wave equations regardless of topography (i.e. including hill slopes and floodplains). This 2D model also simulates vertical infiltration based on the Green-Ampt model and saturated sub-surface flow in mountainous areas for better representations of rainfall runoff processes. The flow inside a river channel is computed with the built-in 1D diffusive wave model, where the lateral inflow and outflow or overbank flow are estimated by coupling with the 2D land model. The flow interaction between the river channel and slope is estimated at each time step based on different overflowing formula, depending on water level and levee height conditions. To solve the diffusive equations, the RRI model employs the fifth-order Runge-Kutta method with adaptive time-step control.

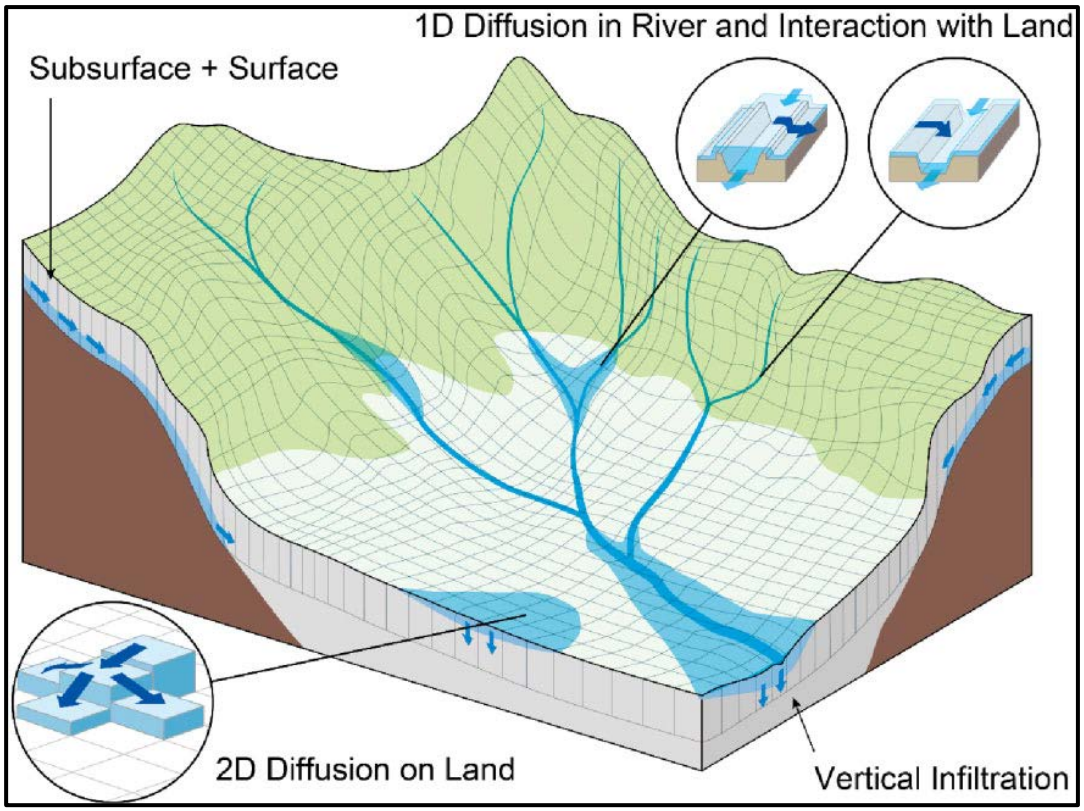

Figure 3.1 Schematic diagram of the RRI model.

3.2.2 Two-dimensional Surface and Sub-Surface Flow Model

The model equations are derived based on the following mass balance equation (3.1) and momentum equation (3.2) for gradually varied unsteady flow:

$$\frac{\partial h}{\partial t}+\frac{\partial q_x}{\partial x}+\frac{\partial q_y}{\partial y}=r-f \tag{3.1}$$

$$\frac{\partial q_x}{\partial t}+\frac{\partial u q_x}{\partial x}+\frac{\partial v q_x}{\partial y}=-gh\frac{\partial H}{\partial x}-\frac{\tau_x}{\rho_w} \tag{3.2}$$

$$\frac{\partial q_y}{\partial t}+\frac{\partial u q_y}{\partial x}+\frac{\partial v q_y}{\partial y}=-gh\frac{\partial H}{\partial y}-\frac{\tau_y}{\rho_w} \tag{3.3}$$

where h is the height of water from the local surface, q_x and q_y are the unit width discharges in x and y directions, u and v are the flow velocities in x and y directions, r is the rainfall

intensity, H is the height of water from the datum, ρ_w is the density of water, g is the gravitational acceleration, and τ_x and τ_y are the shear stresses in x and y directions. The second terms of the right-hand side of equations (3.2) and (3.3) are calculated with Manning's equation:

$$\frac{\tau_x}{\rho_w} = \frac{gn^2 u\sqrt{u^2+v^2}}{h^{1/3}} \tag{3.4}$$

$$\frac{\tau_y}{\rho_w} = \frac{gn^2 v\sqrt{u^2+v^2}}{h^{1/3}} \tag{3.5}$$

where n is Manning's roughness parameter.

Under the diffusion wave approximation, inertia terms (the left side terms of equations (3.2) and (3.3)) are neglected. Moreover, by separating x and y directions (i.e. ignoring v and u terms in equations (3.2) and (3.3), respectively), the following equations are derived:

$$qx = -\frac{1}{n}h^{5/3}\sqrt{\left|\frac{\partial H}{\partial x}\right|}\,\mathrm{sgn}\left(\frac{\partial H}{\partial x}\right) \tag{3.6}$$

$$qy = -\frac{1}{n}h^{5/3}\sqrt{\left|\frac{\partial H}{\partial y}\right|}\,\mathrm{sgn}\left(\frac{\partial H}{\partial y}\right) \tag{3.7}$$

where sgn is the signum function.

The RRI model spatially discretizes mass balance equation (3.1) as follows:

$$\frac{dh^{i,j}}{dt} + \frac{q_x^{i,j-1} - q_x^{i,j}}{\Delta x} + \frac{q_y^{i-1,j} - q_y^{i,j}}{\Delta y} = r^{i,j} - f^{i,j} \tag{3.8}$$

where $q_x^{i,j}$, $q_y^{i,j}$ are x and y direction discharges from a grid cell at (i, j).

By combining equations (3.6), (3.7) and (3.8), water depths and discharges are calculated at each grid cell for each time step. One important difference between the RRI model and other inundation models is that the former uses different forms of the discharge and hydraulic gradient relationship, so that it can simulate both surface and sub-surface flows

with the same algorithm. The RRI model replaces equations (3.6) and (3.7) with the following equations (3.9) and (3.10). These equations were originally developed for a kinematic wave rainfall–runoff model considering both surface and sub-surface flows. For the kinematic wave model, the hydraulic gradient was assumed to be equal to the topographic slope, whereas the RRI model assumes the water surface slope as the hydraulic gradient. The first parts of equations (3.9) and (3.10) describe the saturated sub-surface flow based on Darcy's law, while the second parts describe the combination of the saturated sub-surface flow and the surface flow:

$$q_x = \begin{cases} -k_a h \dfrac{\partial H}{\partial x}, (h \le d_a) \\ -\dfrac{1}{n}(h - d_a)^{5/3} \sqrt{\left|\dfrac{\partial H}{\partial x}\right|} \operatorname{sgn}\left(\dfrac{\partial H}{\partial x}\right) - k_a h \dfrac{\partial H}{\partial x}, (d_a < h) \end{cases} \tag{3.9}$$

$$q_y = \begin{cases} -k_a h \dfrac{\partial H}{\partial y}, (h \le d_a) \\ -\dfrac{1}{n}(h - d_a)^{5/3} \sqrt{\left|\dfrac{\partial H}{\partial y}\right|} \operatorname{sgn}\left(\dfrac{\partial H}{\partial y}\right) - k_a h \dfrac{\partial H}{\partial y}, (d_a < h) \end{cases} \tag{3.10}$$

where k_a is the lateral saturated hydraulic conductivity and d_a is the soil depth times the effective porosity.

Equations (3.11) and (3.12) can be also used to simulate the effect of unsaturated, saturated sub-surface flow and surface flow with the single variable of h.

$$q_x = \begin{cases} -k_m d_m \left(\dfrac{h}{d_m}\right)^{\beta} \dfrac{\partial H}{\partial x}, (h \le d_m) \\ -k_a (h - d_m) \dfrac{\partial H}{\partial x} - k_m d_m \dfrac{\partial H}{\partial x}, (d_m < h \le d_a) \\ -\dfrac{1}{n}(h - d_a)^{5/3} \sqrt{\left|\dfrac{\partial H}{\partial x}\right|} \operatorname{sgn}\left(\dfrac{\partial H}{\partial x}\right) - k_a (h - d_m) \dfrac{\partial H}{\partial x} - k_m d_m \dfrac{\partial H}{\partial x}, (d_a < h) \end{cases} \tag{3.11}$$

$$q_y = \begin{cases} -k_m d_m \left(\dfrac{h}{d_m}\right)^{\beta} \dfrac{\partial H}{\partial y}, \left(h \le d_m\right) \\ -k_a \left(h - d_m\right) \dfrac{\partial H}{\partial y} - k_m d_m \dfrac{\partial H}{\partial y}, \left(d_m < h \le d_a\right) \\ -\dfrac{1}{n}\left(h - d_a\right)^{5/3} \sqrt{\left|\dfrac{\partial H}{\partial y}\right|} \operatorname{sgn}\left(\dfrac{\partial H}{\partial y}\right) - k_a \left(h - d_m\right) \dfrac{\partial H}{\partial y} - k_m d_m \dfrac{\partial H}{\partial y}, \left(d_a < h\right) \end{cases} \tag{3.12}$$

Note that to assure the continuity of the discharge change when $h = d_m$, the lateral hydraulic conductivity in unsaturated zone (k_m) can be computed by $k_m = k_a / \beta$, so that k_m is no longer the model parameter.

The stage discharge relationship equations were originally developed to be applied to humid forest areas with a high permeable soil layer, where a lateral sub-surface flow is the dominant runoff generation mechanism. On the other hand, for relatively flat areas, the vertical infiltration process during the first period of rainfall has more impact on large-scale flooding; therefore, the vertical infiltration can be treated as loss for event-based simulation. The infiltration loss f is calculated with the Green-Ampt model.

$$f = k_v \left[1 + \frac{\left(\phi - \theta_i\right) s_f}{F}\right] \tag{3.13}$$

where k_v is the vertical saturated hydraulic conductivity, ϕ is the soil porosity, θ_i is the initial water volume content, S_f is the suction at the vertical wetting front and F is the cumulative infiltration depth.

Typically for mountainous areas where lateral subsurface flow and saturated excess overland flow dominate, the equations (3.9) and (3.10) (or (3.11) and (3.12) can be used with setting f equals to be zero. Note that the equations (3.9) and (3.10) or (3.11) and (3.12) implicitly assume that the vertical infiltration rate within the soil is infinity. On the other hand, for plain areas where infiltration excess overland flow dominates, the surface flow equations (3.6) and (3.7) can be used with the consideration of vertical infiltration by equation (3.13). If the vertical infiltration f is set to be non-zero and the lateral subsurface equations are used instead of the surface flow equation, the lateral subsurface water is infiltrated to bedrock by the rate of f.

In the study area, there are three types of land-use in common which are urban, agricultural and forest. In the RRI model application, the consideration made as the urban area has only overland flow (no infiltration loss and sub-surface flow) thus the both k_v and k_a set to zero. For the agricultural land, it has vertical infiltration and infiltration excess overland flow then k_a is set to zero. For the forest, it has saturated sub-surface flow and saturation excess overland flow but without unsaturated sub-surface flow considered. The schematic diagram of surface/subsurface flow conditions are illustrated in Figure 3.2.

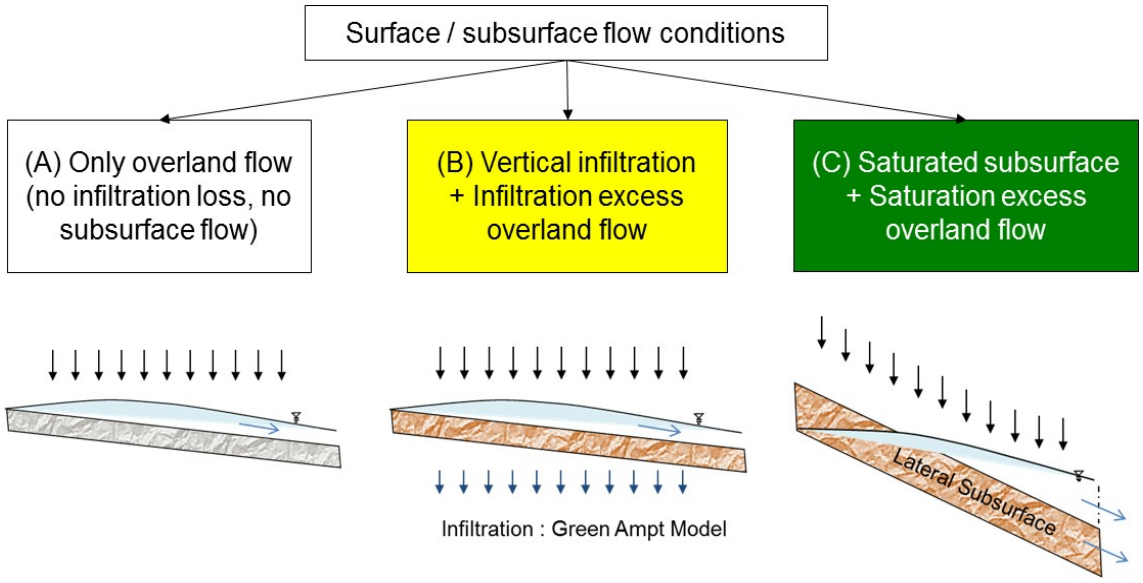

Figure 3.2 Schematic diagram of surface/sub-surface flow conditions.

3.2.3 One-dimensional River Routing Model

Streamflow was also calculated with the diffusion wave approximation. The form of streamflow equations was essentially the same as equations (3.6) and (3.8), but one-dimensional (i.e. $q_y = 0$). The shape of the channel was assumed to be rectangle, where the geometries were defined with three parameters, width, depth and levee height.

3.2.4 Interactions of Water between Slope and River

Water exchange between a slope grid cell and an overlying river grid cell was estimated depending on the relationships between the slope water level, river water level and levee height. The following four different conditions were considered and, for each condition, different overtopping formula were applied to calculate the unit length discharge from slope to river, q_{sr}, or from river to slope, q_{rs}, which were then multiplied by the length of the river vector at each grid cell to calculate the total exchange flow rate:

1) Flow from slope to river under the normal condition: when the water levels on the slope and the river are lower than the levee height, the discharge from the slope into the river is calculated by a step fall formula:

$$q_{sr} = \mu_1 h_s \sqrt{g h_s} \tag{3.14}$$

where μ_1 is the constant coefficient (= 0.544) and h_s is the water depth on a slope cell.

2) No flow exchange between slope and river: when the river water level is higher than the slope water level but still lower than the levee height, no water exchange was considered.

3) Overtopping flow from river to slope: when the river water level is higher than the levee height and the slope water level, the overtopping flow is calculated by an over-bank flow formula:

$$q_{sr} = \mu_2 h_1 \sqrt{2 g h_1} \tag{3.15}$$

where μ_2 is the constant coefficient (= 0.35) and h_1 is the difference between the river water level and the levee crown.

4) Overtopping flow from slope to river: When the river water level is higher than the levee height and the slope water level is even higher than the river water level, the flow exchange is calculated by over-bank flow formula (3.15). In this case, h_1 represents the difference between the two water levels and q_{rs} is replaced with q_{sr} (i.e. slope to river).

3.2.5 Numerical Scheme

To solve equations (3.8), (3.9) and (3.10), the fifth-order Runge-Kutta method with adaptive time-step control is applied. This method solves an ordinary differential equation by the general fifth-order Runge-Kutta formula and estimates its error by an embedded forth-order formula to control the time-step. The general form of the fifth-order Runge-Kutta formula is:

$$\begin{aligned} k_1 &= \Delta t f\left(t, h_t\right) \\ k_2 &= \Delta t f\left(t + a_2 \Delta t, h_t + b_{21} k_1\right) \\ &\cdots\cdots \\ k_6 &= \Delta t f\left(t + a_6 \Delta t, h_t + b_{65} k_5\right) \\ h_{t+1} &= h_t + c_1 k_1 + c_2 k_2 + c_3 k_3 + c_4 k_4 + c_5 k_5 + c_6 k_6 + O\Delta t^6 \end{aligned} \tag{3.16}$$

while the embedded forth-order formula is:

$$h^*_{t+1} = h_t + c^*_1 k_1 + c^*_2 k_2 + c^*_3 k_3 + c^*_4 k_4 + c^*_5 k_5 + c^*_6 k_6 + O\Delta t^5 \tag{3.17}$$

By subtracting h^*_{t+1} from h_{t+1}, the error can be estimated by using k_1 to k_6, as follows:

$$\delta \equiv h_{t+1} - h^*_t = \sum_{i=1}^{6} \left(c_i - c^*_i\right) k_i \tag{3.18}$$

3.2.6 Setting of Model RRI

The RRI model is applied to the Kelantan River Catchment. The model was being set up, the DEM (digital elevation model), flow direction and flow accumulation were delineated from HydroSHEDS 15 arc-seconds resolution (Lehner et al., 2008). The RRI model uses flow direction and accumulation only to determine flood channel locations. Flood direction cannot be determined because they vary depend on the local hydraulic gradients dynamically. The river cross sections used the following simple regression equations:

$$W = C_w A^{S_w} \tag{3.19}$$

$$D = C_w A^{S_D} \tag{3.20}$$

Where A is the upstream contributing area (km^2) in each grid cell (accumulation area) and C_W, S_W, C_D and S_D are regression parameters, where the values were estimated from river cross section data. The parameters obtained were C_W = 5, S_W = 0.186, C_D = 0.95 and S_D = 0.2.

a) Rainfall Set Up

The rainfall data from 17 rainfall stations were converted into Microsoft Excel Comma Separate Value File (.csv). The Figure 3.3 shows the rainfall data in Microsoft Excel Comma Separate Value File (.csv). The rainfall data will abstract into RRI Builder. Figures 3.4 and 3.5 shows the steps how to import the rainfall data into RRI Builder.

17	Brook	Blau	Upper Chil	Gunung Ga	Gua Musa	Kg. Aring	Balai Polis	Gob	Dabong	Kg. Laloh	Ulu Sekor	Kg. Jeli	Kg. Durian	Jps Macha	Bendang N	Rumah Kar	Stor JPS Kot
lat	4.6764	4.7667	4.7653	4.7569	4.8792	4.9375	5.1458	5.2514	5.3778	5.3083	5.5639	5.7014	5.7806	5.7875	5.8444	6.0236	6.1083
lon	101.4847	101.7569	102.1736	102.6556	101.9694	102.3528	102.0486	101.6625	102.0153	102.275	102.0083	101.8389	101.9681	102.2194	102.0736	101.9792	102.2569
2014/12/01 0:00	0	0	0	0	0	0	0	0	0	0	0	0	0	0	0	0	0
2014/12/01 1:00	0	0	0	0	0	0	0	0	0	0	0	0	0	0	0	0	0
2014/12/01 2:00	0	0	0	0	0	0	0	0	0	0	0	0	0	0	0	0	0
2014/12/01 3:00	0	0	0	0	0	0	0	0	0	0	0	0	0	0	0	0	0
2014/12/01 4:00	0	0	0	0	0	0	0	0	0	0	0	0	0	0	0	0	0
2014/12/01 5:00	0	0	0	0	0	0	0	0	0	0	0	0	0	0	0	0	0
2014/12/01 6:00	0	0	0	0	0	0	0	0	0	0	0	0	0	0	0	0	0
2014/12/01 7:00	0	0	0	0	0	0	0	0	0	0	0	0	0	0	0	0	0
2014/12/01 8:00	0	0	0	0	0	0	0	0	0	0	0	0	0	0	0	0	0
2014/12/01 9:00	0	0	0.1	0.1	0	0	0	0	0.1	0.1	0	0	0	0	0	0	0.1
2014/12/01 10:00	0	0	0.1	0.1	0	0	0	0	0.1	0.1	0	0	0	0	0	0	0.1
2014/12/01 11:00	0	0	0.1	0.1	0	0	0	0	0.1	0.1	0	0	0	0	0	0	0.1
2014/12/01 12:00	0	0	0.1	0.1	0	0	0.2	0	0.1	0.1	0	0	0	0	0	0	0.1
2014/12/01 13:00	0	0	11	1.1	0	0	0.3	0	0.1	0.1	0	0	0	0	0	0	0.1
2014/12/01 14:00	0	0	1.1	0	0	0	8	0	0.1	0.1	0	0	0	0	0	0	0.1
2014/12/01 15:00	0	0	0	0	0	0	0	0	0.1	0.1	0	0	0	0	0	0	0.1
2014/12/01 16:00	0	0	0	0	0	0	0	0	2	0	0	0	0	0	0	0	0
2014/12/01 17:00	0	0	0	0	0	0	0	0	0	0	0	0	0	0	0	0	0
2014/12/01 18:00	0	0	0	0	0	0	0	0	0	0	0	0	0	0	0	0	0
2014/12/01 19:00	2.5	0	0	0	0	0	0	0	0	0	0	0	0	0	0	0	0
2014/12/01 20:00	0.1	0	0	0	0	0	0	0	0	0	0	0	0	0	0	0	0
2014/12/01 21:00	0.1	0	0	0	0	0	0	0	0	0	0	0	0	0	0	0	0
2014/12/01 22:00	0.1	0	0	0	0	0	0	0	0	0	0	0	0	0	0	0	0
2014/12/01 23:00	2.7	0	0	0	0	0	0	0	0	0	0	0	0	0	0	0	0
2014/12/02 0:00	7.1	0.3	0	0	0.5	0	0	0	0	0	0	0	0	0	0	0	0
2014/12/02 1:00	2.8	2.2	0	0	0	0	0	0	0	0	0	0	0	0	0	0	0

Figure 3.3 Rainfall Data in Microsoft Excel Comma Separate Value File (.csv).

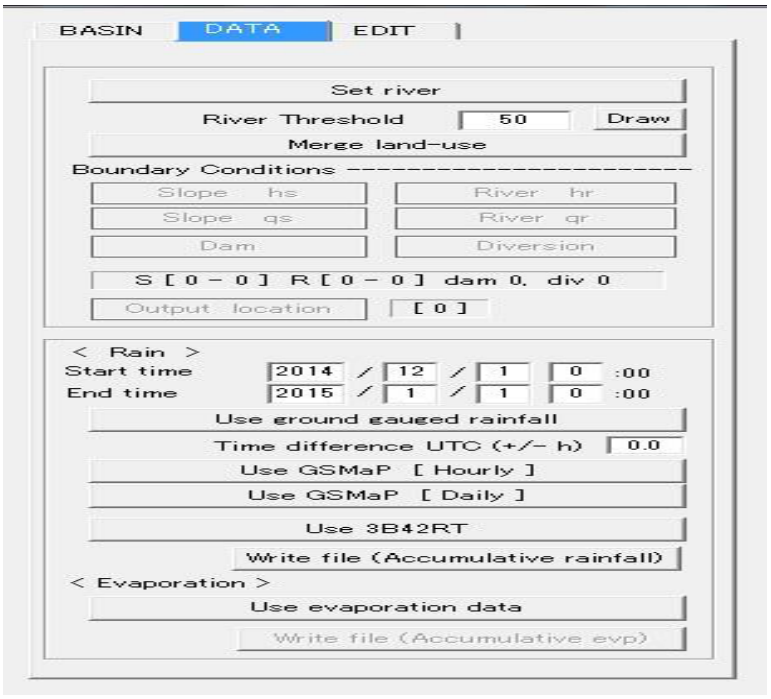

Figure 3.4 Main Window of The RRI Builder (State the duration of the study in the RRI software, and click on use ground gauged rainfall).

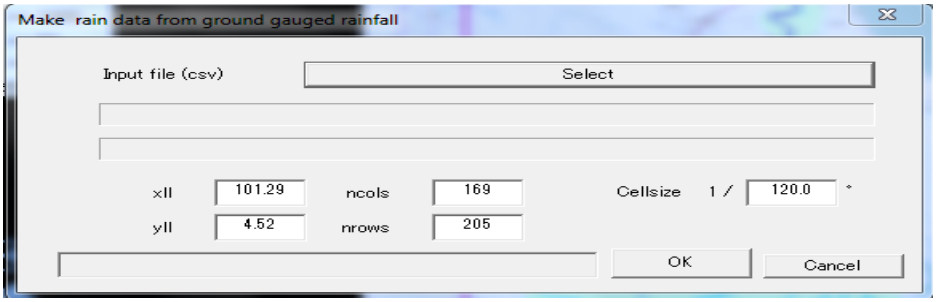

Figure 3.5 Window of Ground Gauged Rainfall from RRI Builder (The 'pop up' window of Ground Gauged Rainfall from RRI Builder was generated after clicking on use ground gauged rainfall. So, select the rainfall data as an input data to RRI).

b) Topography Data

In this study, the topography data at Kelantan catchment were produced by RRI Builder based on HydroSHEDS data. Data that used as input is 15 arc-second HydroSHEDS Digital Elevation Model (DEM). The RRI Builder analysed the topography data to get the hydrological data such as Digital Elevation Model (DEM), Flow Accumulation (ACC) and Flow Direction (DIR). Based on World Wide Fund for Nature (WWF), HydroSHEDS is a mapping product that provides hydrographic information for regional and global-scale applications in a consistent format. It offers a suite of geo-referenced data sets (vector and raster) at various scales, including river networks, watershed boundaries, drainage

directions, and flow accumulations. Furthermore, HydroSHEDS is based on high-resolution elevation data obtained during a Space Shuttle flight for NASA's Shuttle Radar Topography Mission (SRTM).

The initial results are presented from RRI are shown in Figures 3.6, 3.7, and 3.8.
Digital Elevation Model (DEM), flow accumulation (ACC), and flow direction (DIR) were the topography input for RRI Builder. DEM, ACC, and DIR were obtained from HydroSHEDS data. From Figure 3.7, it shows that the topography of the catchment where the upstream areas consist of high elevation.

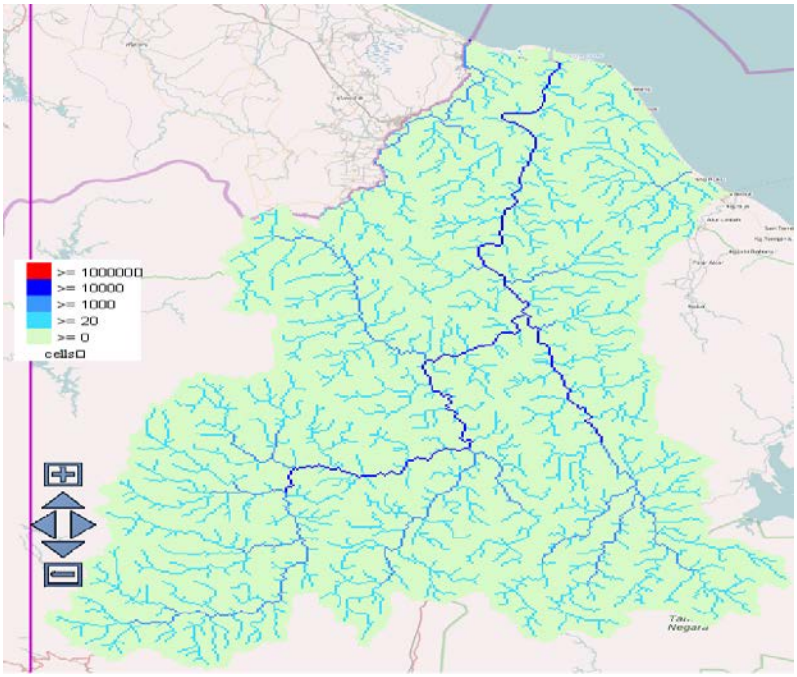

Figure 3.6 Flow accumulation (ACC) with 20 thresholds.

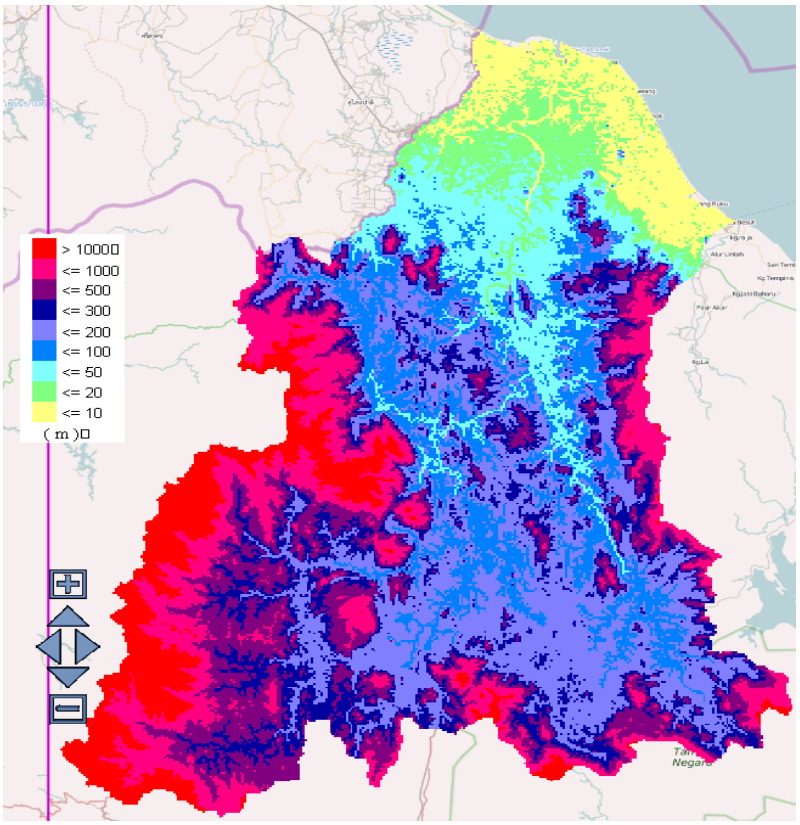

Figure 3.7 Digital Elevation Map (DEM) for Sungai Kelantan.

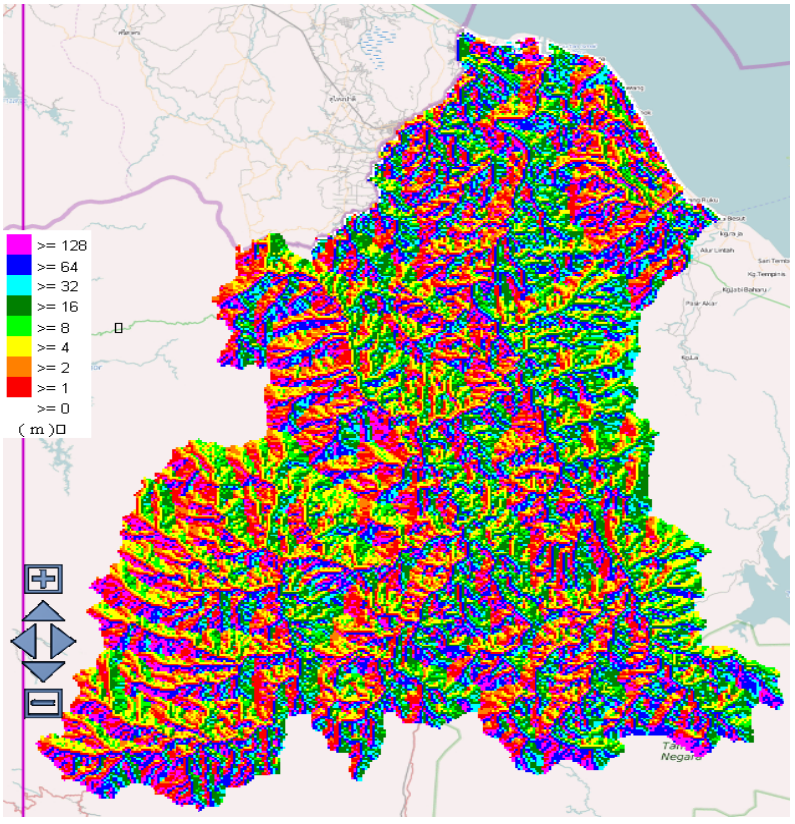

Figure 3.8 Calculated Flow Direction (Dir) for Sungai Kelantan Catchment.

After all the preparation of input data, the RRI model can be run to analyse the flood event at Kelantan from 1st December 2014 to 7th January 2015. The result such as inundation level, water depth and discharge of the river will be generated after running the programme by using RRI model.

c) Parameter Settings

The parameters used in this study for simulation are manning roughness coefficient for river, river section parameters, land use parameters and evaporation rate. Figure 3.9 shows the parameters input data in RRI Builder.

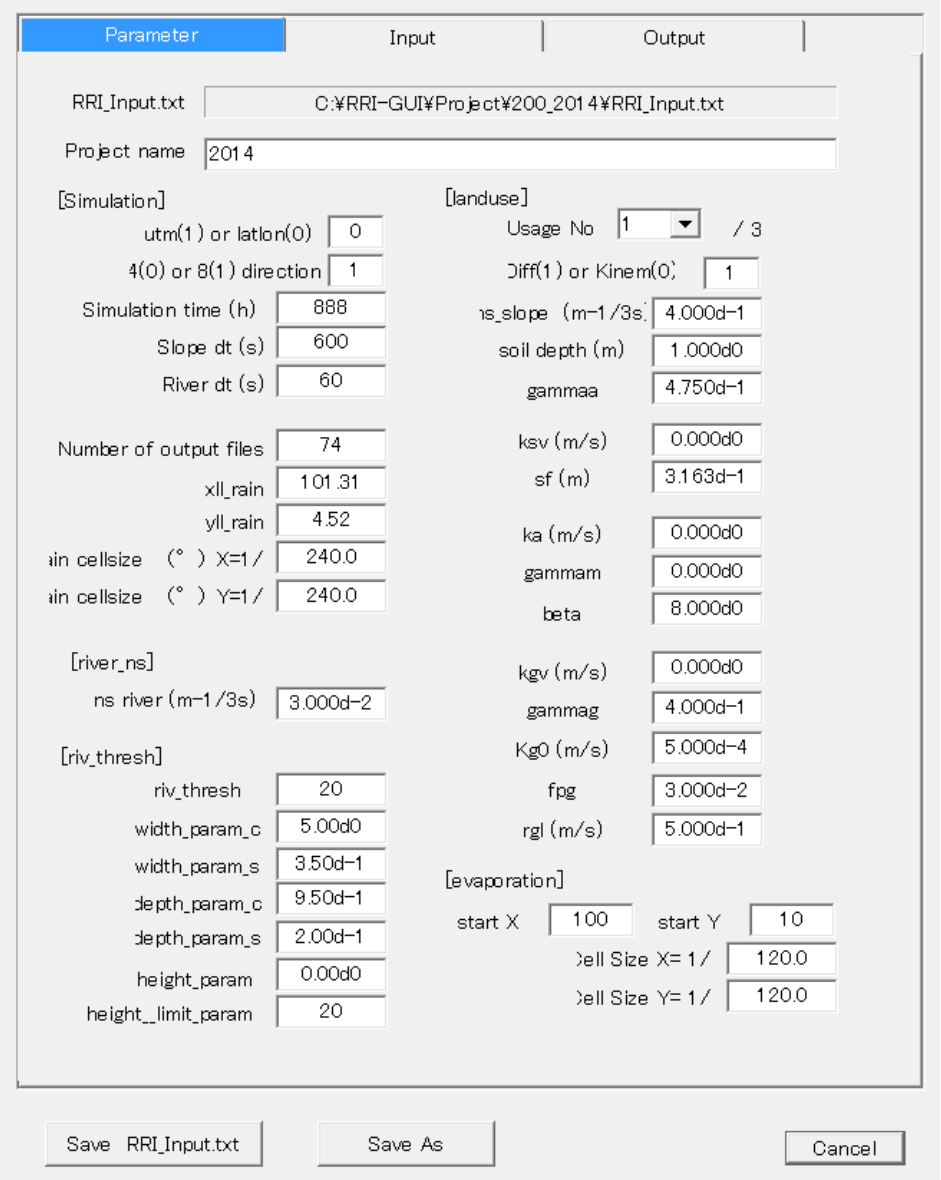

Figure 3.9 The Parameters Input Data in RRI Builder.

3.2.7 Model Calibration

The model is calibrated from the initial ranges of parameters values. The ranges are set manually based on hydrological knowledge and literature values. Based on a 2014 event, the calibration was done with different parameters. There are three land use used in RRI Builder, such as urban, agriculture and forest. For agriculture land, soil type that stated by Department of Geology and Mineral Resources is clay type. Therefore, to obtain the most match parameter value of agricultural land, different types of soil texture were simulated. The sample with the best performance is selected as a calibrated parameter set. The best performance was showed as clay. The model parameters used in simulation are show in Table 3.1.

Table 3.1 RRI Builder Parameters

Parameters	Forest	Urban	Agriculture
Manning's roughness on slope cells, n_s (in $m^{-1/3}$)	0.400	0.400	0.400
Soil depths, d (in m)	1.000	1.000	1.000
Effective porosity, ϕ (-)	0.475	0.475	0.475
Green Ampt Infiltration Model Parameters			
Vertical saturated hydraulic conductivity, k_v (in m/s)	0.000	0.000	1.67×10^{-7}
Suction at the wetting front, S_f (m/s)	3.163	3.163	3.163
Lateral sub-surface and surface model parameters			
Lateral saturated hydraulic conductivity, k_a (m/s)	0.100	0.000	0.000

Nash-Sutcliffe efficiency (NSE) measures the efficiency of a model by relating the errors to the variance in the observations (Strömqvist et al., 2012). Larger NSE values indicate better model performance and a perfect fit corresponds to NSE =1. The performance is evaluated by Nash-Sutcliffe efficiency (NSE) and Correlation Coefficient (R^2) between observations and simulations. The equations for NSE and R^2 are expressed as follows:

$$NSE = 1 - \frac{\sum_{i=1}^{n}\left(Q_{i\_obs} - Q_{i\_sim}\right)^2}{\sum_{i=1}^{n}\left(Q_{i\_obs} - \overline{Q_{obs}}\right)^2} \tag{3.19}$$

$$R^2 = \frac{\sum_{i=1}^{n}\left(Q_{i\_obs} - \overline{Q_{obs}}\right)\left(Q_{i\_sim} - \overline{Q_{sim}}\right)}{\sqrt{\sum_{i=1}^{n}\left(Q_{i\_obs} - \overline{Q_{obs}}\right)^2}\sqrt{\sum_{i=1}^{n}\left(Q_{i\_sim} - \overline{Q_{sim}}\right)^2}} \tag{3.20}$$

in which Q_{i_obs} and Q_{i_sim} are the observed and simulated data, respectively; n is the total number of data records; Q_{obs} and Q_{sim} are the mean observed and simulated data for the evaluation period.

3.2.7.1 Calibration results

Figure 3.10 shows observed and simulated discharge during 2014 Event Flood. The model parameters been calibrated for obtained the most suitable parameter of agricultural land type. The hydrograph in Figure 3.10 shows that the model suitable to be apply in Kelantan Catchment. The evaluation statistics at upstream point (Lebir River) were NSE = 0.810, R^2 = 0.952. For downstream point (Kelantan River), the evaluation statistics were NSE = 0.812, R^2 = 0.823.

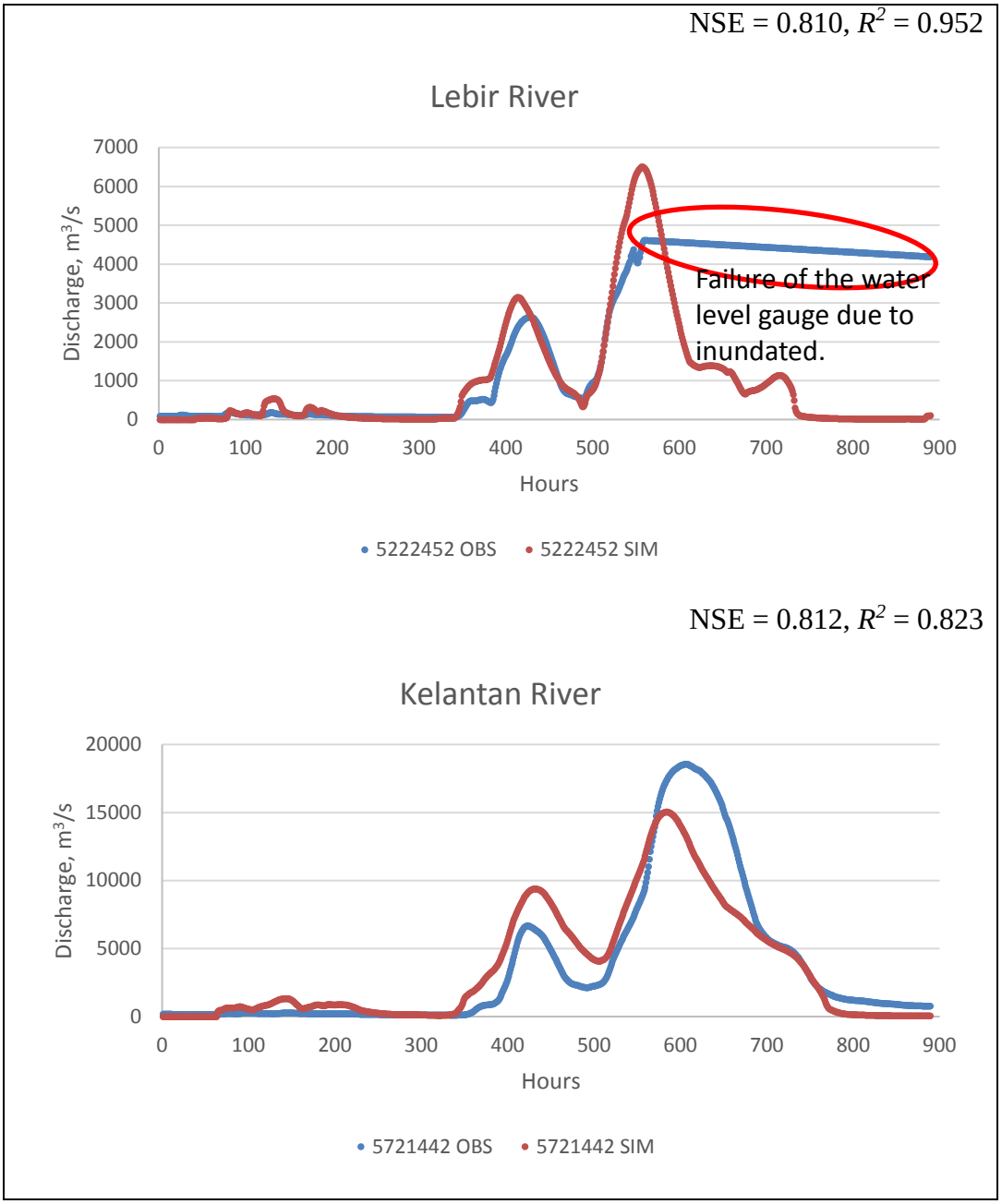

Figure 3.10 2014 event calibrated simulated discharge

3.2.7.2 Validation results

The selected validation events were 2001, 2008 and 2013. The simulated periods are showed in Table 3.2.

Table 3.2 Simulated periods for validation events

Validation events	Simulated periods	Simulated durations (hours)
2001	December 1, 2001 – January 7, 2002	889
2008	November 16, 2008 – December 23, 2008	889
2013	November 16, 2013 – December 23, 2013	889

The calibrated parameters were used in these three events as validation events. Figure 3.11 shows the observed and simulated discharges at the selected discharge points for 2001 event. The evaluation statistics at upstream point (Lebir River) were NSE = 0.786, R^2 = 0.814. For downstream point (Kelantan River), the evaluation statistics were NSE = 0.860, R^2 = 0.881.

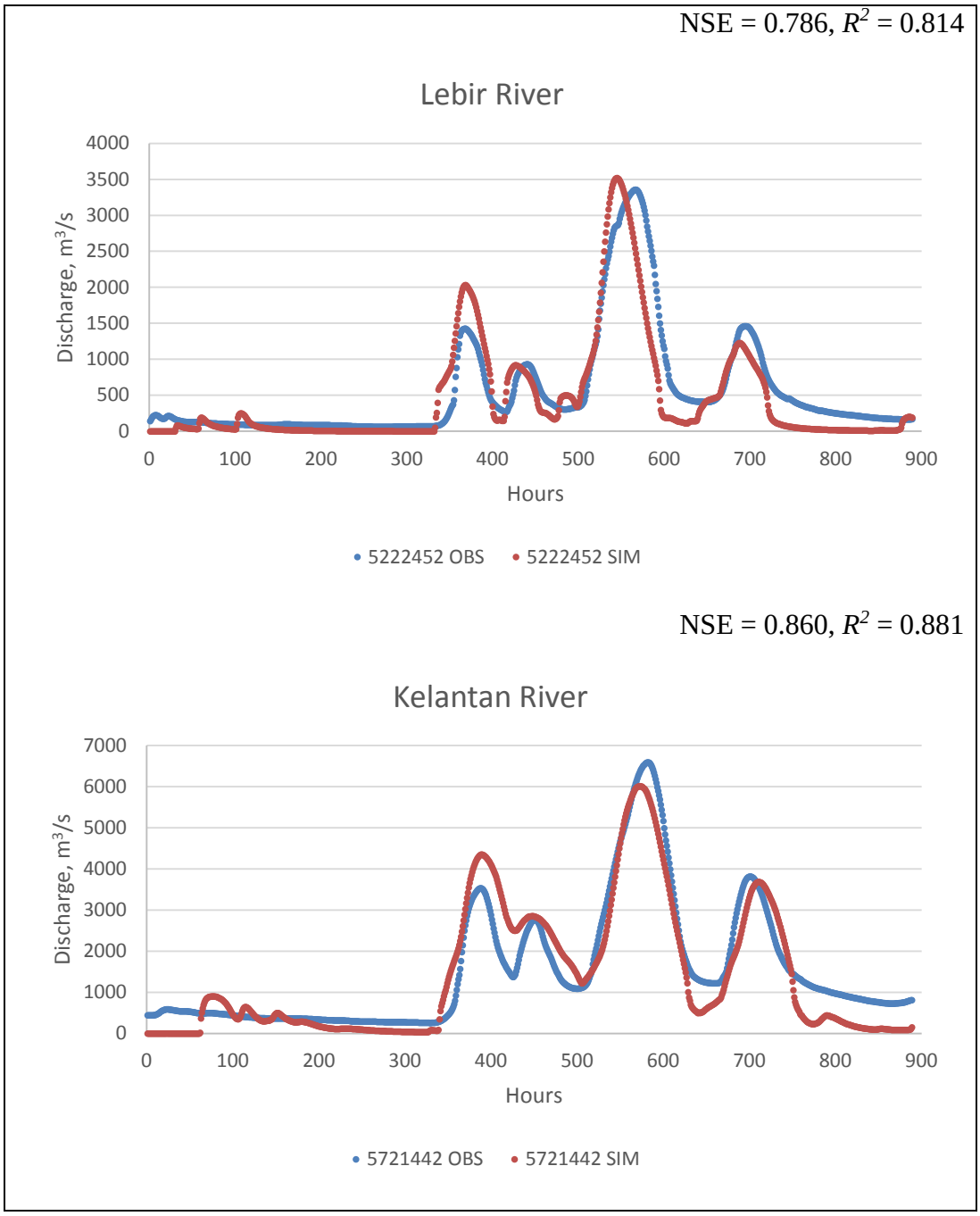

Figure 3.11 2001 event validation simulated discharge

Figure 3.12 shows the observed and simulated discharges at the selected discharge points for 2008 event. The evaluation statistics at upstream point (Lebir River) were NSE = -2.413, R^2 = 0.713. For downstream point (Kelantan River), the evaluation statistics were NSE = 0.282, R^2 = 0.644. The performance of both stations were low in NSE, with the possibly due to the evapotranspiration or the diversion channel from the upstream to downstream. Although the NSE was low, but the R^2 shows better value where it can be explained that both simulated and observed discharge correlated to each other.

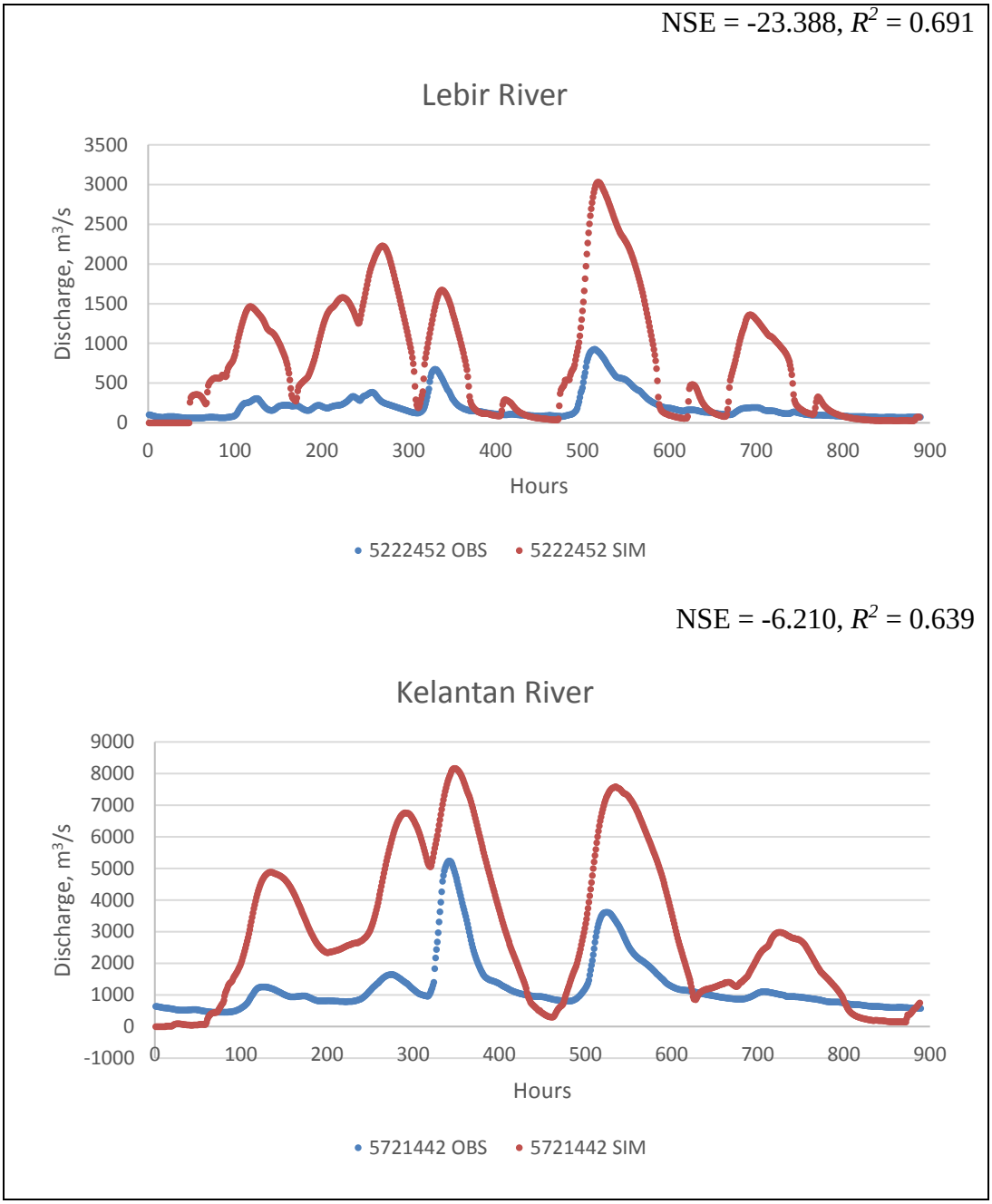

Figure 3.12 2008 event validation simulated discharge.

Figure 3.13 shows the observed and simulated discharges at the selected discharge points for 2013 event. The evaluation statistics at upstream point (Lebir River) were NSE = 0.731, R^2 = 0.814. For downstream point (Kelantan River), the evaluation statistics were NSE = 0.454, R^2 = 0.863. The performance of both stations were low in NSE of Kelantan River and good fit to Lebir River. However, the R^2 shows good value in both discharge point where it can be explained that both simulated and observed discharge correlated to each other.

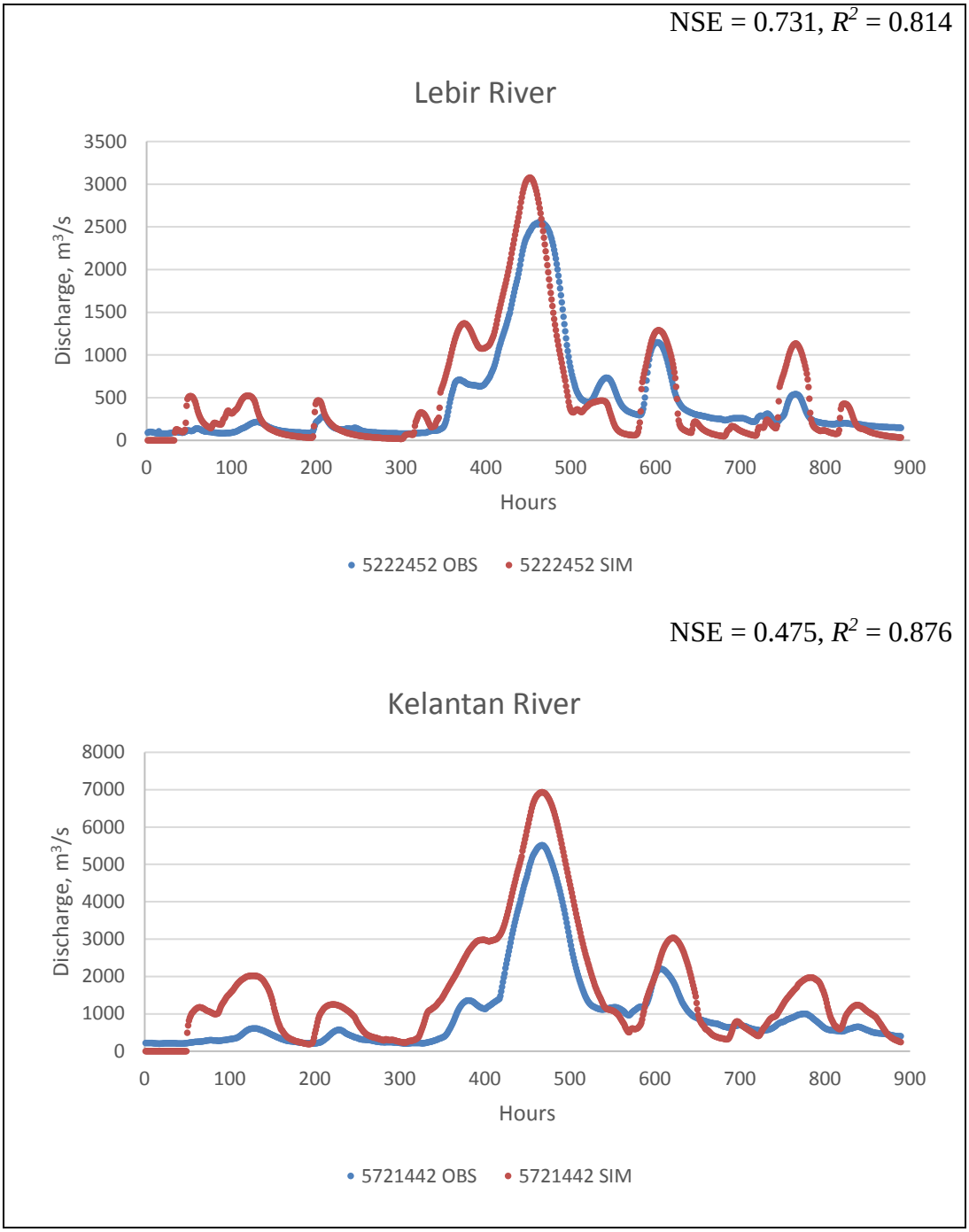

Figure 3.13 2013 event validation simulated discharge.

CHAPTER 4 EFFECTS OF HYDROLOGICAL PROCESSES IN TIME OF CONCENTRATION

4.1 INTRODUCTION

In Malaysia, common practice to design a peak discharge for urban drainage system uses a rational method. Based on Urban Stormwater Management Manual (DID, 2000), the design rainfall intensity used in the rational method is a function of time of concentration T_c. In addition, T_c is used to estimate the timing of flood arrival at different river sections. Hence T_c is an important parameter in drainage system designs and provide early warnings during flooding.

T_c is defined as the wave travel time needed for the most remote point of the catchment to contribute to the surface runoff at the catchment outlet (Su & Fang, 2004). An alternative operating definition is the amount of time required for all portions of a catchment that bring all surface runoff to contribute runoff at the outlet (Su & Fang, 2004). The concept of the time of concentration and its relation to the maximum runoff during the continuance of a uniform rate of rainfall was explained in previous studies (Singh, 1976; Ishihara & Takasao, 1959). The affecting factors of T_c include the size, shape and inclination of catchments. There are experimental studies conducted by the Corps of Engineers (1954) and Izzard (1943), which showed rainfall intensity and rainfall duration also have significant impacts on T_c.

The overland flow is the initial phase of surface runoff. It is sometimes referred to as sheet flow because the water is projected as moving in a sheet down slope over a plane surface to the nearest concentration point or channel. Nearly all surface runoffs start as overland flow in the upper portions of a catchment and travels at least a short

distance in this manner before it reaches a defined channel in which its flow property may usually be characterized by standard hydraulic procedures.

In the estimations of T_c, there are essentially two theoretical approaches, (i) lumped approach which treats T_c of overland flow and channel flow as a single process and (ii) separated approach in which two of the processes are treated separately. Yen (1982) and Kibler and Aron (1983) suggested that the separated approach should be adopted as the two flow components are the distinct systems, and therefore the separated approach provide better estimations of T_c.

In Malaysia, Urban Stormwater Management Manual (DID, 2000) suggests the use of separated approach based on Kinematic Wave (KW) approximations. However, during a severe flood event in the Kelantan River basin, such as the one in December 2014, the estimated flood arrival time based on the KW approach was much shorter than the actual flood arrival time. Therefore, there is a need to estimate more practically reasonable T_c. The working hypothesis of this study is that the short T_c is due to the KW assumption, which may be invalid in fairly flat areas and also no inundation consideration. Both of their effects may reduce the estimations of T_c.

Zakeri et al. (2012) introduced the general form in the derivation of T_c based on Saint-Venant equations and DW approximation. They found DW approximation improved the results of T_c compared to KW approximation especially for flat topography. Regarding the flow depth profile, DW estimation shows the effect of pressure gradient allowing more water to retain in the channel. Wong (2008) studied the effect of river channel shape on wave travel time and detention storage in seven types of river channel. The findings show river channel with high detention storage capacity provide longer T_c.

The main objective of this chapter is to propose an equation for calculating T_c with DW approximation for river channel followed by Zakeri et al. (2012) with considering the effect of inundation extent. Furthermore, the relationship between the proposed methods and other simulation and data based approaches are compared with the estimation of T_c.

4.2 METHODOLOGY

This section explains the methodology that apply for this study. This methodology includes three parts which are simulation, theoretical and empirical. All the topography data, rainfall data and simulation setting will be explained in the next section.

4.2.1 Topographic Parameters

In terms of the topographic parameters assumed in the theoretical T_c estimations, we used the HydroSHEDS DEM with 15-arc second which was also used for the RRI simulation. As shown in Figure 4.1, we defined river grid cells with flow accumulation greater than or equal to 5. We divided the main rivers into seven segments at the gauging stations. Then the average gradients of each river segment were calculated as the average of gradients of all river grid cells in the sub-catchment. The river widths were estimated by the measurement data with Acoustic Doppler Current Profiler (ADCP) at total 31 cross sections and calculated the average widths for each segment by refer to equation (3.19) and (3.20). As for the sub-catchment topographic parameters, the slope is calculated from the average slopes of all grid cells within the sub-catchment. Finally, the representative slope length S_L of each sub-catchment is estimated by equation (4.1) (Takasao & Shiba, 1978).

$$S_L = \frac{A}{2 \times T_L} \tag{4.1}$$

where A is the area of sub-catchment, T_L is total length of the river channel.

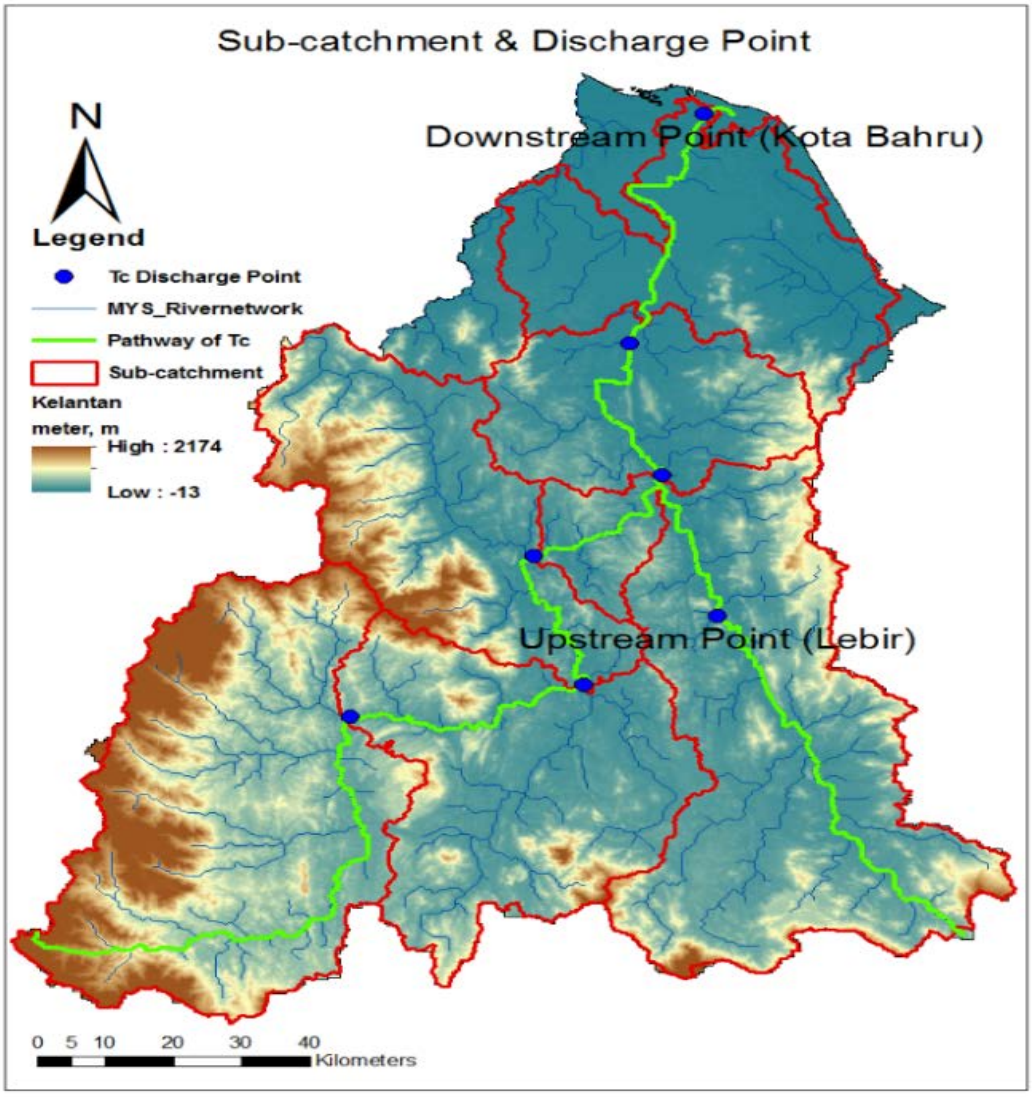

Figure 4.1 Sub-catchment and discharge point for upstream and downstream.

4.2.2 Empirical Study

T_c can be also estimated empirically by examining the relationship between peak discharge and rainfall with different durations. We used 29-year (1986-2014) records of observed hourly rainfall and discharge. The rainfall from 17 stations were interpolated by Thiessen polygon method to compute catchment average rainfall (Figure 4.1). By setting the annual peak discharges as the ending time for each year, we calculated catchment average rainfall prior to the discharge peaks by changing the durations from 6-hours, 12-hours, 18-hours, 24-hours, 2-days, 3-days, 4-days, 5-days, 6-days, 7-days, 2-weeks, 3-weeks and 4-weeks. Then the duration showing the highest coefficient of determination, R^2 with the tolerance level of ±0.01 were selected as the empirically estimated T_c.

4.2.3 Simulation Conditions of RRI Model

T_c is estimated also by a hydrologic model considering runoff on slope, stream flow and flood inundation. Here T_c is approximated by the time for discharge to reach a steady state where a discharge reaches 97% of given constant rainfall followed by previous studies (Machmeier & Larson, 1968). Saghafian and Julien (1995) called the time estimated in this way for more complex catchment with varied catchment characteristics as time to equilibrium T_e. The definitions of T_c and T_e are different because the former one expresses the arrival of wave time from hydraulically longest point to the outlet regardless the conditions of steady rainfall, while the latter one presumes the steady state conditions. However, in the theoretical estimations of T_c presented above, we assume the steady state conditions, and therefore the following sections compare the variables without distinguishing T_c and T_e.

As a hydrologic model, this study used the RRI model, simulating for both rainfall-runoff and inundation simultaneously (Lehner et al., 2008). The topographic data is obtained from HydroSHEDS dataset with 15 arc-second resolution. For the model parameters, we assume no infiltration to make it consistent with the theoretical approach described above, leading to two model parameters; the Manning's roughness coefficients for rivers and slopes. Based on simulations for the 2014 flood event, they were determined as 0.03 $m^{-1/3}s$ and 0.4 $m^{-1/3}s$, respectively, used also for the theoretical T_c calculations.

The simulation was carried out over 13,104 km^2 area, identified as Kelantan River Catchment Area based on topographic data. The simulation used topographic data from HydroSHEDS with 15 arc-second resolution. The resolution was able to give 61594 number of grid cells, which corresponds to 461 m x 460 m of grid resolution in the catchment. The river channel locations were defined by using the flow accumulation datasets included in the HydroSHEDS with 15 arc-second resolution. As such, grid cells more than 5 flow accumulation were confirmed to have a river channel.

The steady state simulation was conducted with 1 mm/h for 360 hours to simulate the base flow conditions followed by various rainfall intensities from 5 mm/h to 25 mm/h to reach the equilibrium conditions. Catchment slope is calculated based on the topography from a

land slope of 0.15 and river channel slope of 0.009 (90/10000) to a very mild slope of 0.0001 (1/10000). Moreover, the RRI model simulations were executed with different assumptions including kinematic wave, diffusive wave and with and without inundation processes (Table 4.1).

Table 4.1 Abbreviation for simulated parameters.

Test Code	Descriptions
Kinematic Wave (KW)	Kinematic wave. The depth of river channel was deepen by 30 m from original depth to avoid flood inundation.
Diffusive Wave (DW)	Diffusive wave. The depth of river channel was deepen by 30 m from original depth to avoid flood inundation.
DW + Inundation (5000 m)	Diffusive wave. The observed river cross sections were used to estimate river width and depth. Flood inundation can occur in the model.

4.3 THEORETICAL DERIVATION

This section presents the methods to calculate T_c based on KW and DW approximations for overland flow and river channel flow. In addition, this section explains the application of a hydrologic model simulating for rainfall-runoff and flood inundation for the T_c estimate with continuous rainfall input.

4.3.1 T_c based on Kinematic Wave (KW)

By referring to Saghafian and Julien (1995), we separated that T_c into two phases: $T_{cs\text{-}KW}$ refers to the time of concentration based on KW approximation on a hillslope to the beginning of stream flow. $T_{cr\text{-}KW}$ refers to the time of concentration with KW approximation along river channels from an upstream point to a downstream point.

As a wave originates from a point at a distance $x = x_1$ and travels to $x = x_2$ in either overland or channel flow phase, the wave travel time t_w is written as equation (4.2),

$$t_w = \int_{x_1}^{x_2} \frac{dx}{c} \tag{4.2}$$

where x is the distance measured along the flow path and c is the wave celerity. The celerity of the wave depends upon an expression for the resistance as well as the wave type. In general, the wave celerity is expressed by equation (4.3),

$$c = \frac{\partial Q}{\partial h} \cdot \frac{dh}{dA_x} \tag{4.3}$$

where Q is the discharge, h is the flow depth, and A_x is the flow cross-section area.
The relationship between discharge Q, flow depth h and flow cross-section area A_x based on Manning resistance law can be written as equation (4.4).

$$Q = \frac{1}{n} \cdot R^{\frac{2}{3}} \cdot S_f{}^{\frac{1}{2}} \cdot (b \times h) \tag{4.4}$$

Here n is the Manning's roughness coefficient, R is hydraulic radius, S_f is friction slope, b is width and h is flow depth.

Based on flow cross-section area A_x the hydraulic radius R can be determined as the functions of flow depth h. Friction slope, S_f can be assumed as bed slope, S_o when the acceleration and pressure gradient terms are assumed negligible in the conservation of the dynamic wave momentum for overland flow.

$$\frac{\partial Q}{\partial h} = \frac{5}{3}\frac{1}{n} \cdot h^{\frac{2}{3}} \cdot S_o{}^{\frac{1}{2}} \cdot b \tag{4.5}$$

$$\frac{dh}{dA_x} = \frac{1}{b} \tag{4.6}$$

By substituting equation (4.5), (4.6) in the wave celerity equation (4.3) and replacing the computed c into the wave travel time equation (4.2) for a rectangular channel, $T_{cr\text{-}KW}$ is expressed as

$$T_{cr-KW} = \frac{3}{5} \cdot n^{\frac{3}{5}} \int_{x_1}^{x_2} \frac{dx}{Q(x)^{\frac{2}{5}} \cdot S_o(x)^{\frac{3}{10}} \cdot b^{-\frac{2}{5}}} \tag{4.7}$$

If the wave travel time is computed for $x_1 = 0$ and $x_2 = L$ with the assumption of $S_o(x)$ are constant along x, $T_{cr\text{-}KW}$ can be further approximated as;

$$T_{cr-KW} = \frac{3}{5} \cdot \frac{n^{\frac{3}{5}} \cdot b^{\frac{2}{5}}}{S_o^{\frac{3}{10}}} \int_0^L \frac{dx}{Q(x)^{\frac{2}{5}}} \tag{4.8}$$

Now let assume that rainfall of constant intensity falling over an impervious watershed. If the uniform rainfall intensity, i falls under a uniform rectangular plane, along the length of the slope S_L, the kinematic wave based T_c for slope overland flow[5)] can be estimated by inserting $Q(x) = i \cdot x \cdot b$ and the unit width (i.e. $b = 1$) in equation (4.8).

$$T_{cs-KW} = \frac{S_L^{0.6} n^{0.6}}{i^{0.4} S_o^{0.3}} \tag{4.9}$$

where S_L is length along the slope, n is the Manning's roughness coefficients, i is rainfall intensity, S_o is the topographic slope.

Hence the $T_{c\text{-}KW}$ can be summed up from the two phases: the wave travel time for overland flow $T_{cs\text{-}KW}$ and river channel flow $T_{cr\text{-}KW}$.

$$T_{c-KW} = T_{cs-KW} + T_{cr-KW} \tag{4.10}$$

4.3.2 T_c based on Diffusive Wave (DW)

In the absence of lateral flow, conservation of the dynamic wave momentum for overland flow over a wide plane can be expressed as follows:

$$S_f = S_o - \frac{\partial h}{\partial x} \tag{4.11}$$

With the function of discharge Q and friction slope S_f, flow depth $\frac{\partial h}{\partial x}$ can be expressed as

$$\frac{\partial h}{\partial x} = \frac{\partial h}{\partial Q} \cdot \frac{\partial Q}{\partial x} + \frac{\partial h}{\partial S_f} \cdot \frac{\partial S_f}{\partial x}$$

$$\frac{\partial S_f}{\partial x} = \frac{\partial S_o}{\partial x} - \frac{\partial^2 h}{\partial x^2} \tag{4.12}$$

By assuming $\frac{\partial S_o}{\partial x} = 0$ and $\frac{\partial^2 h}{\partial x^2} = 0$, $\frac{\partial h}{\partial x}$ can be written as equation (4.13).

$$\frac{\partial h}{\partial x} = \frac{\partial h}{\partial Q} \cdot \frac{\partial Q}{\partial x} \tag{4.13}$$

Based on the Manning resistance law, flow depth h can be written as

$$h = \left(\frac{n \cdot Q}{b \cdot S_f^{\frac{1}{2}}} \right)^{\frac{3}{5}}$$

$$\frac{\partial h}{\partial Q} = \frac{3}{5} \left(\frac{n}{b \cdot S_f^{\frac{1}{2}}} \right)^{\frac{3}{5}} Q^{-\frac{2}{5}} \tag{4.14}$$

Discharge at the position x along river is expressed as

$$Q(x) = 2S_L \cdot x \cdot i + Q_{up}$$

$$\frac{\partial Q}{\partial x} = 2S_L \cdot i \tag{4.15}$$

where $Q(x)$ is discharge at distance x, Q_{up} is discharge from upstream catchment that flow into the river channel, b is the width.

By substituting equations (4.14) and (4.15) in equation (4.13),

$$\frac{\partial h}{\partial x} = \frac{3}{5}\left(\frac{n}{b \cdot S_f^{\frac{1}{2}}}\right)^{\frac{3}{5}} Q^{-\frac{2}{5}} \cdot 2S_L \cdot i \tag{4.16}$$

Wave travel time in diffusive wave for $x_1 = 0$ and $x_2 = L$ the integral may similarly be defined based on equation (4.7) by replacing $S_f = S_o - \frac{\partial h}{\partial x}$ and the wave travel time in river channel flow $T_{cr\text{-}DW}$ is expressed as

$$T_{cr-DW} = \frac{3}{5} \cdot n^{\frac{3}{5}} \int_0^L \frac{dx}{\left(2S_L \cdot x \cdot i + Q_{up}\right)^{\frac{2}{5}} \cdot \left(S_o - \frac{\partial h}{\partial x}\right)^{\frac{3}{10}} \cdot b^{-\frac{2}{5}}} \tag{4.17}$$

Note that the solution becomes imaginary numbers when S_f is smaller or equal to zero. In such a case Zakeri et al. (2012) proposed to divide the integral into two parts with the boundary of x_b calculated by the equation (4.18).

$$x_b = S_o^{-\frac{13}{4}} \cdot \left(\frac{5}{3}\right)^{-\frac{5}{2}} \cdot \left(\frac{n}{b}\right)^{\frac{3}{2}} \cdot (2S_L)^{\frac{3}{2}} \cdot i^{\frac{3}{2}} - Q_{up} \cdot (2S_L)^{-1} \cdot i^{-1} \tag{4.18}$$

Refer to Zakeri et al. (2012), wave travel time $T_{cr\text{-}DW}$ is calculated as equation (4.19).

$$T_{cr-DW} = \frac{3}{5} n^{\frac{3}{5}} b^{\frac{2}{5}} \left[\frac{1}{S_o^{\frac{3}{10}}} \int_0^{1.01x_b} \frac{dx}{\left(2S_L \cdot x \cdot i + Q_{up}\right)^{\frac{2}{5}}} + \int_{1.01x_b}^{L} \frac{dx}{(2S_L \cdot x \cdot i + Q_{up})^{\frac{2}{5}} \cdot (S_o - \frac{\partial h}{\partial x})^{\frac{3}{10}}} \right] \tag{4.19}$$

Since the equations (4.17) and (4.19) have no analytical solution, it has to be numerically integrated to obtain the $T_{cr\text{-}DW}$. Note that if x_b is within the range of *0* and *L*, the equation (4.19) has to be used instead of (4.17). In other words, if the following condition (4.20) is satisfied with inflow Q_{up} from the upstream, x_b will be always smaller than 0 (i.e. outside

the range of 0 to L). In such a case the equation (4.17) can be used.

$$Q_{up} > S_o^{-\frac{13}{4}} \cdot \left(\frac{5}{3}\right)^{-\frac{5}{2}} \cdot \left(\frac{n}{b}\right)^{-\frac{3}{2}} \cdot 2S_L^{\frac{5}{2}} \cdot i^{\frac{5}{2}} \tag{4.20}$$

The above derivation focused on the diffusive wave for river channel $T_{cr\text{-}DW}$. The equation can be derived in the similar way as the $T_{cs\text{-}DW}$.

4.3.3 T_c based on Diffusive Wave (DW) with Flood Inundation

Figure 4.2 shows the assumption that made for calculate T_{cr} which considers DW and flood inundation.

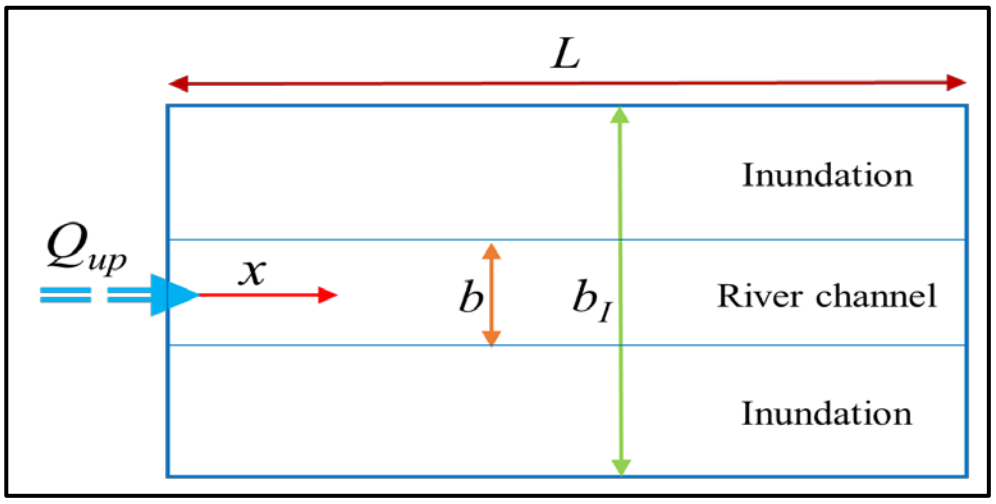

Figure 4.2 Schematic of assumption of $Q(x)$.

T_{cr} for DW and flood inundation can be calculated by equation (4.17) or (4.19) with simply replacing the b with b_I to represent the area of inundation extent.

$$T_{cr-DWI} = \frac{3}{5} \cdot n^{\frac{3}{5}} \int_0^L \frac{dx}{\left(2S_L \cdot x \cdot i + Q_{up}\right)^{\frac{2}{5}} \cdot \left(S_o - \frac{\partial h}{\partial x}\right)^{\frac{3}{10}} \cdot b_I^{-\frac{2}{5}}} \tag{4.21}$$

where b_I is width of the inundation boundary, Q_{up} is discharge from upstream catchment that flow into the river channel, L is distance along of the river channel.

Time of concentration of DW and flood inundation $T_{c\text{-}DWI}$ is calculate in two parts: the wave travel time on slope $T_{cs\text{-}DW}$ equation (4.9) and river channel with inundation $T_{cr\text{-}DWI}$ equation (4.21).

$$T_{c-DWI} = T_{cs-DW} + T_{cr-DWI} \tag{4.22}$$

4.4 RESULTS AND DISCUSSIONS

This section is to discuss all the results and findings from the theoretical, empirical and simulation approaches. The results of theoretical and simulation include three conditions which are kinematic wave (KW), diffusive wave (DW) and diffusive wave including inundation. Results for theoretical approach obtained from MATHLAB by apply all the parameters to the equation in section 4.3. Results for empirical assumption obtained by the coefficient of determination, R^2. The value of R^2 that close to 1 means the higher correlation of relationship.

4.4.1 Theoretical Results

Table 4.2 Summary of theoretical T_c in hours based on different methods.

		Lebir					Kota Bharu				
Method	Rainfall, mm/h	5	10	15	20	25	5	10	15	20	25
Theory	KW	6	4	4	3	3	12	9	8	7	6
	DW	8	6	5	5	4	14	11	10	9	8
	DW + Inundation b_I=5,000 m	16	12	11	10	9	205	158	136	123	114

According to the theoretical calculations in Table 4.2, the results indicate that T_c decreases with the increase of rainfall intensity both at Lebir and Kota Bharu. This result agrees to the previous studies (Ishihara & Takasao, 1959; Izzard, 1943; Singh, 1976), which stated rainfall intensity is an important influence on the T_c. For the Lebir, T_c calculated by using KW and DW show almost the same values. Table 4.2 shows T_c of KW decreases from 6 hours to 3 hours with rainfall intensities 5 mm to 25 mm, while T_c of DW decrease from 8

hours to 4 hours. On the other hand, for the Kota Bharu, T_c calculated by DW has longer T_c compared to the one by KW by 2 hour. Table 2 shows T_c at Kota Bharu with 5 mm rainfall is 12 hours for KW and 14 hours for DW. Followed by 10 mm rainfall, 9 hours T_c for KW and 11 hours T_c for DW. T_c of KW and DW slightly decreases 1 hour each from 10 mm rainfall to 25 mm rainfall. This can be explained as DW effect occurs at mild slope area (Su & Fang, 2004; Zakeri et al., 2012; Saghafian & Julien, 1995). T_c that includes the effect of DW and inundation shows even higher increase in the time compared to the T_c without inundation. At 5 mm rainfall, T_c of DW is 8 hours at Lebir and 14 hours at the Kota Bharu without inundation. However, T_c of DW with inundation is 16 hours for upstream and 205 hours for downstream.

4.4.2 Simulated Results

In Figure 4.3, T_c at Lebir with different conditions were shown. There are three conditions such as KW, DW without inundation and DW with inundation. The T_c is approximated by the time for discharge to reach a steady state where a discharge reaches 97% of given constant rainfall followed by previous studies (Machmeier & Larson, 1968). Discharge starts to increase after 360 hours and reach steady state at 380 hours for KW and 384 hours for DW. However, for DW with inundation more travel time needed for the discharge reaching steady state which is 436 hours. For Kota Bharu, the T_c is much longer compared to Lebir as Lebir is the upstream point and Kota Bharu is the downstream point. Figure 4.3 shows discharges reach steady state at 384 hours and 390 hours for DW. Moreover, DW with inundation reach steady state at 580 hours. KW and DW for both Lebir and Kota Bharu show almost the same T_c due to no inundation occur during the travel of water from upstream to downstream.

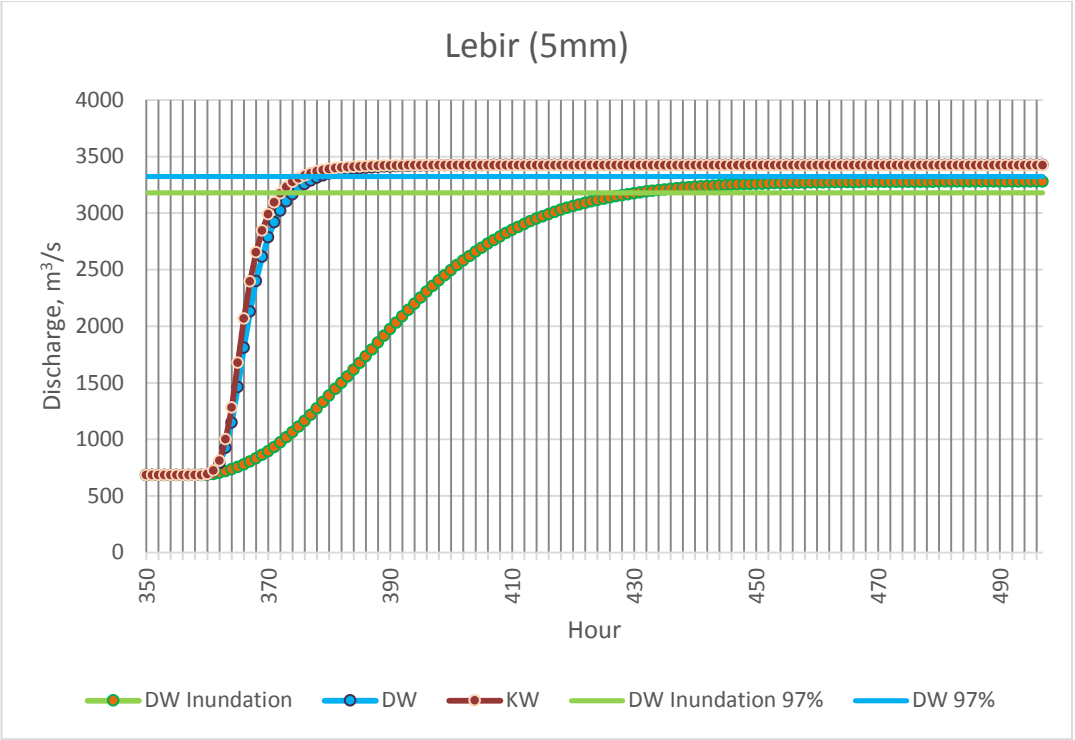

Figure 4.3 Tc of Lebir for different condition at steady state.

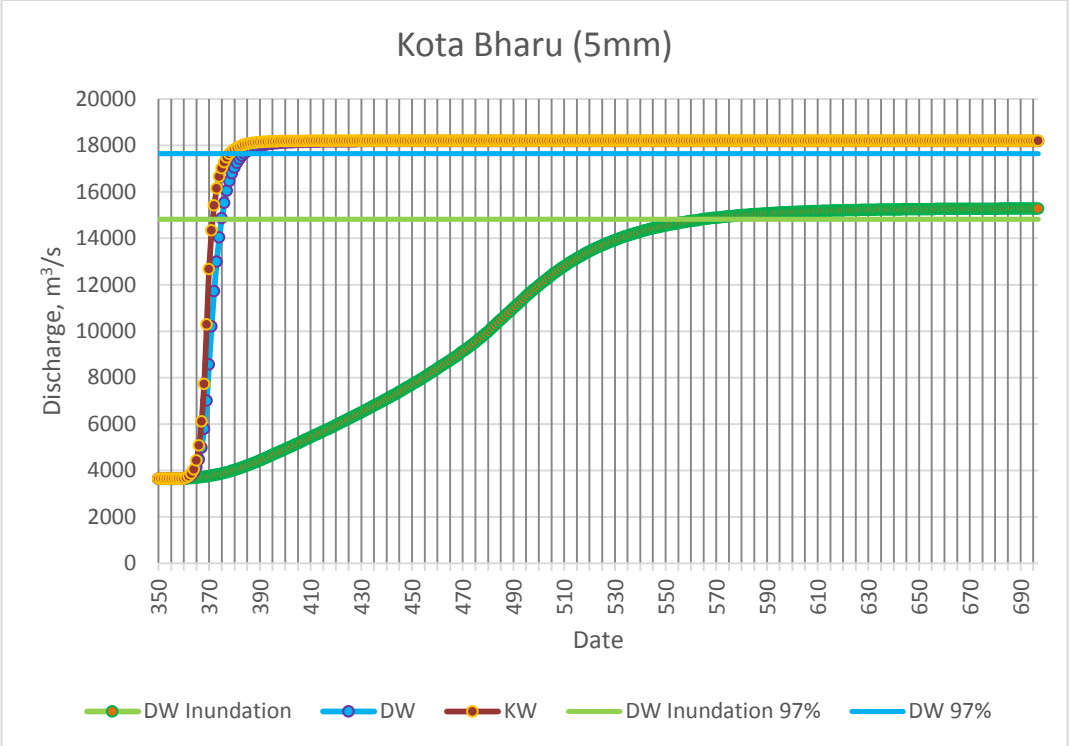

Figure 4.4 Tc of Kota Bharu for different condition at steady state.

Su and Fang defined T_c as the amount of time required for all portions of a catchment that bring all surface runoff to the contribute runoff to the outlet (Su & Fang, 2004). However, Figure 4.3 and 4.4 show that DW with inundation didn't reach the same maximum discharge as KW and DW. The loss of discharge DW with inundation in Lebir is smaller than Kota Bharu because of the water in the downstream is not only flow in the river channel but also flow along the riverside due to the flood inundation.

Table 4.3 Summary of simulated Tc in hours based on different methods.

		Lebir					Kota Bharu				
Method	Rainfall, mm	5	10	15	20	25	5	10	15	20	25
RRI Model	KW	20	16	14	12	10	22	18	14	12	12
	DW	24	18	15	15	15	30	24	20	30	60
	DW + Inundation	76	74	71	72	74	210	236	250	250	260

The summary of simulation results in Table 4.3 showed that KW presents a smaller T_c which is gradually decreasing from 20 hours to 10 hours with rainfall intensity from 5 mm to 25 mm at the Lebir; compared with DW which is 24 hours for 5 mm rainfall, 18 hours for 10mm rainfall, 15 hours for 15 mm, 20 mm and 25 mm rainfall. For Kota Bharu, the T_c is decreasing from 22 hours to 12 hours with rainfall intensity 5 mm to 25 mm. T_c of DW is longer compared to KW where the T_c is decreasing at the rainfall intensity of 5 mm, 10 mm and 15 mm for T_c 30 hours to 20 hours. However, the T_c increase to 30 hours and 60 hours when the rainfall intensity increase. This may cause of the inundation occur at 20 mm and 25 mm rainfall. Moreover, from the simulation results at Lebir, T_c with inundation shows longer T_c compared to the one without inundation. T_c with inundation is about three times longer than T_c without inundation with 5 mm rainfall, 76 hours for T_c with inundation and 24 hours for T_c without inundation. T_c at the downstream point (Kota Bharu) shows high T_c compared to the DW, where the T_c increased from 210 hours to 260 hours with rainfall intensity of 5mm to 25 mm. This happens due to the inundation extent slow down the water travel time.

4.4.3 Empirical Approach

T_c can be also estimated empirically by examining the relationship between peak discharge and rainfall with different durations. We used 29-year (1986-2014) records of observed hourly rainfall and discharge. The rainfall from 17 stations were interpolated by Thiessen polygon method to compute catchment average rainfall (Figure 4.1). The relationships between rainfall amounts for different durations and peak discharges are shown in Figure 4.5 and 4.6. They plot cumulative rainfall (*x*-axis) counted backwards from the peak discharge of each year (*y*-axis).

By setting the annual peak discharges as the ending time for each year, we calculated catchment average rainfall prior to the discharge peaks by changing the durations from 6-hours, 12-hours, 18-hours, 24-hours, 2-days, 3-days, 4-days, 5-days, 6-days, 7-days, 2-weeks, 3-weeks and 4-weeks. Then the duration showing the highest coefficient of determination with the tolerance level of ±0.01 were selected as the empirically estimated T_c in this study.

Based on the analysis, Figure 4.5 shows that the 3, 4, 5, 7-days cumulative rainfall at Lebir shows the highest correlation (R^2 = 0.68±0.01). This means that 3 to 7-days cumulative rainfall intensity have high affect to the peak discharge at Lebir. T_c for Lebir by using empirical study is between 3 to 7-days periods. Furthermore, Figure 4.6 shows the analysis results at Kota Bharu. The highest correlation at Kota Bharu is 0.7±0.01. This value can be identified with 5, 7, 14-days cumulative rainfall. From the analysis, it can be decided that the effects of rainfall intensity towards discharge at Kota Bharu will be significant with 5 to 14-days cumulative rainfall due to the high coefficient of determination. The results from this analysis will be used in the next chapter for time series analysis. Time series analysis need to be analyze by refer to the empirical analysis results because empirical analysis shows the most significant cumulative rainfall to the discharge.

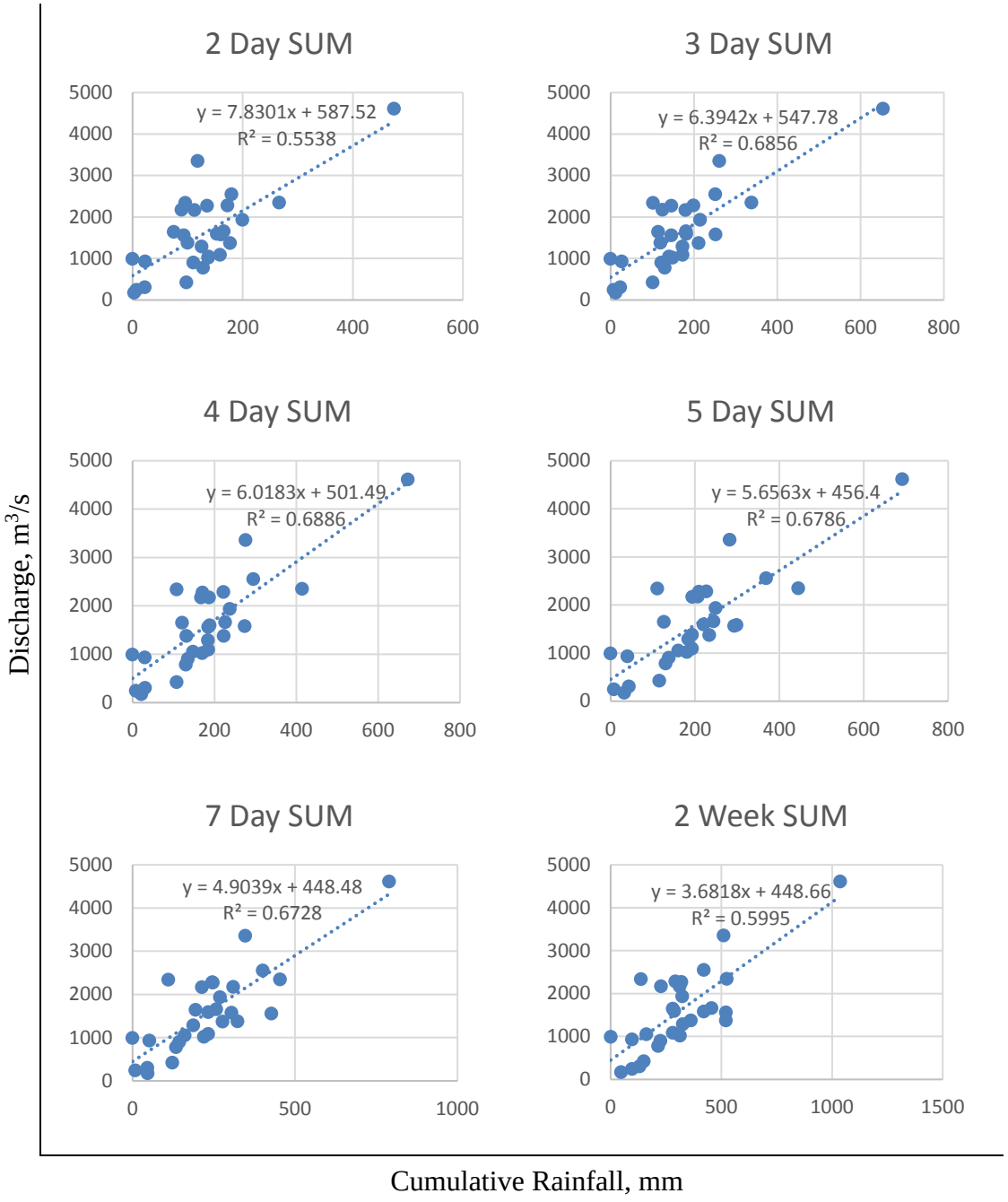

Figure 4.5 Relationships between annual maximum discharge (*y*-axis) and cumulative rainfall for different durations (*x*-axis) at Lebir.

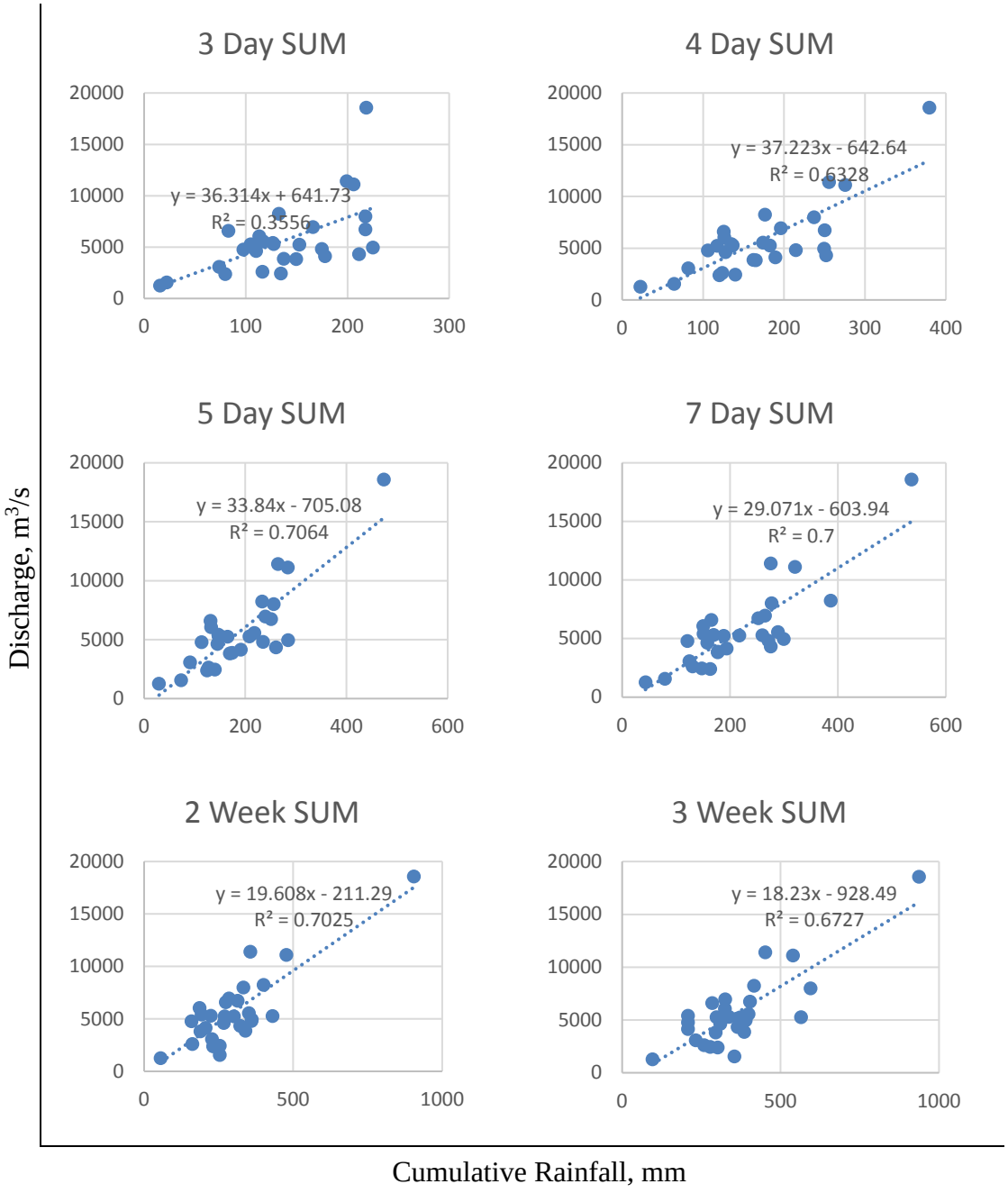

Figure 4.6 Relationships between annual maximum discharge (*y*-axis) and cumulative rainfall for different durations (*x*-axis) at Kota Bharu.

4.5 SUMMARY

This study proposed a method to estimate T_c that considers diffusive wave and inundation effects along stream flow. From the comparison between the proposed theoretical approach and RRI model results, we can conclude that the diffusive wave and inundation extent shortens T_c. For flat topography areas, it is therefore important to consider these factors for estimating more reasonable T_c to be used to estimate flood arrival times or in designing drainage systems.

From the analysis of empirical study, it can be conclude that cumulative 3-days to 7-days rainfall will bring affects to the upstream discharge point (Lebir). Then, for the downstream discharge point (Kota Bharu), the analysis results show that 5-days to 14-days cumulative rainfall has the highest R^2 (0.7), which means the cumulative rainfall brings high impact to the related discharge point. These findings will be used for the chapter 5 and 6, where the frequency analysis and trend analysis need to be conducted for the most high relationship parameters rather than all the parameters. As example: The findings from the analysis shows the cumulative rainfall that affect discharge is 3-days to 14-days.

Regardless the discrepancies, our analysis supported that T_c becomes longer with the considerations of flood inundation effects. According to the RRI simulated results, the T_c values are generally longer than the theoretical ones possibly due to the different assumptions in the calculation. One of the reasons may be associated to the assumption of 5,000 m inundation extent for the theoretical calculation based on Kelantan 2014 flood event. With the constant inundation extent, the theoretical T_c becomes shorter with the higher rainfall intensities. On the other hand, the inundation extent by the RRI model increases without the limitation of 5,000 m for to the higher rainfall intensity cases. This leads to even longer T_c by the model estimations. Hence the reason for the underestimation by the theoretical approach especially for the high intensity rainfall cases may be related to the assumptions of the inundation extents.

CHAPTER 5 TIME SERIES ANALYSIS: FREQUENCY AND TREND ANALYSIS

5.1 INTRODUCTION

The recent severe flood in 2014 in Kelantan River Catchment caused severe losses both in human lives and properties. In order to efficiently manage extreme or rare event, there is a need to understand the peculiarity of the 2014 event and find the best method to understand how frequent these extreme events occur and how is the trend of rainfall in the last four decades. Understanding extreme event occurrences and the trend of rainfall is valuable to better management of flood risks. The aim of this chapter is to understand the extreme event frequency and the rainfall trend in Kelantan River Catchment. In this chapter, historical hydrological data was used to investigate the frequency analysis and rainfall trends for the Kelantan River for a 44 (1971 – 2014) year period.

The increased of extreme events brings large challenge for disaster prevention infrastructure, such as 2011 Tohoku tsunami, Thailand floods and 2014 Kelantan Yellow floods. Water resource structures such as dams, bridges, railways are designed for return periods exceed 50-years (Rajczak *et al.*., 2013). Therefore, it is crucial to understand the changes in the past and thereby predict what will happen in the future and finally to improve the ability to manage the risks associated with precipitation extreme events.

The floods' critical peak discharges are often determined by meso-scale processes than small and require to be analysed in basin-specific approaches (Lehner *et al.*., 2006). It is necessary to conduct research on each basin with local historical data. Due to the northeast monsoon, the Kelantan River basin is vulnerable to floods and suffered from some disastrous floods in the history. The previous sections found the correlation between

rainfall with different durations and peak discharge in the river basin. Findings from Chapter 4 showed that continuously 3 to 7-days rainfall will be seriously affect to upstream areas, and 5 to 14-days continuous rainfall will be seriously affect to the downstream areas. The relationships between the changes of extreme precipitation and peak discharges are contribution to understand the differences level of floods. However, many previous studies did not include the duration of continuous rainfall in the analysis of rainfall trends. Therefore, the previous rainfall trend analysis does not accurately express the trend of rainfall.

This chapter attempts to apply statistical methods to understand the frequency of extreme events (frequency analysis) and rainfall trend (trend analysis) using statistical methods. Rainfall data used for frequency analysis was 44 years (1971 – 2014) rainfall data from 17 stations in Kelantan River Basin. The distribution models used for the frequency analyses were the Generalized Extreme Value (GEV) and the Gumbel distributions. After distribution parameters were estimated, the compatibility of data and the two theoretical distributions were then quantified with goodness to fit tests, namely the standard least-square test (SLSC), the correlation coefficient test (COR), the Kolmogorov-Smirnov test (KS), and the Anderson-Darling (AD) test to fit the sample data. The Mann-Kendall (MK) test was used to detect time-series trends (increasing or decreasing) of rainfall in the catchment. Furthermore, in order to determine the magnitude of rainfall change in the catchment, the non-parametric Sen's slope test was used. The trend analysis is using 45 years of rainfall data at 17 stations in the catchment.

5.2 FREQUENCY ANALYSIS

5.2.1 Distribution Function and Return Period

The use of probability theory and frequency analysis are important for understanding and describing stochastic hydrological phenomena. Besides, probability theory and frequency analysis are needed because of there are non-determinable hydrologic processes which can provide a fully understanding on the hydrological phenomena (Yevjevich, 1972). In the recent years, extreme rainfall events are more common in the hydrological phenomena due

to climate change. Extreme rainfall events are reflected as random variables in frequency analysis where random variables are assumed to be independent and come from identical distribution. Probability distribution can be used to identify the magnitude of random variables happened to within a particular frequency of occurrence.

By understanding the historical data of hydrological events, probability distribution can be explained in term of future probability of occurrence (Chow, 1964) which helps in engineering structure design in flood protection and flood risk management.

There are two common ways to present probability distribution such as probability density function (PDF) and cumulative distribution function (CDF). Equation (5.1) described that CDF is probability distribution of a random variable *X* with a probability *P* at a value of less than or equal to *x*.

$$F(x) = P[X \leq x] \tag{5.1}$$

$$F(x) = \int_{-\infty}^{x} f(x)dx \tag{5.2}$$

which $F(x)$ is the cumulative distribution function (CDF) and $f(x)$ is the probability density function (PDF). It is also regarded as the non-exceedance probability. The CDF is also related to PDF as in equation (5.2). A cumulative of the PDF produces the CDF.

The design life of hydraulic structures depends on the return period, *R*. If a hydrologic event, *X* equal to or greater than *x* occurs once in *R*-years, the exceedance probability $P(X \geq x)$ is equal to 1 in *R* cases, or

$$P(X \geq x) = \frac{1}{R} \tag{5.3}$$

For an extreme hydrological event with specific value O_{max}, there is a relationship:

$$R = \frac{1}{1 - P[X \leq O_{\max}]} \tag{5.4}$$

In the equation, R is the return period (year) of $X=O$, and O_{max} is often called as R-year event (Takara, 2009). According to equation (5.4), the R-year event O_{max} can be obtained by using the following equation:

$$O_{\max} = F^{-1}(1-\frac{1}{R}) \tag{5.5}$$

Now, the frequency of extreme index is related to return period. The extreme changes can be quantified in magnitude by the changes of R-year event O_{max} or frequency by the changes of return period with the same value of O_{max}.

5.2.2 Probability Distributions

There are several families of probability distribution methods used for modelling extreme events such as normal, log-normal, extreme-value type I (Gumbel) and type II, and Pearson type III (Gamma) distributions (Takara and Stedinger, 1994). The most commonly used in the frequency analysis of extreme events is the family of the extreme value distribution (Takara and Tosa, 1999). In this study, two types of distribution model, the distributions of Generalized Extreme Value (GEV) and Gumbel were used and compared. The goodness-of-fit test were used to choose which distribution model fits to Kelantan River Catchment data.

The *CDFs* of Gumbel and GEV distributions are:

$$F(x) = \begin{cases} \exp\left[-\exp\left(-\dfrac{x-b}{\sigma}\right)\right] & k = 0 \\ \exp\left[-(1-k\dfrac{x-b}{\sigma})^{\frac{1}{k}}\right] & k \neq 0 \end{cases} \tag{5.6}$$

In the equation (5.6), k, σ, and b are the shape, scale and location parameters, respectively. When k=0, it is the cumulative function of Gumbel distribution. Whereas $k\neq0$, it is the cumulative function of GEV distribution.

5.2.3 Parameter Estimation Methods

Parameter estimation method is used as a step to fit the data into several hypothesized distribution functions. There are some common parameter estimation methods in extreme value analysis, as example standard least square fitting method, method of moments (MOM), maximum likelihood method (MLM), Graphical method and *L*-moments method. Details explanations of each method could be referred to literature review of Yevjevich (1972) and Hosking and Wallis (2005). Each method has different level of simplicity and accuracy and some have limitations.

The suitability of parameter estimation method is selected based on the type of distribution that need to be tested. Referring to Alias (2014), although there are few methods but least square fitting method, method of moments or graphical method are simple methods compared to others. However, these methods only limit to the distribution with less than three parameters. In this study, the L-moments method is used for parameter estimation.

5.2.4 Goodness of Fit Tests

Based on the goodness of fit test, the best fit distribution is used to estimate the return periods and quantiles of the extreme values. Stephens (1986) introduced a modified Anderson-Darling (AD) criterion to validate the probability distribution models. Also, there are some studies using Kolmogorov-Smirnov (KS) criterion (Conover, 1980). However, Takara and Stedinger (1994) suggested four different approach for goodness-of-fit criteria which are standard least-square criterion (SLSC), correlation coefficient (COR), maximum loglikelihood (MLL) and Akaike's information criterion (AIC).

Additionally, Castillo et al. (2005) suggested that using graphical displays such as Quantile-Quantile (Q-Q) plots and Probability-Probability (P-P) plots. Graphic displays method can be said as simple and useful method for distribution model validation. In this study, the criteria of SLSC, COR, AD and KS are used for goodness of fit test. And the graphical displays are used as reference to suppose the test statistics from vision.

a) Standard least-square test (SLSC)

Takara (2009) mentioned that SLSC is one of the easiest methods for evaluating linearity of the data. The calculation equation is as follows:

$$SLSC = \frac{\sqrt{\sigma^2_{\min}}}{\left|S^*_{1-p} - S^*_p\right|} \tag{5.7}$$

$$\sigma^2 = \frac{1}{N}\sum_{i=1}^{N}(S_i - r_i)^2 \tag{5.8}$$

Where S^*_p is a value of the reduced variate S_i, which is corresponding to the non-exceedance probability p; σ^2_{min} obtained by minimizing σ^2; N is the sample size of observations; S_i obtained from the function $f(x)$:

$$S_i = f(y_i) \tag{5.9}$$

$$r_i = f(F^{-1}(p_i)) \tag{5.10}$$

Where y_i is the variable x which arranged from low to high; r_i is the standard variate of empirical data; p_i the non-exceedance probability which can be calculated as:

$$p_i = \frac{i-\alpha}{N+1-2\alpha} \tag{5.11}$$

In the equation (5.11), α is a constant based on probability distributions. Takasao et al. (1986) had compared six formula to determine the best α that suitable in the p_i estimation. From the comparison, Takasao et al. (1986) found that α=0.5 from Hazen's formula is the recommended compared to the others, e.g.: Weibull (a=0), Adamowski (a=0.25), Bolm (a=0.375), Cunnane (a=0.4) and Gringorten (a=0.44). The smaller the SLSC is, the better the fitting of the distribution is. Takasao et al. (1986) suggested SLSC<0.03 as a good fit for precipitation extremes analysis.

b) Correlation coefficient test (COR)

The criterion of correlation coefficient between y_i and r_i is describe as equation (5.12). Value of COR closer to 1 shows good fits of the distribution (Takara and Takasao, 1988).

$$COR = \frac{\sum_{i=1}^{N}(y_i - \bar{y})(r_i - \bar{r})}{\sqrt{\sum_{i=1}^{N}(y_i - \bar{y})^2 \sum_{i=1}^{N}(r_i - \bar{r})^2}} \tag{5.12}$$

c) Kolmogorov-Smirnov test (KS)

The KS test is used to test if a sample of data came from a hypothesized continuous distribution in which the theoretical distribution function of the test distribution is compared with the empirical distribution function of the time series data (Conover, 1980). The smaller value of *Y* is, the better the fitting of the distribution is. The statistic *Y* is described as:

$$Y = sup\left|Fn(x) - S(x)\right| \tag{5.13}$$

where *Fn(x)* is the empirical cumulative distribution function of the random sample *X*; *S(x)* is the theoretical cumulative distribution function.

d) Anderson-Darling test (AD)

The Anderson-Darling test (Stephens, 1974) is used to test if a sample of data came from a population with a specific distribution. The AD is an alternative goodness-of-fit tests to the KS. The AD makes use of the specific distribution in calculating critical values and puts more weight to tails compared to KS. The AD statistics can be calculated as equation (5.14).

$$AD^2 = -N - \sum_{i=1}^{N}\frac{2i-1}{N}\left[lnf_{CD}(y_i) + ln(1 - f_{CD}(y_{N+1-i}))\right] \tag{5.14}$$

where y_i is the i^{th} case in the sample *X*; *N* is the number of the sample. The smaller value is, the better the fitting of the distribution.

5.2.5 Results

5.3.5.1 Goodness of fit

Statistical parameters were estimated for two probability distributions, GEV and Gumbel, based on these datasets and afterwards the compatibility of these distribution functions and data was quantified with four goodness-of-fit tests, namely, SLSC, COR, KS and AD. According to Tanaka and Takara (1999), distribution functions shows good fit when SLSC test shows value less than 0.045 for extremes analysis. The other three criteria are less likely to reject the good fit, and are successfully used to compare the goodness of fit of different fitted distributions.

Table 5.1 shows the results of goodness of fit of the extreme rainfall. GEV showed to be the best distribution in four goodness of fit test. In all four criteria test, GEV has the lowest value compared to Gumbel. However, the value difference between GEV and Gumbel not significant showed. Thus, Quantile-Quantile (Q-Q) plots of GEV and Gumbel are compared to provide the best distribution between GEV and Gumbel. The results indicated that GEV shows better fit (Figure 5.1). This results showed agreement with results obtained by Abdulkareem and Sulaiman (2016) at station level which showed that GEV distribution function is best fit in 15 out of 17 stations using KS test and 14 out of 17 stations using AD test. Alias et al. (2016) also stated that GEV distribution model fits most of extreme values series in the Kelantan River Catchment. The GEV distributions were developed for annual maximum series for 1-day, 3-day, 5-day, 7-day and 14-day for catchment scale.

Table 5.1 Results of goodness of fit for extreme rainfall.

		Max1day	Max3day	Max5day	Max7day	Max14day
SLSC	GEV	0.026*	0.034*	0.035*	0.034*	0.038*
	Gumbel	0.030	0.036	0.036	0.040	0.056
COR	GEV	0.99*	0.981*	0.981*	0.982*	0.978*
	Gumbel	0.987	0.980	0.980	0.976	0.952
KS	GEV	0.081*	0.104*	0.075*	0.093*	0.097*
	Gumbel	0.097	0.104*	0.080	0.106	0.115
AD	GEV	0.328*	0.44*	0.339*	0.331*	0.337*
	Gumbel	0.429	0.468	0.347	0.405	0.770

"*" the best ranking under each criterion.

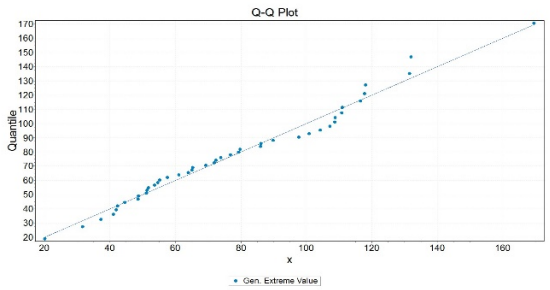

a) Max1day GEV

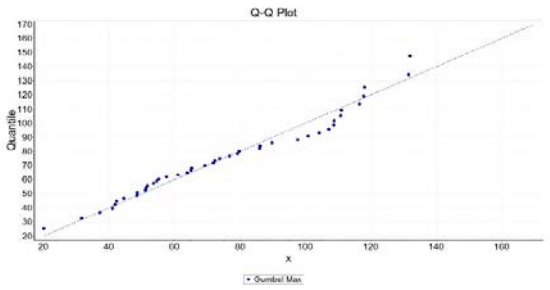

b) Max1day Gumbel

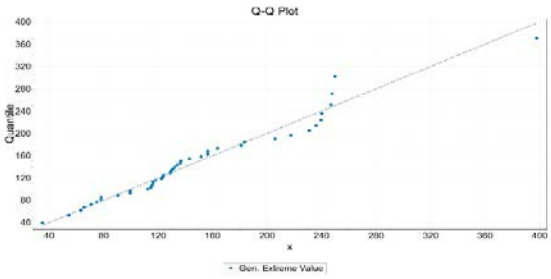

c) Max3day GEV

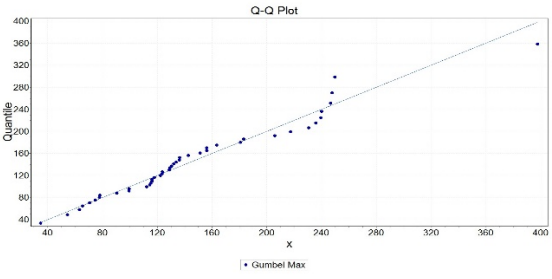

d) Max3day Gumbel

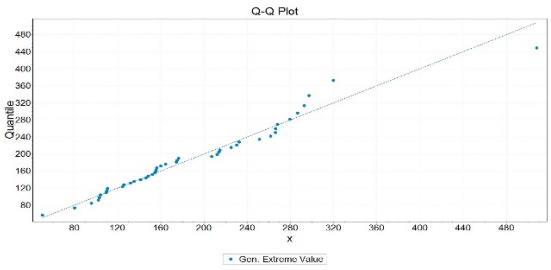

e) Max5day GEV

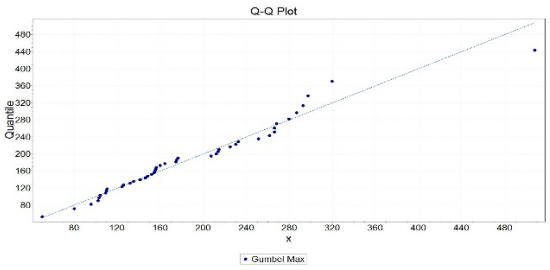

f) Max5day Gumbel

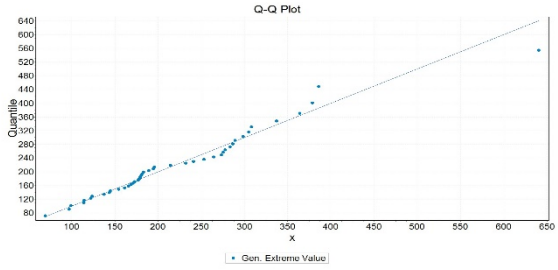

g) Max7day GEV

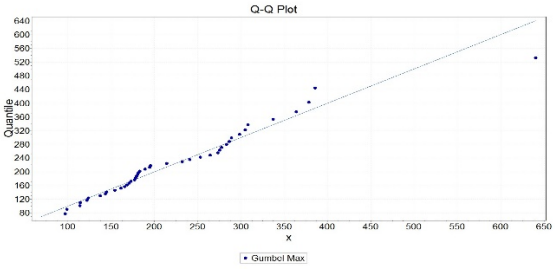

h) Max7day Gumbel

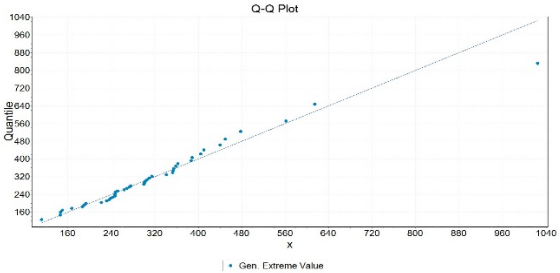

i) Max14day GEV

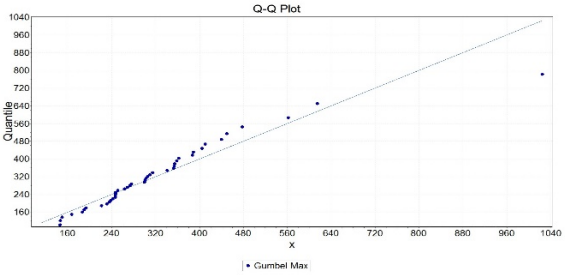

j) Max14day Gumbel

Figure 5.1 Q-Q plots for GEV and Gumbel in different durations of rainfall.

5.3.5.2 Frequency analysis for extreme events at each station

Frequency analysis of the extreme values was conducted to estimate the return period of the rainfall events using the GEV distributions fitted for extreme values data of each stations. The results from frequency analysis can show the average recurrence interval (ARI) of a magnitude of rainfall or return period of a particular rainfall. This research compares the December 2014 Kelantan flood to these return periods and assessed the peculiarity of the rainfall event against historical records. A rainfall event having a return period of 2-years means that the possibility of exceeding the magnitude is 0.5 for each year. The higher the return period values, the rarer the rainfall event is. The analysis uses the annual maximum rainfall series of more than 40 years of data. The GEV distribution model for the 1-day, 3-days, 5-days, 7-days and 14-days extreme rainfalls were fitted to and used to estimate the return periods.

The assessment of ARI for 2014 event's results are delivered in Table 5.2 and Table 5.3. The stations in Table 5.2 and 5.3 are arranged starting from stations located at the most upstream of the river basin to the downstream. The assessment shows that the return period or average recurrence interval (ARIs) of rainfall event in 2014 for most of the stations located at the upstream of the Kelantan river basin experienced high ARIs rainfall events (ARIs near or over 50-years) compared to stations at the downstream of the river basin (ARIs near or less than 20-years), especially for rainfall periods higher than 3-days. Stations which have the recorded rainfalls experiencing ARIs near to 500 years are stations Gob (3 and 5-days rainfall) and Brook (5-days rainfall). This result is in line with Alias et al (2016) who stated that max. 7-day rainfall in Gob Station has 496-year ARI and max. 5-day rainfall in Brook has >200 year ARI. Fourteen out of seventeen stations also recorded rainfalls in 2014 to be the highest value in historical records. Alias et.al (2016) who conducted up max 7-day rainfall mentioned that 9 out of 16 stations recorded rainfalls exceeding their historical values, namely JPS Machang, Kg. Durian Daun, Ulu Sekor, GOB, Kg. Aring, Gua Musang, Blau, Gunung Gagau, and Brook. The ARIs value is getting higher with number of day precipitations in the 2014 event, in particular for the upstream stations.

Table 5.2 ARIs for the 2014 rainfall in continuous of 1-day to 7-day.

	Max 1-Day Rainfall			**Max 3-Day Rainfall**		
Station	2014	ARIs (Years)	Historical highest	2014	ARI (Years)	Historical highest
Brook	132.7	50	132.7*	252.7	150	252.7*
Blau	145.2	10	196.9	311.1	50	311.1*
Upper Chiku	240.9	20	240.9*	567.8	50	567.8*
Gunung Gagau	502.8	20	541.9	1175.9	50	1175.9*
Gua Musang	216.3	50	216.3*	480.2	100	480.2*
Kg. Aring	282.2	20	304.1	616.1	50	616.1*
Balai Polis Bertam	208.5	150	208.5*	454.1	130	454.1*
GOB	257	50	257*	584.7	500	584.7*
Kg. Laloh	462.2	50	462.2*	1002.2	100	1002.2*
Dabong	243.6	10	778.5	498.2	20	781
Ulu Sekor	200.2	5	305	419.9	5	579.9
Kg. Jeli	220	5	294	399.2	5	486.8
Kg. Durian Daun	299.7	10	366	575.1	20	619.5
JPS Machang	539	10	612*	755.2	10	755.2*
Bendang Nyior	442	20	512.3	576.7	5	662.6
Rantau Panjang	411.9	20	829.6	565.9	10	1121
Kota Bharu	195.3	2	506.5	356.7	2	1058.8
	Max 5-Day Rainfall			**Max 7-Day Rainfall**		
Station	2014	ARI (Years)	Historical highest	2014	ARI (Years)	Historical highest
Brook	354.9	500	354.9*	400.9	300	400.9*
Blau	386.8	50	386.8*	428.4	50	443.4
Upper Chiku	653.4	50	653.4*	751.2	50	751.2*
Gunung Gagau	1367.6	50	1367.6*	1613	110	1613*
Gua Musang	534.7	50	534.7*	612	50	612*
Kg. Aring	656.7	20	656.7*	825.6	50	825.6*
Balai Polis Bertam	547.3	240	547.3*	651.3	250	651.3*
GOB	668.8	450	668.8*	712.8	240	712.8*
Kg. Laloh	1246.8	110	1246.8*	1430.2	110	1430.2*
Dabong	594.2	20	781	678.1	20	781
Ulu Sekor	594.9	10	657	804.7	20	804.7*
Kg. Jeli	520.1	5	608.5	699.4	10	858.5
Kg. Durian Daun	701.5	20	701.5*	858.6	50	858.6*
JPS Machang	876.1	10	876.1*	1063.6	20	1063.6*
Bendang Nyior	642.7	5	759.3	648.3	5	833.6
Rantau Panjang	646.8	10	1217.7	800.8	10	1270.2
Kota Bharu	499.5	5	1084.3	550.1	5	1177.4

"*" indicates historical highest rainfall occurred in 2014.

Table 5.3 ARIs for the 2014 rainfall in continuous of 14-days.

	Max 14-Day Rainfall		
Station	2014	ARI (Years)	Historical highest
Brook	563.2	100	563.2*
Blau	565.1	110	565.1*
Upper Chiku	1096.3	50	1096.3*
Gunung Gagau	2424.2	140	2424.2*
Gua Musang	834.9	120	834.9*
Kg. Aring	977.6	20	977.6*
Balai Polis Bertam	927.7	240	927.7*
GOB	1010.7	250	1010.7*
Kg. Laloh	2270.2	150	2270.2*
Dabong	1119.7	50	1119.7*
Ulu Sekor	1351.8	20	1351.8*
Kg. Jeli	1190	20	1333
Kg. Durian Daun	1249.2	150	1249.2*
JPS Machang	1625.1	50	1625.1*
Bendang Nyior	655.1	2	1205.4
Rantau Panjang	1119.7	10	1654
Kota Bharu	644.9	2	1393.1

"*" indicates historical highest rainfall occurred in 2014.

5.3.5.3 Frequency analysis for extreme event at the catchment scale

Another GEV distributions was fitted to the extreme values at catchment scale (rainfall intensities for each station for one particular time was averaged based on Thiessen polygon method and distributed in the catchment). Frequency analysis of the extreme values were conducted to estimate the return period of the historical extreme values. By estimating these return periods, historical floods and ARI can be compared and thus patterns can be understood. Also, it may help to explain the peculiarity of rainfall event are during the December 2014 Kelantan flood compared to the historical records. The analysis uses the hourly rainfall series of 44 years of data.

A single point precipitation measurement is quite often not representative of the volume of precipitation falling over a given catchment area. A dense network of point measurements and/or radar estimates can provide a better representation of the true volume over a given area. The Thiessen Polygon approach is probably the most common method used in hydrometeorology for determining average precipitation over an area when there is more than one measurement. The basic concept is to divide the watershed into several

polygons, each one around a measurement point, and then take a weighted average of the measurements based on the size of each one's polygon, i.e., measurements within large polygons are given more weight than measurements within small polygons (DID, 2000). The weighted average is calculated by equation (5.15):

$$P_{avg} = \frac{P_1A_1 + P_2A_2 + P_3A_3 + \ldots + P_nA_n}{A_1 + A_2 + A_3 + \ldots + A_n} = \frac{\sum_{i=1}^{n} P_iA_i}{\sum_{i=1}^{n} A_i} \quad (5.15)$$

where n is the sample size, P_{avg} is the weighted average, P_i are measurements of rainfall, and A_i are areas of each polygon, i is represents each rain gauge stations.

The parameters are estimated to fit all the samples (1-day, 3-days, 5-days, 7-days and 14-days extreme rainfalls) to GEV distribution. It is used to estimate the return periods of the catchment scale. The results are delivered in Table 5.4. Assessment shows that the return period or average recurrence interval (ARIs) in the past 44 years are not rare in records. As mentioned in the Chapter 1, flood used to occur every year, the return periods that showed in the Table 5.4 are commonly 1 and 2-years ARIs which can be support from the flood events that occurred in the past. However, there are few years in the historical showed the return periods with more than 5-years in maximum daily, such as 1983, 1984, 1988, 1993, 2001, 2004, 2007, 2009, 2011, 2012, 2013. The most severe case happened in 2014, where the return period is higher than 50-years in maximum daily and exceed 100-years return periods at maximum 3, 5, 7 and 14-days rainfall.

These findings is in line with Chan (1995) for floods 1925-1993 and Global Active Archive of Flood Events (Brakenridge, 2017). The archive listed out that in Kelantan Area floods with different magnitude caused by heavy rain, torrential rain, and monsoonal rain happened with different of severity such as large flood with less than 20-year return period happened in the year 1993, 1999, 2003, 2006, 2007, 2008, 2009, 2010 and 2013, and between 20-year and 100-year period happened in the year of 1988, 2000, 2001, 2004, and 2006. More than 100-year magnitude of flood happened in 2014 (Brakenridge, 2017).

Table 5.4 ARIs for the 2014 rainfall in catchment scale.

Year	**Max 1-Day**		**Max 3-Day**		**Max 5-Day**		**Max 7-Day**		**Max14-Day**	
	Rainfall	ARI	Rainfall	ARI	Rainfall	ARI	Rainfall	ARI	Rainfall	ARI
1971	42.36	1	65.72	1	104.54	1	122.08	1	242.35	1
1972	48.79	1	136.22	2	154.53	1	161.55	1	193.25	1
1973	41.11	1	78.25	1	103.46	1	114.36	1	189.93	1
1974	54.70	1	115.61	1	146.65	1	154.70	1	167.80	1
1975	55.34	1	99.49	1	126.04	1	173.20	1	302.39	2
1976	41.98	1	78.08	1	109.74	1	124.00	1	247.69	1
1977	44.59	1	70.70	1	80.40	1	97.00	1	150.34	1
1978	57.66	1	74.93	1	102.41	1	114.50	1	146.90	1
1979	79.82	2	136.67	2	176.68	2	194.77	1	301.41	2
1980	31.76	1	54.66	1	96.03	1	99.26	1	146.28	1
1981	48.66	1	116.38	1	124.88	1	137.78	1	187.12	1
1982	73.90	2	156.37	2	174.58	2	195.85	1	247.30	1
1983	111.02	5	249.66	10	319.84	10	364.15	10	561.61	15
1984	108.83	5	205.92	5	251.41	5	283.37	4	315.23	2
1985	51.17	1	90.51	1	110.19	1	143.62	1	305.57	2
1986	86.02	2	163.40	3	230.33	4	277.80	4	341.48	3
1987	69.40	1	99.59	1	141.57	1	183.39	1	300.38	2
1988	110.85	5	240.12	10	261.86	5	275.51	4	389.51	4
1989	20.22	1	35.18	1	50.76	1	69.79	1	112.09	1
1990	72.38	1	122.30	1	135.45	1	181.70	1	247.70	1
1991	71.88	1	151.41	2	214.95	3	241.28	3	276.12	1
1992	76.86	2	130.70	1	155.75	1	180.74	1	269.07	1
1993	118.15	5	246.80	10	292.85	5	378.61	10	478.32	5
1994	65.38	1	129.26	1	207.35	2	264.63	3	440.48	5
1995	53.71	1	117.94	1	132.13	1	177.20	1	231.23	1
1996	51.78	1	112.39	1	152.52	1	165.92	1	236.05	1
1997	61.07	1	114.80	1	160.13	1	168.93	1	246.94	1
1998	63.96	1	156.33	2	266.33	5	308.25	5	354.44	3
1999	51.40	1	116.26	1	212.27	3	289.13	5	352.88	3
2000	86.20	2	124.02	1	148.48	1	171.11	1	238.56	1
2001	116.52	5	123.63	1	156.03	1	179.82	1	309.72	2
2002	37.29	1	63.49	1	110.78	1	144.87	1	221.53	1
2003	100.90	4	142.90	2	213.98	3	253.41	3	358.97	3
2004	108.65	5	230.78	5	279.70	5	298.32	5	362.55	3
2005	89.89	3	134.10	2	175.42	2	189.17	1	273.34	1
2006	97.68	3	180.90	4	225.30	3	232.01	2	251.58	1
2007	131.96	15	217.38	5	297.53	10	385.71	10	614.99	20
2008	79.29	2	128.79	1	164.78	1	214.28	2	354.95	3
2009	107.24	5	239.56	10	268.19	5	305.08	5	387.06	4
2010	65.13	1	132.23	1	156.56	1	178.26	1	263.65	1
2011	131.51	15	235.90	5	286.72	5	337.22	5	404.74	5
2012	117.80	5	183.22	3	232.57	4	273.31	4	410.58	5
2013	104.23	5	247.76	10	266.50	5	286.72	4	449.90	5
2014	169.46	80	397.61	130	507.85	200	640.38	200	1024.64	240

5.3.5.4 Frequency analysis for future prediction

The most commonly used in the frequency analysis of extreme events is the family of the extreme value distribution (Takara and Tosa, 1999). From the analysis in previous sub-chapter, the probability distribution used for modelling extreme events decided as distribution of Generalized Extreme Value (GEV). The results in goodness of fit tests show the better agreement to GEV than Gumbel. For the decision of maximum precipitation decided based on the empirical study result in Chapter 4 where the maximum 14-days bring the highest correlated to the downstream discharge. Also, the goodness of fit explained better result compared to others. Table 5.5 shows the estimation of rainfall in different return periods with catchment scale. The estimation of rainfall was included 2014 events. The predicted rainfall will be used in the next chapter for flood hazard map development.

Table 5.5 Rainfall prediction used for flood hazard map.

Non-exc prob	Return period	Gen. Extreme Value (GEV)				
		1-day	3-days	5-days	7-days	14-days
0.5	2	73.30	133.45	173.68	200.94	281.90
0.8	5	103.03	194.59	247.28	288.31	401.08
0.9	10	121.42	236.77	296.95	350.14	492.05
0.95	20	138.16	278.54	345.30	412.62	589.60
0.98	50	158.57	334.61	408.95	498.38	732.75
0.99	100	173.00	378.14	457.44	566.45	854.10
0.995	200	186.67	422.85	506.44	637.71	988.48

5.3 TREND ANALYSIS

5.3.1 Mann-Kendall (MK) Trend

MK is a non-parametric statistical procedure used to test for trends in time series data (Yu et al., 1993). The method MK1 was developed by Mann (1945) and later improved by Kendall (1975). However, MK1 assumes there is no serial correlation among observations, which has great effects on the variance of the test statistics (Yue et al., 2002; Hamed and Rao, 1998; Hamed, 2009; Tabari and Talaee, 2011). There are a lot of authors suggested

additional treatments for autocorrelation in MK analysis. With the consideration of all significant autocorrelation, a modified MK test had developed by Hamed and Rao (1998) which is MK3. The MK1 and MK3 were applied in this study in order to calculate the trend values for precipitation. MK1 and MK3 were selected is because MK2 (Yue et al., 2002) that improved with Trend-free Pre-whitening (TFPW) produce is not sufficient to remove the effects of serial correlation in the data series (Hu et al., 2017; Fathian et al., 2016).

The null hypothesis, H_0 that been stated as independent and random distribution sample data is tested by MK 1 test, i.e. there is no trend or serial correlation structure in the time-series (Hamed and Rao, 1998). For independent and randomly ordered data in a time-series x_i $\{x_i, i = 1, 2, \ldots, n\}$, the null hypothesis H_0 is tested on the observations xi against the alternative hypothesis H_1, where there is an increasing or decreasing monotonic trend (Yu et al., 1993). According to the condition of $n \geq 10$, the variance S, $Var\ (S)$ is described according to equation (5.16) below:

$$Var(S) = \frac{n(n-1)(2n+5) - \sum_m m(m-1)(2m+5)}{18} \tag{5.16}$$

where S has a normal distribution under H_0; n is the analyzed time series; m is the extent of any give tie; x is the observation values to be compared.

The statistical S test is given as follows:

$$S = \sum_{i=1}^{n-1} \sum_{t=i+1}^{n} \mathrm{sgn}(x_t - x_i) \tag{5.17}$$

$$\mathrm{sgn}(\phi) = \begin{cases} 1 & if\ \phi > 0 \\ 0 & if\ \phi = 0 \\ -1 & if\ \phi < 0 \end{cases} \tag{5.18}$$

where x is the observation values to be compared and $\phi = x_t - x_i$; sgn is the directional information (+1 if value > 0; 0 if value = 0; and -1 if value < 0).

The normal approximation Z test by using the statistical value S and the variance value Var(S) are written in the following form:

$$Z = \begin{cases} \dfrac{S-1}{\sqrt{Var(S)}} & if \quad S > 0 \\ 0 & if \quad S = 0 \\ \dfrac{S+1}{\sqrt{Var(S)}} & if \quad S < 0 \end{cases} \tag{5.19}$$

The presence of a statistically significant trend is evaluated using the Z value. A positive (negative) value of Z indicates an upward (downward) trend. The statistic Z has a normal distribution. To test for either an upward or downward monotone trend (a two-tailed test) at α level of significance, H_0 is rejected if the absolute value of Z is greater than $Z_{1-p/2}$, where $Z_{1-p/2}$ is obtained from the standard normal cumulative distribution table (Table 5.6).

Table 5.6 Standard normal cumulative distribution table.

p	0.0002	0.002	0.01	0.02	0.05	0.1	0.2	0.3	0.5	0.8	1
$1 - p/2$	0.9999	0.999	0.995	0.990	0.975	0.95	0.90	0.85	0.75	0.60	0.50
$Z_{1-p/2}$	3.72	3.090	2.576	2.326	1.960	1.645	1.282	1.04	0.67	0.25	0.00

Refer to Hu et al., 2017 and Kumar et al., 2009, the calculation of MK3 is used when there is significant autocorrelation in the dataset. Autocorrelation coefficient, R_k is calculated by using the Equation (5.20) with (k=1).

$$R_k = \frac{\dfrac{1}{n-k}\sum_{i=1}^{n-k}\left(x_i - \bar{x}\right)\left(x_{i+k} - \bar{x}\right)}{\dfrac{1}{n}\sum_{i=1}^{n}\left(x_i - \bar{x}\right)^2} \tag{5.20}$$

Refer to Kumar et al., 2009 stated that, the data are assumed to be serially independent at 10% significant level and no pre-whitening is required when the R_k is with the range $\frac{-1-1.645\sqrt{n-2}}{n-2} \le R_k \le \frac{-1+1.645\sqrt{n-2}}{n-2}$. Else the data are serially correlated and pre-whitening is required before applying the MK test.

The modified variance *S, Var(S)** that proposed by Hamed and Rao (1998) is used for calculating the MK3 *Z* value.

$$Var(S)^* = Var(S) \times \left(1 + \frac{2}{n(n-1)(n-2)} \sum_{i=1}^{n-1} (n-1)(n-i-1)(n-i-2) R_k \right) \quad (5.21)$$

where R_k is the lag-*k* significant autocorrelation coefficient of rank *k* of time series.

5.3.2 Sen's Slope

The Mann-Kendall test only provides increase or decrease trends indicated by the positive and negative values of *S*, the magnitude of the trend (change per unit time) was computed using Sen's Slope procedure (Sen, 1968). The Sen's slope method, used to estimate the magnitude of change, requires a time-series of equally spaced data (Changnon and Demissie, 1996; Burn and Hag Elnur, 2002; Salmi, 2002). Normality was also examined using skewness, kurtosis and Anderson–Darling statistics. The slope *Q* is defined as:

$$Q = median\left[\frac{x_j - x_k}{j-k} \right], \; for \quad all \; k < j \quad (5.22)$$

where x_j and x_k are the data values at time *j* and *k*; *j* is the time after time *k*. A positive value of slope *Q* indicates an increase trend while a negative value indicates a decrease trend.

5.3.3 Results and Discussions

The observed precipitation data for the period 1970-2014 were used as inputs of the two types of MK analysis, which were described in the previous sub-chapter, the MK1 and MK3. The reason to use of these two types of MK analysis was to increase the level of confidence in increasing/decreasing trend of precipitation level. As such, if the two analyses are in agreement, the likelihood of decreasing/increasing trend in the station is higher. The trend analysis was conducted for total annual precipitation, maximum precipitation (max 1 day, max 3 days, max 5 days, max 7 days, max 14 days), and seasonal precipitation (wet monsoon season from October to March and dry monsoon season from April to September). The precipitation values of the 17 meteorological stations were interpolated by Thiessen Polygon method in GIS software. The trend values of all stations were plotted on a spatial map with red/blue dots with different sizes (Figure 5.2-5.4). Red color indicates increasing trend and blue color indicates decreasing trend. The size of the dots indicates the Z value of increasing/decreasing trend and its confident level. The trend values were classified into 3 levels: S (Small), M (Middle), and L (Large). The small dots represent Z value of 0 to |1.96| with confidence level of $p > 0.05$, the middle dots represent Z value of >|1.96| to |2.576| with confidence level of $0.01 < p \leq 0.05$ and finally the large dots represent Z value of more than |2.576| with confidence level of $p \leq 0.01$. The plus (+) or (-) sign of the Z values represent increasing and decreasing trend respectively with color indicator, red and blue, for better visualization. The rain gauge stations located at southern part of catchment known as the upstream area, northern part is downstream area. There are seven rain gauges located at the upstream area and six rain gauges located at the downstream area.

The results of trend identification in rainfall gauge stations are shown in Table 5.7. The calculation using MK1 and MK3 methods gave good agreement in increasing and decreasing trends in almost all stations. Disagreements of results were seen in Kota Bharu Station for max 3, 5, 7, and 14-days calculations, in Kg. Jeli Station for max 1-day and 14-days calculations, and in Ulu Sekor Station for max 7-days calculation. The Z value calculated for these three stations in the precipitation calculations showed small Z value with confidence level of p=0.05. The calculation using MK3 method resulting smaller Z values than using MK1 method, particularly in Total Annual Precipitation and Wet Monsoon Season calculations. In the maximum precipitation calculations, although both

methods showed good agreement in decreasing/increasing trends, the magnitude of trends varies both in terms of stations and precipitation calculations. As an example, for max 1-day calculation, 5 stations gave smaller results in MK1 calculation and 5 stations gave smaller results in MK3 calculation, and 7 other stations showed agreement. The other maximum precipitation calculation showed more or less the same results. Calculation using MK1 and MK3 methods showed best agreement in the calculation of dry monsoon season with only 4 number of stations difference (in magnitude).

Table 5.7 Z value in MK1, MK3, Sen's Slope.

Station	Annual Total			Max daily			Max 3-days		
	MK1	MK3	Sen's Slope	MK1	MK3	Sen's Slope	MK1	MK3	Sen's Slope
Brook	1.63	1.34	19.55	2.15	1.81	0.53	1.74	1.79	0.91
Blau	1.57	1.71	16.37	1.55	2.17	0.82	1.77	2.91	0.75
Upper Chiku	3.20	2.07	53.44	4.02	1.98	1.39	4.39	2.42	2.53
Gunung Gagau	2.53	1.70	68.24	2.52	2.19	4.71	2.94	2.20	9.61
Gua Musang	1.49	1.98	6.99	0.16	0.24	0.05	-0.59	-1.19	-0.19
Kg. Aring	3.02	2.55	16.86	1.46	2.20	0.94	2.37	2.82	2.79
Balai Polis Bertam	2.53	1.78	19.32	0.73	0.84	0.31	2.04	2.09	1.14
GOB	3.92	2.00	61.05	3.34	2.28	1.84	3.12	2.47	2.83
Kg. Laloh	1.94	1.64	11.69	0.28	0.44	0.12	0.82	1.76	0.67
Dabong	1.41	1.46	12.89	1.93	2.71	1.14	1.25	1.90	1.45
Ulu Sekor	3.81	2.12	54.87	3.38	2.18	2.93	3.53	2.69	5.02
Kg. Jeli	1.29	1.91	14.31	-0.53	-0.58	0.05	0.10	0.14	1.30
Kg. Durian Daun	2.60	1.95	34.71	1.78	1.99	2.35	1.38	1.75	4.23
JPS Machang	2.74	1.69	28.04	2.65	1.87	3.42	2.63	1.62	6.45
Bendang Nyior	2.73	1.89	40.55	3.75	2.31	6.46	2.98	1.90	9.87
Rantau Panjang	3.61	1.99	39.27	1.98	2.07	1.74	2.55	2.56	4.08
Kota Bharu	-0.68	-0.63	-4.80	-1.03	-0.64	-0.82	-0.61	-0.42	0.16

Station	Max 5-days			Max 7-days			Max 14-days		
	MK1	MK3	Sen's Slope	MK1	MK3	Sen's Slope	MK1	MK3	Sen's Slope
Brook	2.34	1.94	1.79	1.78	1.56	1.55	1.91	1.80	2.46
Blau	1.83	2.62	1.03	1.70	2.57	1.29	1.04	1.58	1.30
Upper Chiku	4.18	2.31	2.40	4.23	2.30	2.11	4.10	2.22	3.34
Gunung Gagau	2.94	2.25	11.20	2.82	2.26	11.62	2.40	2.02	15.44
Gua Musang	-0.37	-0.81	-0.18	0.33	0.71	0.18	-0.64	-1.33	-0.63
Kg. Aring	1.99	2.39	3.09	2.11	2.67	3.00	1.19	1.93	2.28
Balai Polis Bertam	1.77	1.75	1.27	1.52	1.49	1.26	2.13	1.84	2.15
GOB	2.56	2.02	3.02	2.44	2.00	3.66	2.56	2.12	4.88
Kg. Laloh	0.31	0.72	0.46	0.27	0.58	0.41	0.33	0.70	0.54
Dabong	1.08	1.78	1.57	0.87	1.47	1.10	0.60	0.87	1.39
Ulu Sekor	3.22	2.35	5.86	3.32	2.37	6.68	3.19	2.71	7.99
Kg. Jeli	0.26	0.41	1.60	0.36	0.62	2.15	-0.12	-0.17	1.95
Kg. Durian Daun	1.76	2.22	4.29	2.06	2.36	5.66	1.91	2.07	7.35
JPS Machang	2.63	1.61	7.59	2.81	1.75	8.44	2.61	1.60	10.28
Bendang Nyior	3.44	2.31	10.31	3.18	2.17	10.05	2.73	2.37	11.51
Rantau Panjang	2.60	2.47	4.67	2.87	2.50	5.09	2.60	2.06	8.92
Kota Bharu	-0.54	-0.35	0.49	-0.42	-0.28	0.81	-0.58	-0.37	0.22

Station	Wet season			Dry season		
	MK1	MK3	Sen's Slope	MK1	MK3	Sen's Slope
Brook	1.53	1.57	1.53	2.20	1.82	2.2
Blau	1.04	0.99	1.04	1.63	2.24	1.63
Upper Chiku	3.06	1.97	3.06	2.36	1.95	2.36
Gunung Gagau	2.03	1.63	2.03	1.96	1.56	1.96
Gua Musang	2.54	2.29	2.54	0.46	1.10	0.46
Kg. Aring	3.56	2.26	3.58	-0.29	-0.48	-0.29
Balai Polis Bertam	2.57	1.89	2.57	1.40	1.22	1.4
GOB	3.89	2.13	3.89	3.28	1.74	3.28
Kg. Laloh	2.09	1.72	2.09	0.48	0.66	0.48
Dabong	1.95	1.77	1.95	-0.30	-0.47	-0.3
Ulu Sekor	3.39	2.08	3.39	3.47	2.06	3.47
Kg. Jeli	1.56	2.01	1.56	-0.17	-0.25	-0.17
Kg. Durian Daun	3.28	2.46	3.28	1.10	1.07	1.1
JPS Machang	3.02	1.79	3.29	0.92	1.11	0.92
Bendang Nyior	3.38	1.95	3.38	0.97	1.29	0.97
Rantau Panjang	4.12	2.13	4.12	1.65	1.62	1.65
Kota Bharu	-0.27	-0.25	-0.27	-1.29	-1.34	-1.29

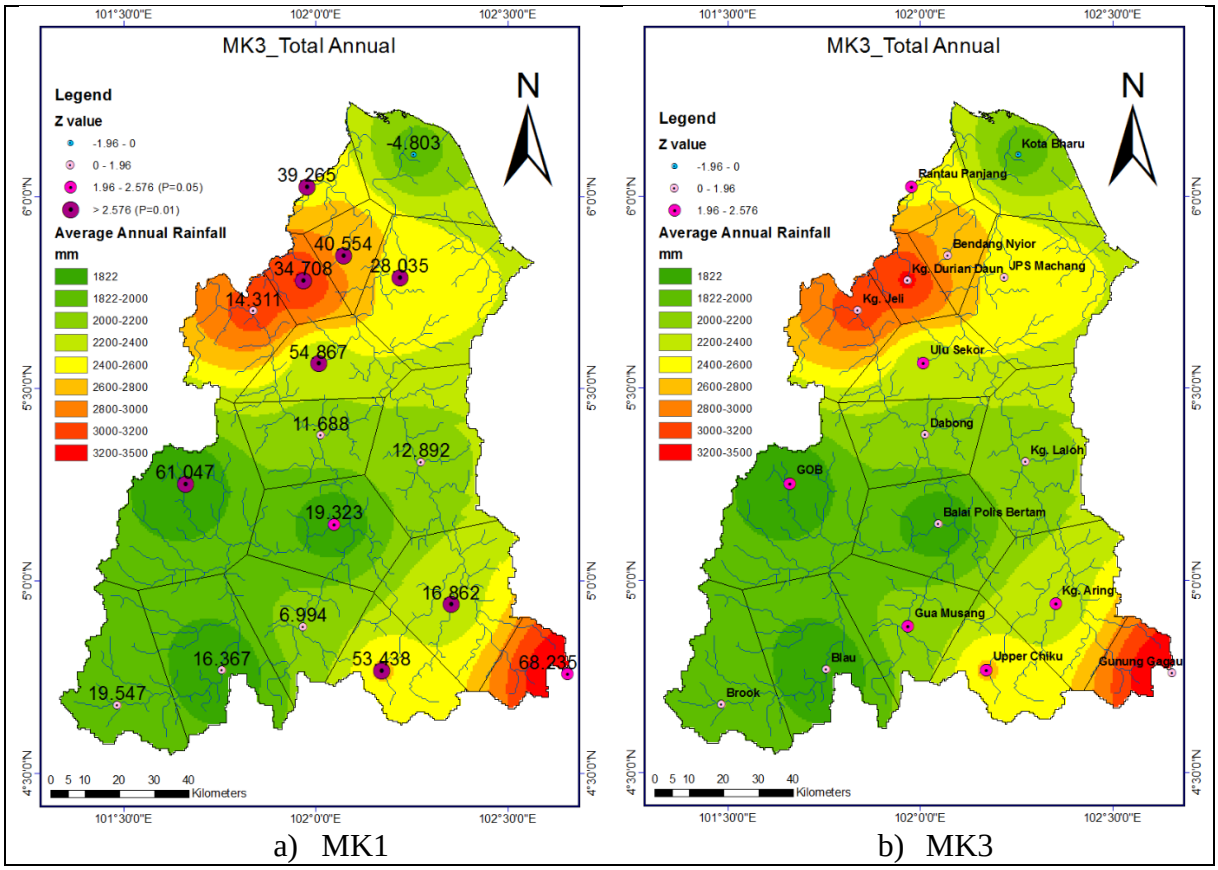

a) MK1 b) MK3

Figure 5.2 Total annual precipitation Kelantan.

Figure 5.2 shows the distribution map of historical average total annual precipitation and the spatial map of long term for MK1 and MK3 trend of total annual precipitation in Kelantan. Significant increasing trends in annual total precipitation calculations were detected in 16 out of 17 rain stations using both MK1 and MK3 methods with at least p =0.05 confidence level and Z value ≥ 1.96. The increasing statistical values of Z for total annual precipitation were from 1.29 to 3.92 by using MK1 and from 1.34 to 2.55 by using MK3 for the 16 stations. The only station with decreasing trend is the Kota Bharu station, with Z value of -0.68 by MK1 and -0.63 by MK3. The Sen's Slope values increased from 6.994 to 68.235 for 16 rain gauge station except Kota Bharu station showed -4.8 Sen's Slope value. From the Sen's slope, it shows that GOB, Ulu Sekor, Kg. Daurian Daun, Bendang Nyior, Rumah Kastam, JPS Machang and Gunung Gagau show high magnitude of increase in annual total, which are 61.047, 54.867, 34.708, 40.504, 39.265, 28.035 and 68.235. From the figure, it shows that the total annual precipitation with increasing trend average distributed at the catchment and provide a good agreement on MK1 and MK3. Figure shows the rain gauges located at upstream with increasing trend will be high risk of debris flow as the average annual rainfall was high at the region too. Also, at the

downstream area the average annual rainfall is high as the trend analysis also show increasing trend. Therefore, extra consideration needed.

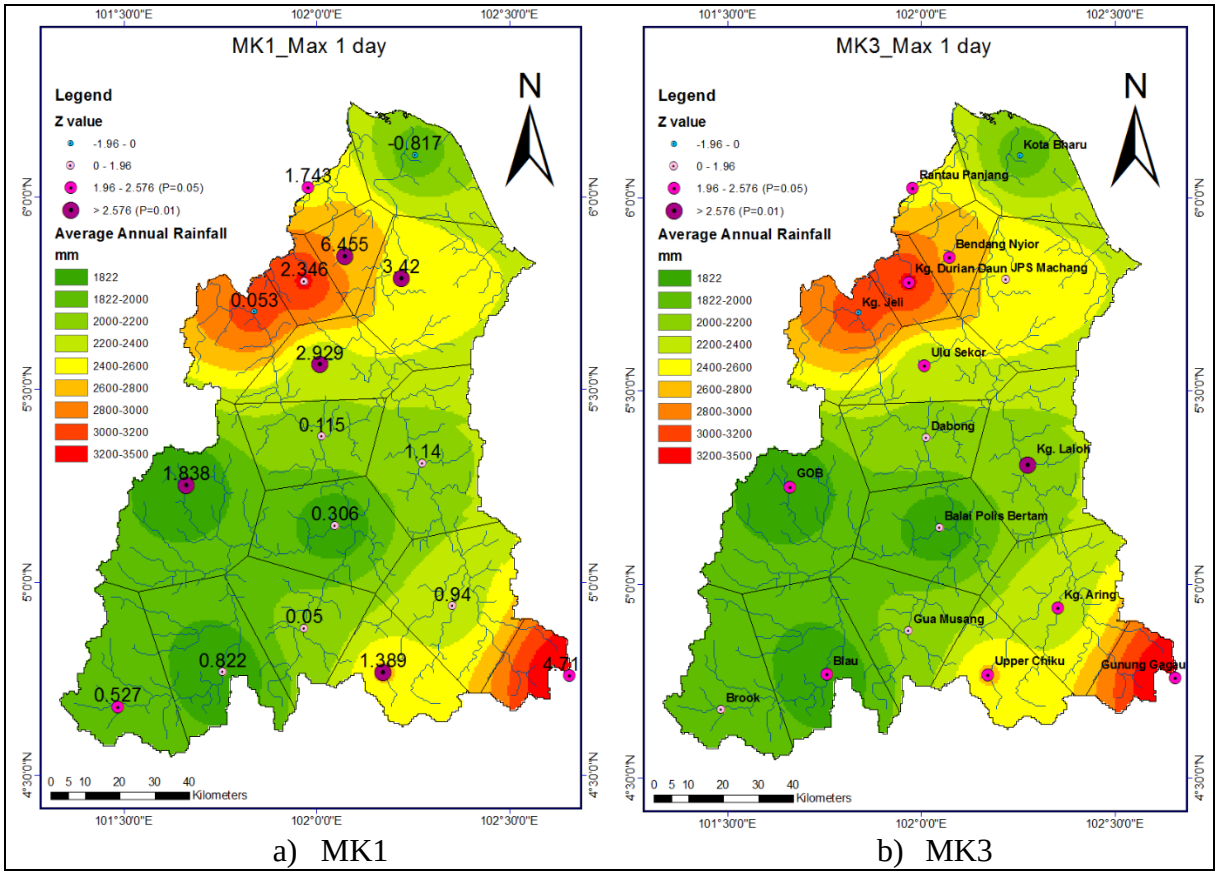

a) MK1 b) MK3

Figure 5.3 Max 1-day precipitation Kelantan.

Figure 5.3 shows the spatial map of annual maximum 1-day precipitation for MK1 and MK3 in Kelantan. From the figure, it shows that the annual daily maximum precipitation with increasing trend average distributed at the catchment. The increasing trend show high significant at the upstream stations (GOB, Brook, Gunung Gagau) and downstream station (Ulu Sekor, JPS Machang, Bendang Nyior, Rumah Kastam) by using MK1. There was slightly decrease in the Mann-Kendall statistic value Z by MK3. The Sen's slope highest at Bendang Nyior with value 6.455, followed by Gunung Gagau 4.71 with the significant level 95%. For Station GOB, Ulu Sekor, Kg. Durian Daun and Rumah Kastam show increase trend with the sen's slope value 1.838, 2.929, 2.346 and 1.743 at significant level 99%.

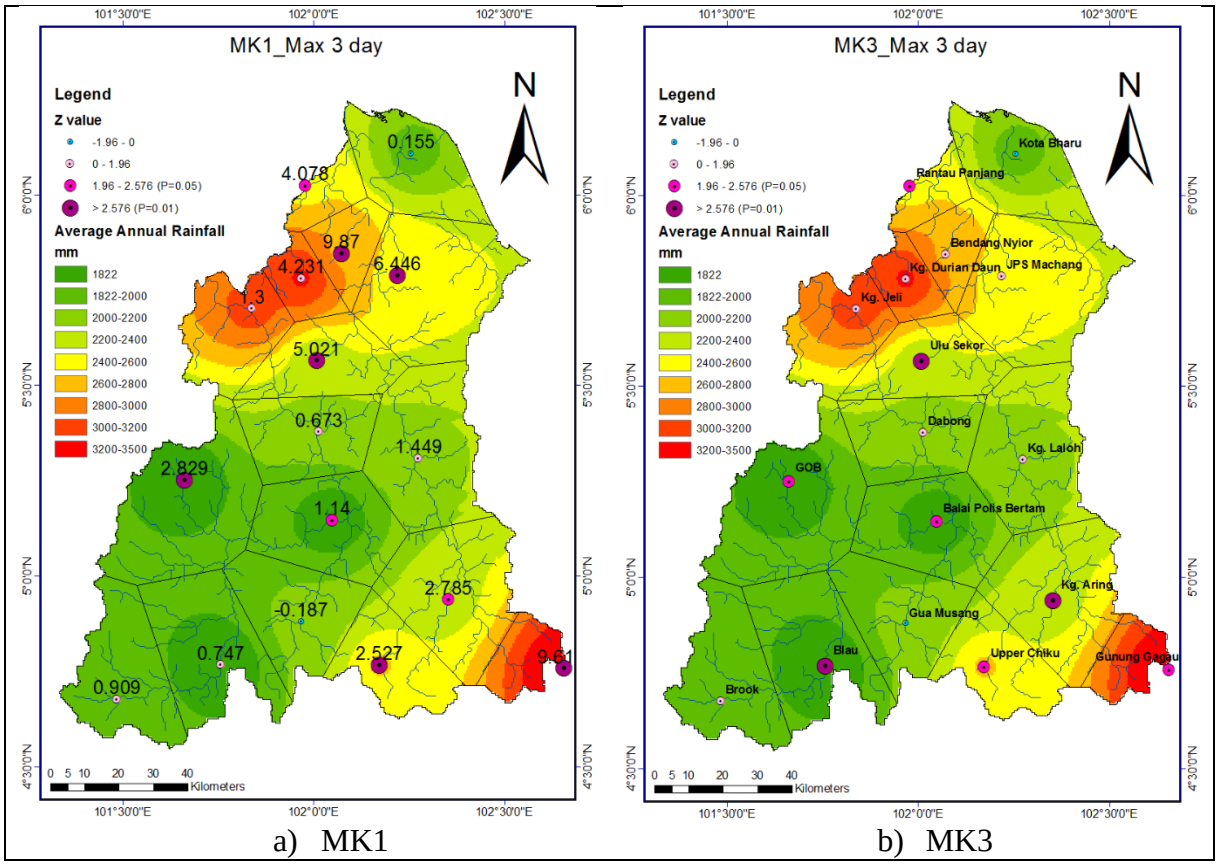

a) MK1 b) MK3

Figure 5.4 Max 3-day precipitation Kelantan

Figure 5.4 shows the spatial map of annual 3-day maximum precipitation trend analysis. From the figure, it shows that the annual 3-day maximum precipitation with increasing trend average distributed at the catchment except the Gua Musang Station is decreasing trend. The increasing trend show high significant at the upstream stations (Blau, GOB, Balai Polis Bertam, Upper Chiku, Kg. Aring, Gunung Gagau) by using MK1 and MK3. The Sen's slope value for the increasing trend is 0.747, 2.829, 1.14, 2.527, 2.785 and 9.61. Moreover, the downstream station (Ulu Sekor, JPS Machang, Bendang Nyior, Rumah Kastam) show the increasing trend by MK1 and MK3 at significant level 95% with the magnitude 5.021, 6.446, 9.87 and 4.078. The statistical values of *Z* for annual 3-day maximum precipitation were from -0.59 to 3.12 by using MK1 and from -1.185 to 2.91 by using MK3.

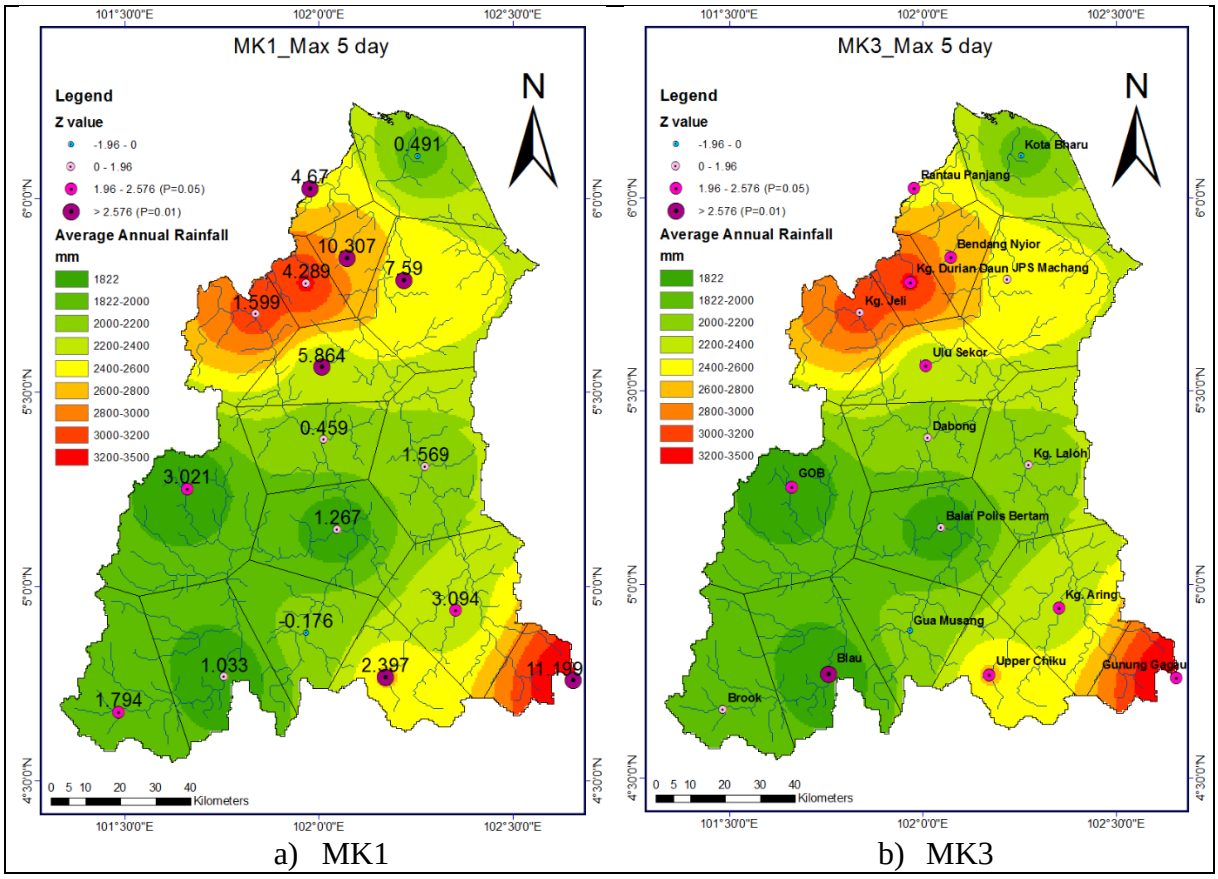

a) MK1 b) MK3

Figure 5.5 Max 5-day precipitation Kelantan.

Figure 5.5 shows the spatial map of annual 5-day maximum precipitation trend analysis. The statistical values of Z for annual 5-day maximum precipitation were from -0.37 to 3.44 by using MK1 and from -0.806 to 2.617 by using MK3. From the figure, it shows that the annual 5-day maximum precipitation with increasing trend average distributed at the catchment. However, Gua Musang station shows decreasing trend. The increasing trend show high Sen's slope value of 11.199 at the Gunung Gagau with significant level 99%. Besides, at the downstream station (Bendang Nyior) shows high significant level of increasing with the Sen's slope 10.307. Also, Ulu Sekor and Rumah Kastam are show increasing trend by MK1 and MK3 too.

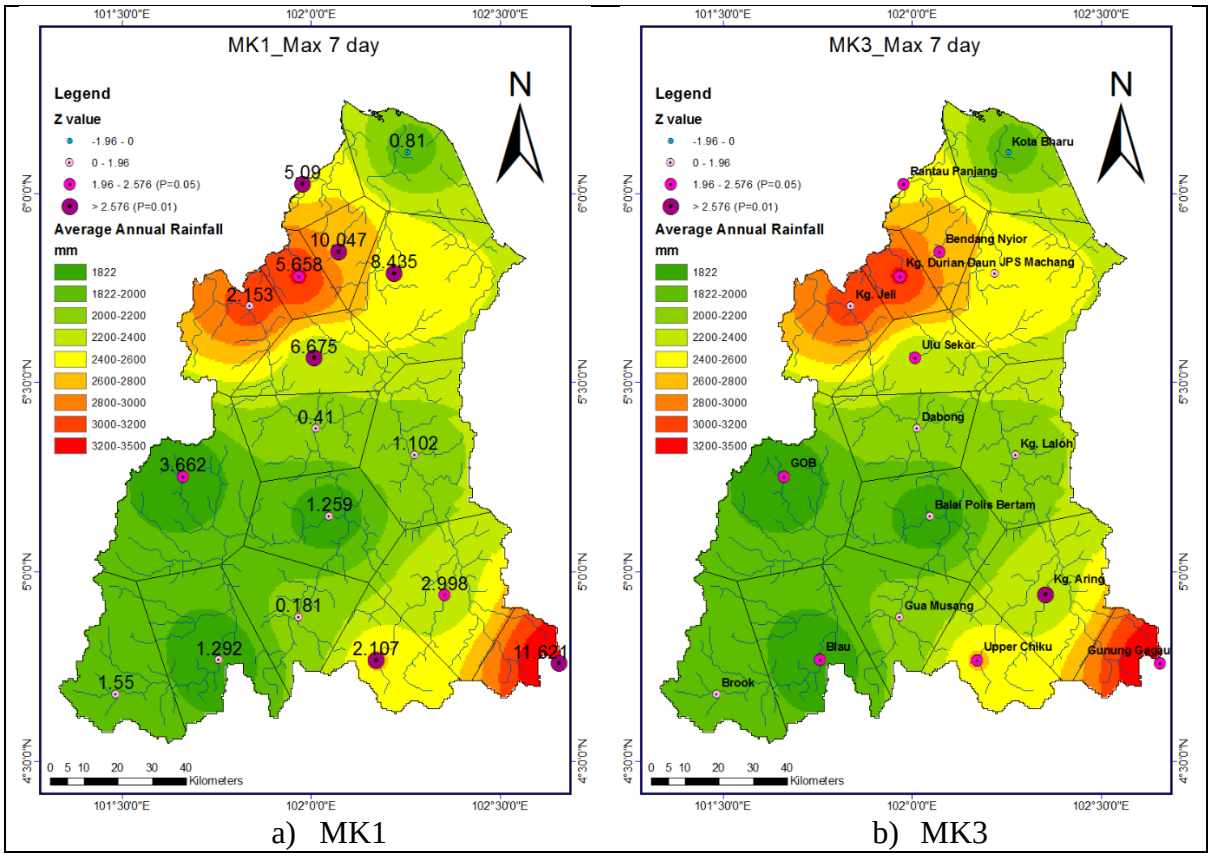

a) MK1 b) MK3

Figure 5.6 Max 7-day precipitation Kelantan.

Figure 5.6 shows the spatial map of annual 7-day maximum precipitation trend analysis. From the figure, it shows that the annual 7-day maximum precipitation with average increasing trend over the catchment. There are upstream stations (GOB, Kg. Aring, Gunung Gagau) and downstream station (Ulu Sekor, Kg. Durian Daun, JPS Machang, Bendang Nyior, Rumah Kastam) that shows high significantly increase by using MK1. However, MK3 only shows agreement to few station which are Gunung Gagau, Kg. Aring, GOB, Ulu Sekor, Kg. Durian Daun, Bendang Nyior and Rumah Kastam. The statistical values of Z for annual 7-days maximum precipitation were from 0.33 to 3.18 by using MK1 and from -0.276 to 2.671 by using MK3. By using MK3, there are 9 stations shows good agreement with significant level p=0.01 (Z=2.576) and 7 stations shows increasing trend at the significant level 95%. The highest sen's slope value goes to Gunung Gagau with 11.624, and followed by Bendang Nyior 10.047. Sen's slope value for most downstream is high compared to upstream. There are four downstream stations display Sen's slope value higher than 5.

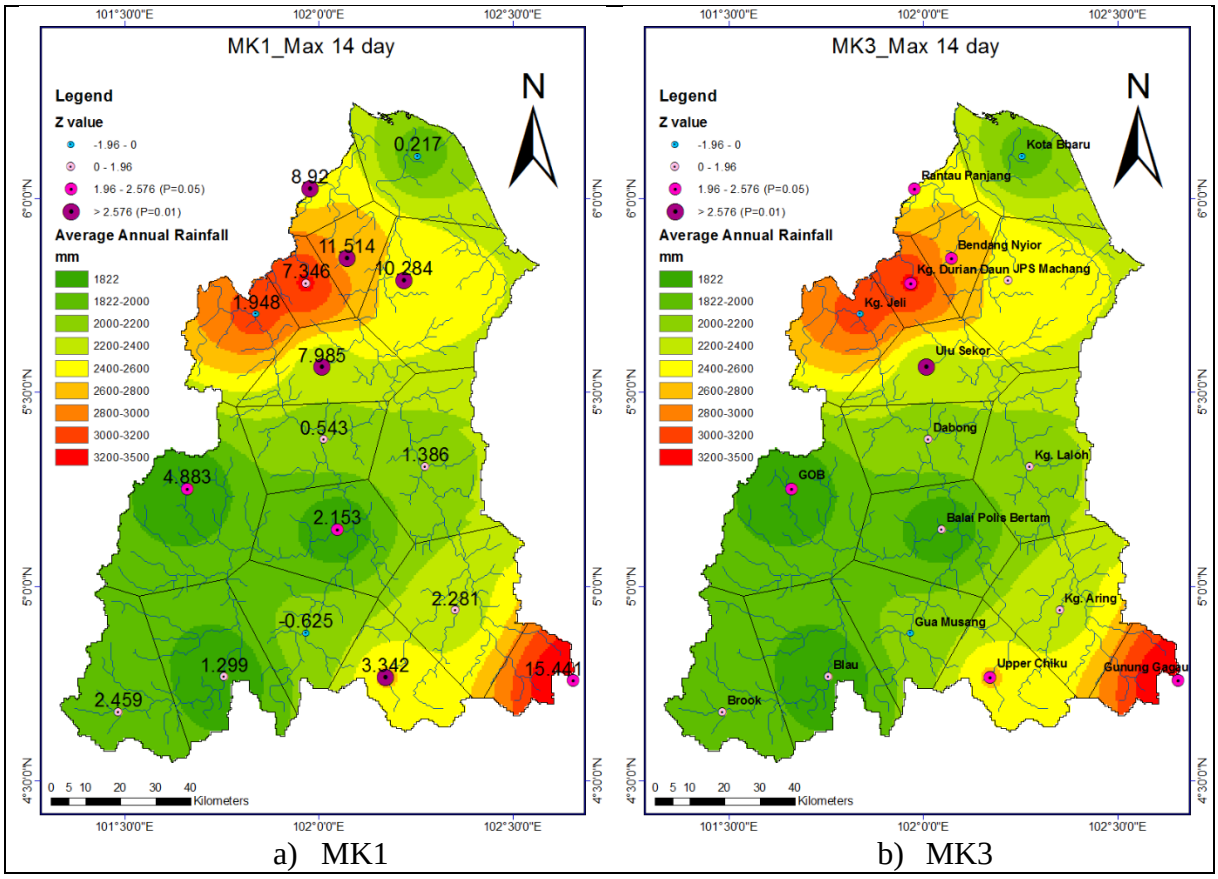

a) MK1 b) MK3

Figure 5.7 Max 14-day precipitation Kelantan.

Figure 5.7 shows the spatial map of annual 14-day maximum precipitation trend analysis. The statistical values of Z for annual 14-day maximum precipitation were from -0.64 to 2.73 by using MK1 and from -1.332 to 2.708 by using MK3. From the figure, it shows that the annual 14-days maximum precipitation with increasing trend average distributed at the catchment except Gua Musang station. The increasing trend show high significant level 99% by MK1 and MK3 at the upstream stations (GOB and Gunung Gagau) with sen's slope value of 4.883 and 15.441; downstream station (Ulu Sekor, Bendang Nyior, Rumah Kastam) with sen's slope value 7.985, 11.514 and 8.92. For station Upper Chiku and Kg. Durian Daun, MK3 shows high significant level than MK1 which is 95% to 99%. However, Kg. Jeli and Kota Bharu show decreasing trend by MK3 with magnitude 1.948 and 0.217.

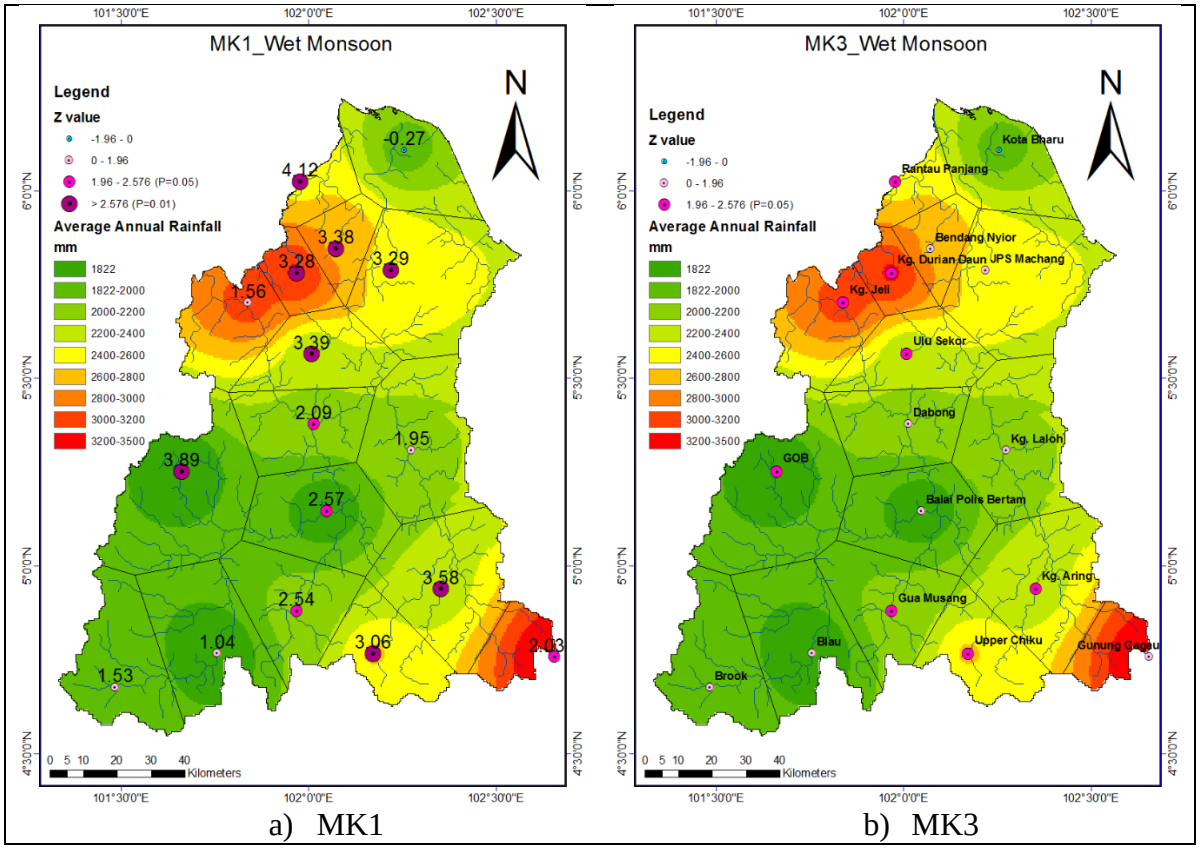

a) MK1 b) MK3

Figure 5.8 Wet monsoon season precipitation Kelantan.

Figure 5.8 shows the spatial map of wet season in Kelantan catchment. In MK1, 12 rain stations show high increasing trend in the catchment with the significant level of p=0.01; 3 rain station increase with p=0.05. However, there are only 7 stations out of 12 stations in MK3 show significant level 99% and 8 stations in MK3 with significant level 95%. MK3 shows low statistic value Z compared to MK1. The statistical values of Z for wet season were from -0.27 to 4.12 by using MK1 and from -0.25 to 2.458 by using MK3. Kg. Jeli station shows increase trend with magnitude of 1.56 at p=0.05 (MK1) to p=0.01 (MK3). The sen's slope for wet season show the high increasing along the river channel from upstream to downstream with the value 1.04 to 4.12. The increasing trend is high significant and correlated to the average annual rainfall intensity. The upstream of high average annual rainfall that with increasing trend will bring high flood risk to the downstream. Besides, for the downstream area, rain gauges (Ulu Sekor, Kg. Jeli, Kg. Durian Daun and Rumah Kastam) also located in the high average annual rainfall region. The risk of flood to occur will increase due to the trend increase and high average annual rainfall.

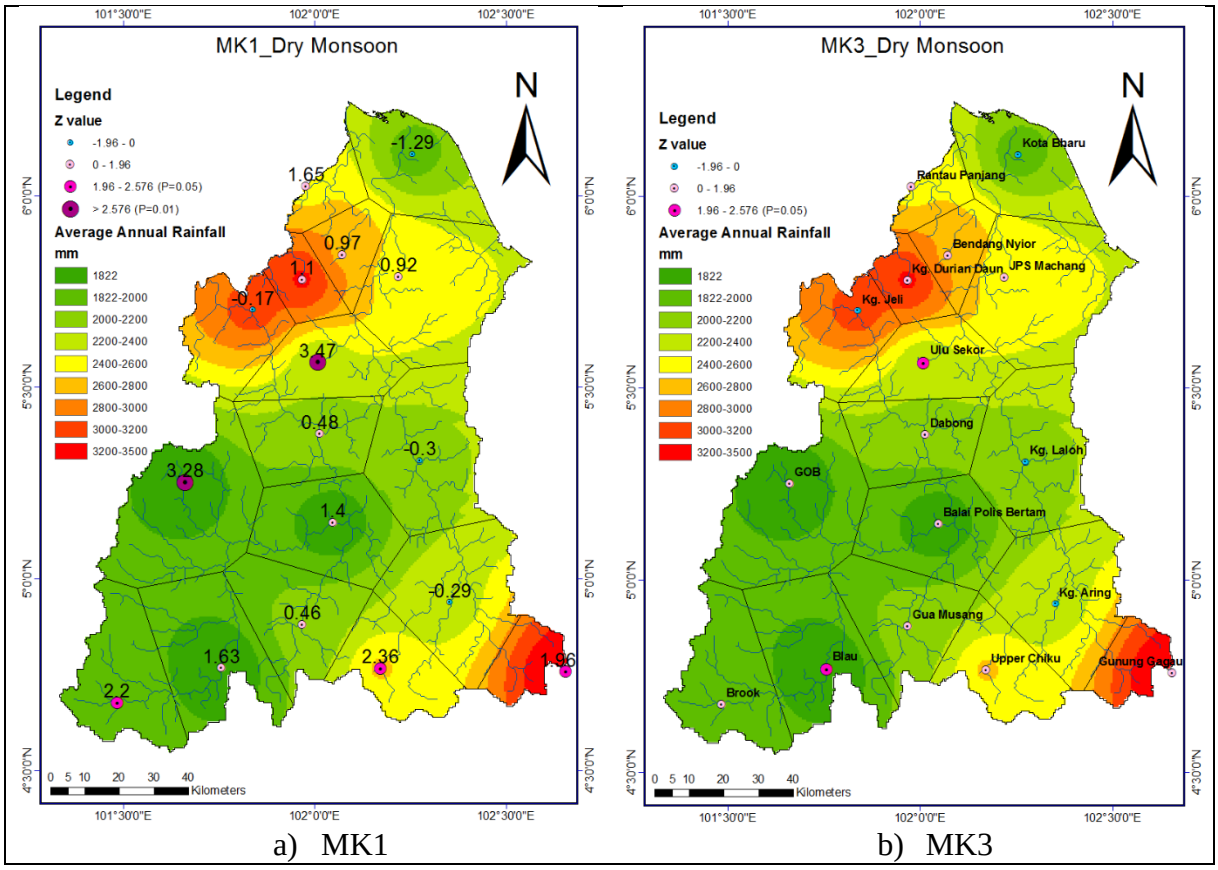

a) MK1 b) MK3

Figure 5.9 Dry monsoon season precipitation Kelantan.

Figure 5.9 shows the spatial map of dry season in Kelantan catchment. In MK1, 5 rain stations show high increasing trend in the catchment with the significant level of p=0.01; 8 rain station increase with p=0.05 and 4 rain stations shows decreasing trend. However, in MK3 only 2 stations increase at p=0.01, 11 stations increase at p=0.05 and 4 stations show decreasing trend with sen's slope value -1.29 to -0.17. Sen's slope value increase with magnitude from 0.46 to 3.28. The statistical values of Z for wet season were from -1.29 to 3.47 by using MK1 and from -1.34 to 2.242 by using MK3. MK3 shows low statistic value Z compared to MK1. For the upstream rain stations (GOB, Gunung Gagau, Brook, Upper Chiku) may need to be aware as the increasing trend in dry season may cause unwanted hazards to the catchment.

5.4 SUMMARY

In this chapter, frequency analysis and two types of non-parametric Mann-Kendall test were applied to characterize the causes of precipitation variability in Kelantan during 1970-2014. We would like to understand the probability of flood occurrence in the catchment and also the latest precipitation trends in the region. In addition, the change per year year (magnitude of slope) was quantified by using linear regression coefficient or Sen's slope estimator based on their distributions and records integrity.

Major conclusions can be summarized as follows:

(i) In the frequency analysis, station scale shows that 2014 flood event is an extreme event among historical records. There are two stations receive rainfall for 500-year ARI such as GOB (max 3-day) and Brook (max 5-day). Besides, station Balai Polis Bertam receive 150-year ARI at max daily rainfall.

(ii) In the frequency analysis, catchment scale shows that 2014 flood event is an extreme event among historical records with 240-year return period in catchment scale. For max daily rainfall, it is an 80-year return period's event. 200-year return period's event happened at max. 5-day rainfall. During the cumulative 14-days rainfall, the return periods is 240-year.

(iii) 5-year return period's event has increase the frequency after 2010. For the max 1-day rainfall, 15-year ARI in 2011, 5-year ARI for 2012 and 2013. For the events of max. 14-day, start 2011 till 2013 every year is 5-year ARI.

(iv) Precipitation tended to increase across Kelantan during 1970-2014 at both MK1 and MK3 with annual total precipitation, maximum precipitation (max. 1 day, max 3 days, max 5 days, max 7 days, max 14 days) and seasonal.

(v) Station located at upstream (Gunung Gagau, Upper Chiku, Brook and Blau) tends to bring more precipitation from analysis results. The trend increase will increase more surface flow if the land use change not well preserved. The increasing of surface flow may trigger more debris flow from upstream to downstream.

(vi) GOB station is located at the upstream with increasing trend of precipitation at annual, maximum precipitation and seasonal. However, the average annual rainfall at GOB was the lowest at the catchment, therefore increasing trend of precipitation will provide more water to the area. However, it may need more attention to be

given for the awareness preparedness because it is rare to receive heavy rainfall.

(vii) Station located at downstream (Ulu Sekor, Jps Machang, Bendang Nyior, Rumah Kastam and Kg. Durian Daun) show increasing trend for annual, maximum and seasonal precipitation. Downstream station with increase trend tends to cause severe flood and big flood extent. These can be high risk area for future development. Therefore, future concerns need to be consider by the policy maker.

(viii) MK3 used to increase the confidential level of the precipitation trend. From the analysis, it shows that MK1 has good agreement with MK3.

CHAPTER 6 HAZARD MAPPING

6.1 INTRODUCTION

This chapter presents proposed hazard maps in the Kelantan River Catchment. These maps were developed to give better visualization of inundated areas in floods with 2-year, 5-year, 10-year, 20-year, 50-year, 100-year and 200-year return periods. The maps were developed based on rainfall frequency analysis presented in chapter 5 and simulated with the RRI Model. This chapter also discusses high hazard and low hazard zones in the catchment by referring to the different hazard maps. The functions of the map will be further explained in this chapter.

6.2 Importance of Hazard Mapping

Hazard is defined as threatening event, or the probability of occurrence of a potentially damaging phenomenon within a given time period and area. Hazard refers to the probability of a potentially dangerous phenomenon occurring in a given location within a specified period of time (Alexander, 1993; Alaghmand et al., 2010). Hazard mapping is a visual method of showing local perceptions of areas or people in a community (such as settlements, infrastructure, and resources) that face different levels and types of hazard. The functions of a hazard map are to know the phenomenon and to make it known to residents. Hazard maps can help to decrease the impacts from disasters but cannot stop a disastrous phenomenon.

Flood hazard mapping was first initiated in 1988 in the United States by the Hydrologic Engineering Centre (HEC) of the U.S. Army Corps of Engineers (Smith, 1996; Feldman and Owen, 1997; Alaghmand et al., 2010). The purpose of the study is mainly to produce flood hazard maps for the National Insurance Program (NFIP) due to the reluctance of private insurance industry in providing insurance policies as a result of catastrophic losses (Smith, 1996).

Udono and Sah (2002) informed that there are two types of hazard map which are resident-educating type and administrative information type. Resident educating type is to inform the residents living within the damage forecast area of the risk of danger. The information on areas of danger or places of safety and the basic knowledge on disaster prevention are given to residents. Therefore, it is important that such information is represented in an understandable form. Administrative information type is used as the basic materials that the administrative agencies utilize to provide disaster prevention services. These hazard maps can be used to establish a warning system and the evacuation system, as well as evidence for land use regulations.

The main objectives of flood hazard mapping is to provide residents with the information on the range of possible damage and the disaster prevention activities. Also it can be sorted as follows: to prevent loss of life, to minimize property damage, to minimize social disruption and to encourage coordinated approach for land/water use. The role of flood mapping in river engineering is an important feature in planning and management: basis for managing flood plains, engineering & planning tool, first step in flood plain management, part of legislation for regulating development and basis for pursuing structural and non-structural measures.

6.2.1 Flood Management in Malaysia

After the disastrous flood of 1971, beside the Natural Disaster Relief Committee (1972), the Government has also established the Permanent Flood Control Commission in December 1971 to implement flood control measures to reduce flood occurrence and to minimise flood damage (Islam *et al.*, 2016). This commission is presently chaired by the Minister of Natural Resources and Environment (previously headed by the Minister of Agriculture) and DID acting as the secretariat. Since 1971, the Department of Irrigation and Drainage (DID) has been designated with the task of implementing flood mitigation plans. There are 17 major river basins, and 27 towns had developed in flood mitigation plans.

There are two common approaches to solving flood problem that recognised are structural and non-structural measure. The structural measures include improving river channel sections, the building of flood protection bunds, perimeter bunds, by-pass floodways, use

of former mining ponds for flood attenuation and construction of flood retention dams to regulate flood flows and minimise flood occurrence. Although structural measure plays a significant role in flood hazard management, it is economically not viable to provide the means of total protection against all floods. More to this, it has been observed that application of structural measures may increase vulnerability to the society downstream area. Refer to Andjelkovic, 2001, as the structural measures provide protection against certain magnitude of floods and reduces the frequency of inundation in certain places, the society became less aware with the sense of safety against all types of floods. At the end, when a high magnitude of flood strikes, damages in human lives and properties are unprecedentedly high. This fact showed the importance of non-structural flood mitigation measures.

A lot of flood hazard studies reflect a techno centric approach, which strongly emphasises the use of structural/engineering methods, and to a lesser degree on non-structural methods in solving flood problems (Chan, 1995). However, in the recent years, the complexity of intertwine of natural and anthropological causes of floods requires more accurate calculation which enables engineers to apply flood management measures effectively. As such, interests in the development of the non-structural methods are increasing in the recent years as a complementary measures in supporting decisions in the application of flood management measures. The development of the non-structural methods include a good cooperation among government, community, private sector and NGO's. In the recent years the use of tools such as computer model to quantify the effects of human interference on the river system is increasing. It is important to understand flood behaviour by carrying out thorough analysis before applying any structural measures. Therefore, with such tools, river engineers are able to evaluate the potential impacts of floods and thus, provide recommendations to the implementing agencies for further prevention measures. As the development, non-structural methods are becoming more popular and considering the importance of social factors in flood management, the non-structural methods are further developed to fit the needs of societies, policy makers and decision makers. A sample of non-structural flood protection measures include: source control (watershed/landscape structure management), laws and regulations, zoning, economic instruments, an efficient flood forecast-warning system, a system of flood risk assessment, awareness raising and improving information, flood-related data bases (Kundzewicz, 2002). Looking at recent specific examples of floods, it is clear that more attention should be paid to non-structural

flood protection measures. The importance of non-structural measures is also illustrated by the power of adaptation. Where a flood visits a place twice in a short time period (e.g., on the Rhine in December 1993 and January 1995), losses during the second flood occurrence are typically far lower than during the first occurrence.

Also, according to Levy et al. (2005), the proposal for a framework of Disaster Support Systems (DSS) is a non-structural method introduced to improve the planning and effectiveness of flood management. Among the vital elements of DSS are communication, knowledge transfer, skill improvement in forecasting ability and the transparency of strategic flood decision management. According to Vari (2002) the public do not need the details in the methods of flood control measures hence they need to understand the level of protection (in spatial and temporal terms) and risks that are associated with the flood control measures. The non-structural measure will give understanding in the society that the structural mitigation measures can only provide a certain flood extend in a certain are, as such it will give them understanding to what extend do their living and working places are protected against flood and thus they can choose how to mitigate the floods wisely. This will therefore reduce the panic of the community during the flood significantly and the loss in human life and properties.

The development of flood hazard maps is one of a fundamental non-structural methods to understand the impact of of floods with certain return periods to the inundation areas of one particular catchment. The hazard maps were developed using different methods and hydrological models, as such it is essential to compare results of different types of hazard maps using different methods in order to improve the existing flood management practices. This research uses the GEV frequency analyses (Chapter 5) and RRI model in order to visualize the inundated areas of floods with different return periods. This research benefits from the momentum of the unprecedent flood in 2014 in order to propose an updated inundation maps.

6.3 METHODOLOGY

The development of inundation maps in this research is as an attempt to combine the previous calculated results, namely the calibrated and validated RRI model parameters in Chapter 3 and the frequency analysis calculation in Chapter 5. In the results and

discussions, this research will discuss on the impact of increasing/decreasing trends in rainfall according to results of calculations in Chapter 5. As the final results of the research, there are 7 inundation maps for the Kelantan River Basins developed for 2, 5, 10, 50, 100 and 200-year of floods.

6.3.1 Rainfall Input for RRI Model

The rainfall input to produce these inundation maps were obtained from the results of extreme event frequency analysis using GEV methods, which were explained in Chapter 5. The maximum 14-days precipitation values (Chapter 4) were chosen as the rainfall input in RRI model. The rainfall intensities for different return periods are determined by the percentage of decreases from 2014 event.

6.3.2 Simulation Conditions of RRI Model

The simulation was carried out over 15,141 km^2 area, identified as Kelantan River Catchment Area based on topographic data. The simulation used topographic data from HydroSHEDS with 15 arc-second resolution. The resolution was able to give 71,176 number of grid cells, which corresponds to 461 m x 460 m of grid resolution in the catchment. The river channel locations were defined by using the flow accumulation datasets included in the HydroSHEDS with 15 arc-second resolution. As such, grid cells more than 20 flow accumulation were confirmed to have a river channel. The map of river networks in Malaysia was used to do visual checking for the river channel. The river cross sections used the following simple regression equations: width (m) = $5A^{3.5}$, depth (m) = $9.5A^2$, where A is the upstream catchment area for (in km^2) in each grid cell (accumulation area). The width and depth parameters for the regression equations were obtained by comparing river width in several locations. The levee height was set to zero.

Based on the calibration results obtained from Chapter 3 and the land use map of Malaysia in 2002, the development of inundation maps was using model parameters: n_s = 0.4 $m^{-1/3}$ s, d = 1 m, ϕ = 0.475 for all types of land use and k_v = 0 and k_a = 0.1 m/s for forest/mountainous area, k_v *and* k_a = 0 m/s for urban area, and USDA Green-Ampt parameters for "clay" k_v = 1.67 10^{-7} *and* S_f = 0.3163 m (From Rawls, W.J. *et al.*., 1992. Infiltration and soil water movement. In: Handbook of hydrology. New York: McGrow-

Hill Inc., 5.1–5.51. (Units are converted for RRI Model). These parameters are presented in Table 6.1. The Manning roughness of the river channel was set to 0.03 $m^{-1/3}$ s.

Table 6.1 Model Parameters.

Parameters	Forest	Urban	Agriculture
Manning's roughness on slope cells, n_s (in $m^{-1/3}$)	0.400	0.400	0.400
Soil depths, d (in m)	1.000	1.000	1.000
Effective porosity, ϕ (-)	0.475	0.475	0.475
Green Ampt Infiltration Model Parameters			
Vertical saturated hydraulic conductivity, k_v (in m/s)	0.000	0.000	1.67×10^{-7}
Suction at the wetting front, S_f (m/s)	3.163	3.163	3.163
Lateral sub-surface and surface model parameters			
Lateral saturated hydraulic conductivity, k_a (m/s)	0.100	0.000	0.000

In order to develop inundation maps for floods with magnitude of 2, 5, 10, 50, 100 and 200-year, the simulation was carried out for period of 37 days. In the first 14-days, the rainfall input was set to 0.1 mm per hour in every station in Kelantan River Catchment in order to allow the catchment to have base flow in the river basin. Day 15 to 28, the hourly rainfall was set based on the calculated maximum 14-days precipitation which resulting 2, 5, 10, 50, 100 and 200-years flood. The rainfall input for the remaining 9 days was set back to 0.1 mm in order to let the model calculated the maximum inundation depth in the catchment. The RRI Builder automatically saved the maximum inundation depth values, which can be retrieved to be visualized in GIS Software.

6.4 RESULTS AND DISCUSSIONS

6.4.1 Results

The RRI Model was applied to Kelantan River Catchment using rainfall inputs for 2, 5, 10, 20, 50, 100, and 200-year ARIs and Figure 6.1 to 6.7 show the maximum inundation depth and area for each magnitude of flood. The simulation showed that the inundated area and the inundation depth are increasing following the magnitude of floods. Due to the characteristics of topography of the area, in the 2-year flood inundation maps (Figure 6.1)

most of the inundated area happened in the flat and/or urbanized places (Machang, Kota Bharu, Rumah Kastam, Kg. Durian and Ulu Sekor). The inundation depth in this area ranged between 30 cm to 3 m and is not caused by overflowing of the Kelantan River. Inundated area in these areas are due to other smaller rivers or sub-catchment of another river such as the Golok River. Along the main river channel, the inundation areas are confined along the river channel at downstream area, particularly after the merge of two rivers at Kuala Krai, with inundation depth, up to 5 m in the 2-year flood magnitude. Some inundated areas close to the river channel happened in sub-rivers of the Kelantan River in the downstream area namely at the Bagan River and the Sat River.

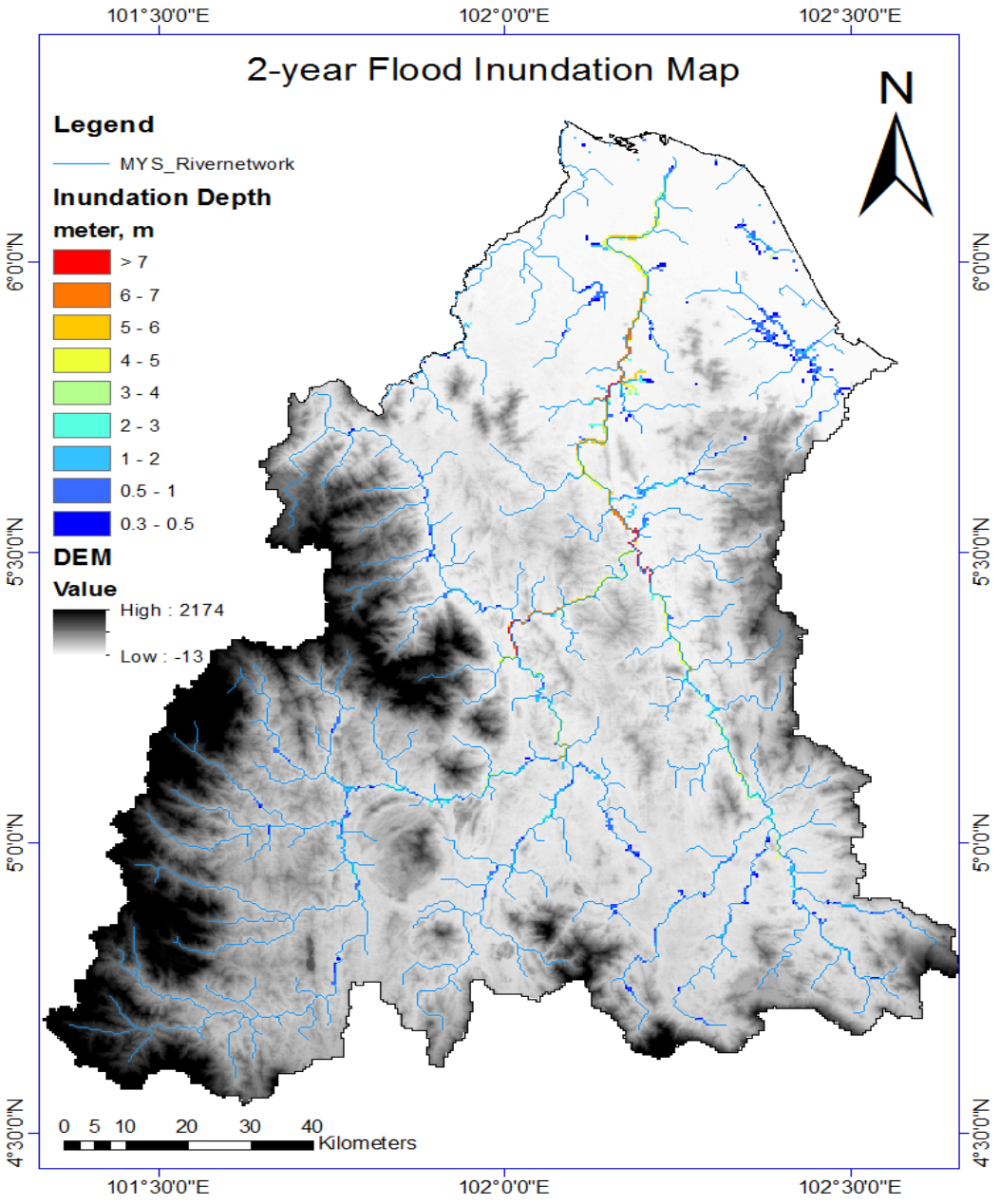

Figure 6.1 Flood inundation map 2-year ARIs.

The inundation map of 5-year magnitude floods showed larger inundation area and deeper inundation depth. In this map, the inundated area in the flat areas which are not caused by the Kelantan River have more or less the same inundation area and inundation depth (30 cm to 3 m). Whereas along the Kelantan River channel, the inundation depth is more than 7 m and start to affect the sub-river channels. The high depth of inundation area is still confined along the main river channel, however the inundation area from the small sub-rivers of Kelantan River in the downstream areas increase.

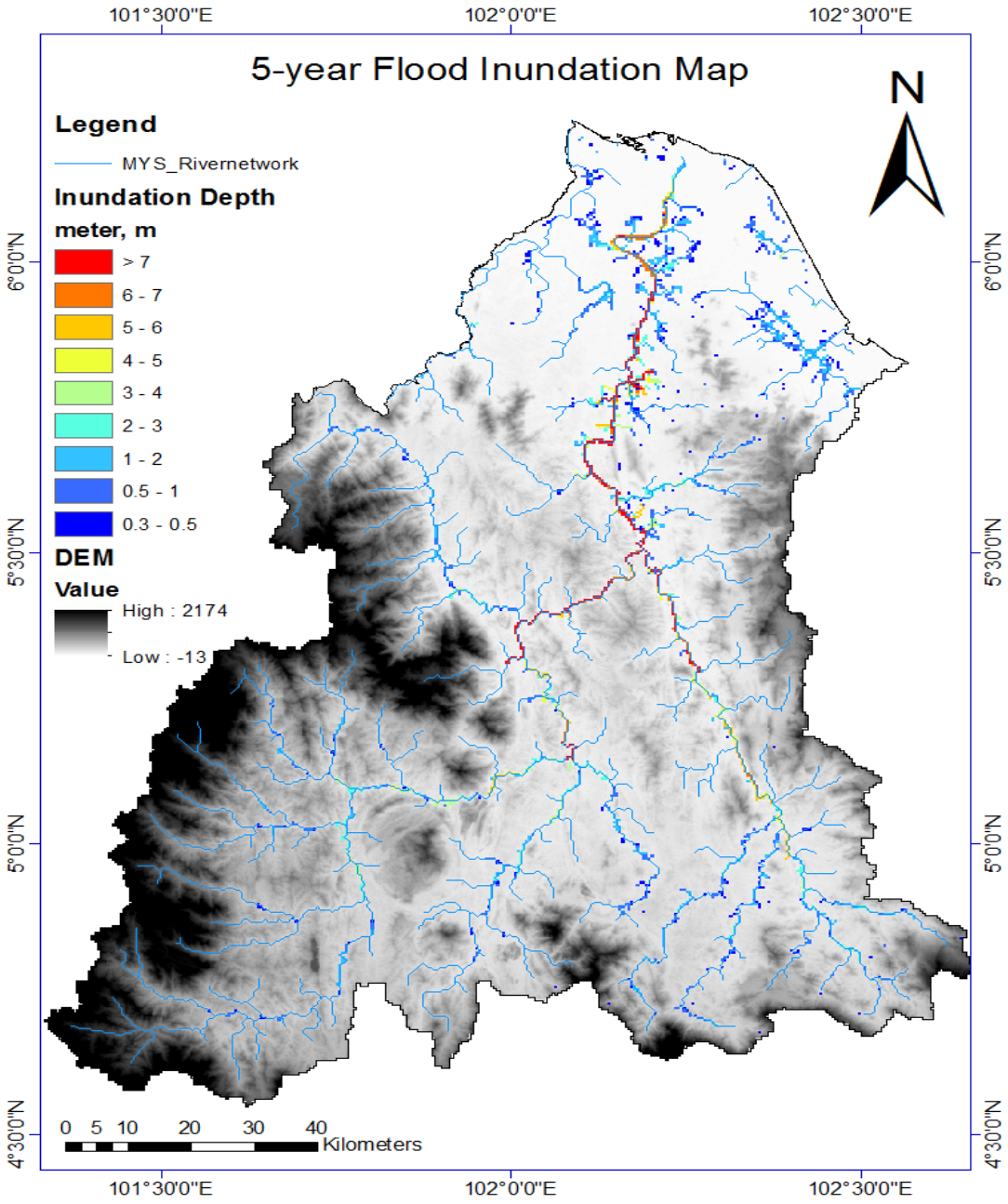

Figure 6.2 Flood inundation map 5-year ARIs.

The inundation area caused by high water level in the main river channel showed significant increase in 10-year flood (Figure 6.3) in the downstream area. Some areas were inundated more than 7 meters and most of the low land areas are inundated with inundation depth of 30 cm to 3 m. Some spots of inundated area in the upper catchments including the mountainous region can be seen in this inundation map with inundation depth of 30 - 50 cm. The 20-year flood inundation maps (Figure 6.4) show similar result to the 10-year flood inundation map.

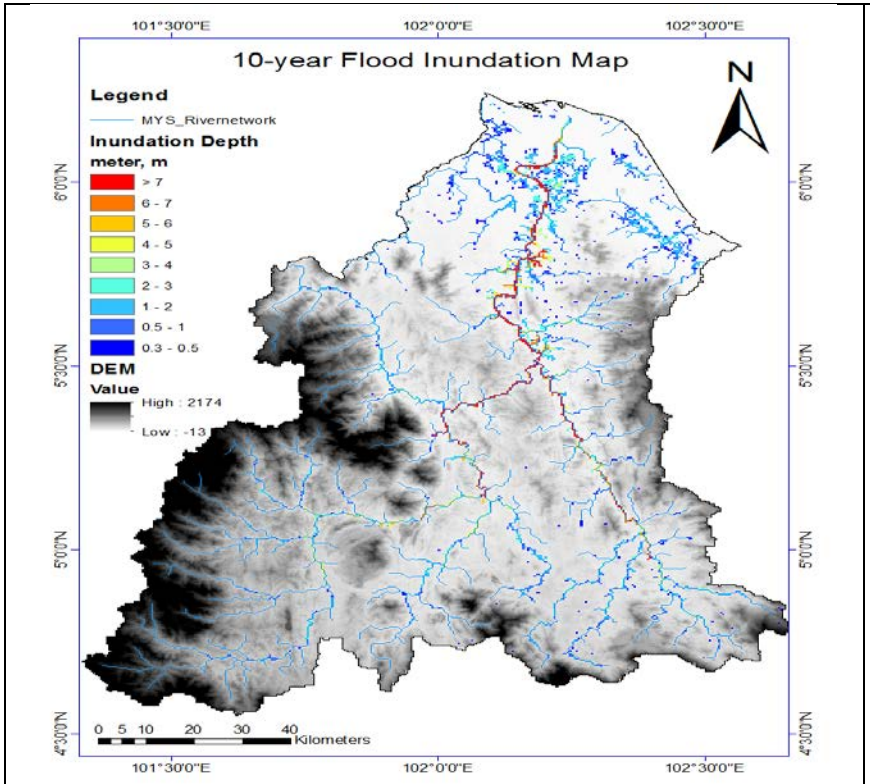

Figure 6.3 Flood inundation map 10-year ARIs.

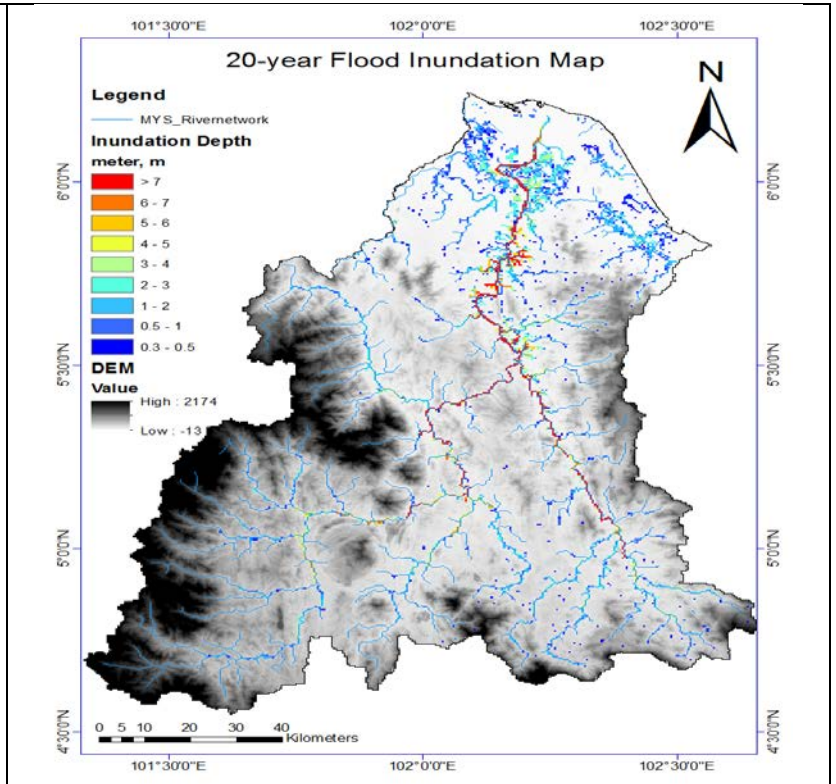

Figure 6.4 Flood inundation map 20-year ARIs.

Severe floods can be seen in the 50-year inundation map (Figure 6.5), where most of the lowland areas are covered with water with depth of 30 cm to 5 m. In the middle catchments, inundated spots are detected nearby the sub-river channels although not necessarily caused by the overflow of the sub-rivers. Inundation areas can be seen in the mountainous areas such as Gagau Mountain, Upper Chiku, and Gua Musang. These areas consist of mainly protected forest and less urbanized area. The 100-year inundation map (Figure 6.6) shows similar result to 50-year inundation map.

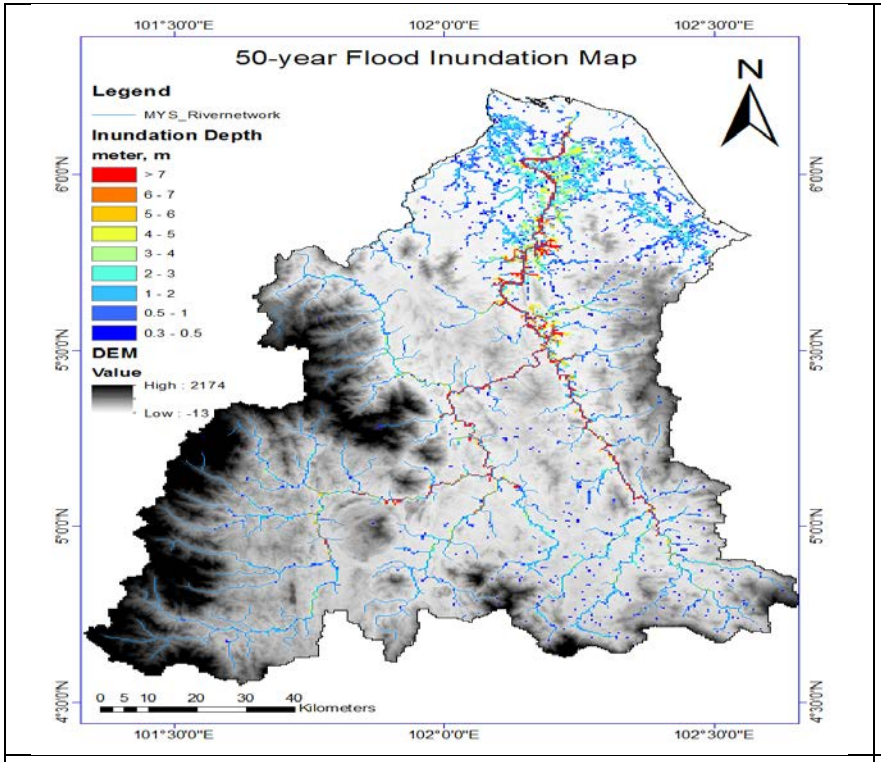

Figure 6.5 Flood inundation map 50-year ARIs.

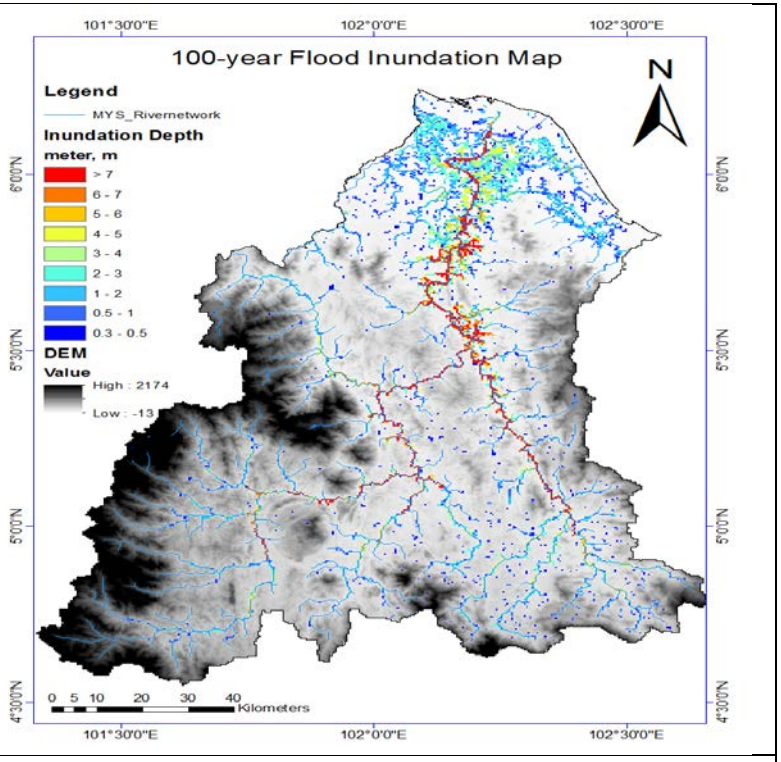

Figure 6.6 Flood inundation map 100-year ARIs.

The 200-year inundation map shows that most of the areas are inundated. Inundation maps shows that there are some spots where inundation depths are more than 7 m due to the overflow of the main river channel. The lowland areas are almost all inundated and the inundation depth reaches 6 m. High water level (more than 7 m) are detected in most of the main river channels.

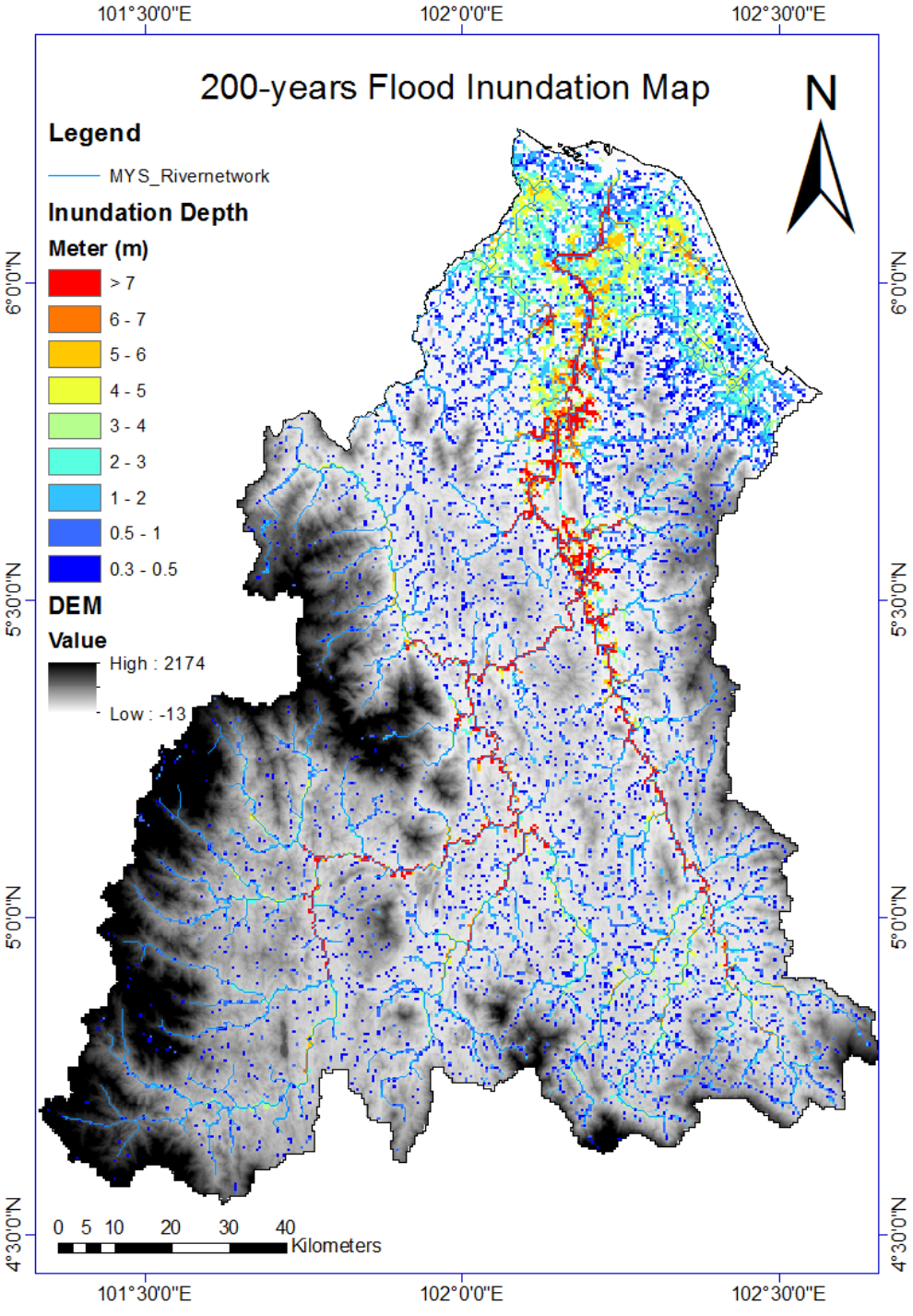

Figure 6.7 Flood inundation map 200-year ARIs.

6.4.2 Discussions

Based on these inundation maps, floods are more likely to happen in the lowland areas. The 2 and 5-years of flood inundation maps shows that most of the inundated areas in the lowland are not due to the overflow of Kelantan River (main channel) but other smaller rivers (see red circles in Figure 6.8). These small rivers linked directly to the South China Sea or another large river such as Golok River and inundation areas are located in the area of Pasir Mas and Pasir Puteh. These areas mostly consist of agricultural land. The inundation caused by these small rivers are less than 3 m depth.

The inundation area caused by the main river channel can be seen along the river channel (up to 4 m in 2-years flood and > 7 m in 5-year flood) and in Machang area (see pink circle in Figure 6.8). The inundation in the northern of Machang area, due to the high water level in the main channel, can reach up to 5 m in 2-year flood and >7 m in 5-year flood. This particular area is where the East-West Highway crosses the Kelantan River. Machang Area is well known as a flood prone area.

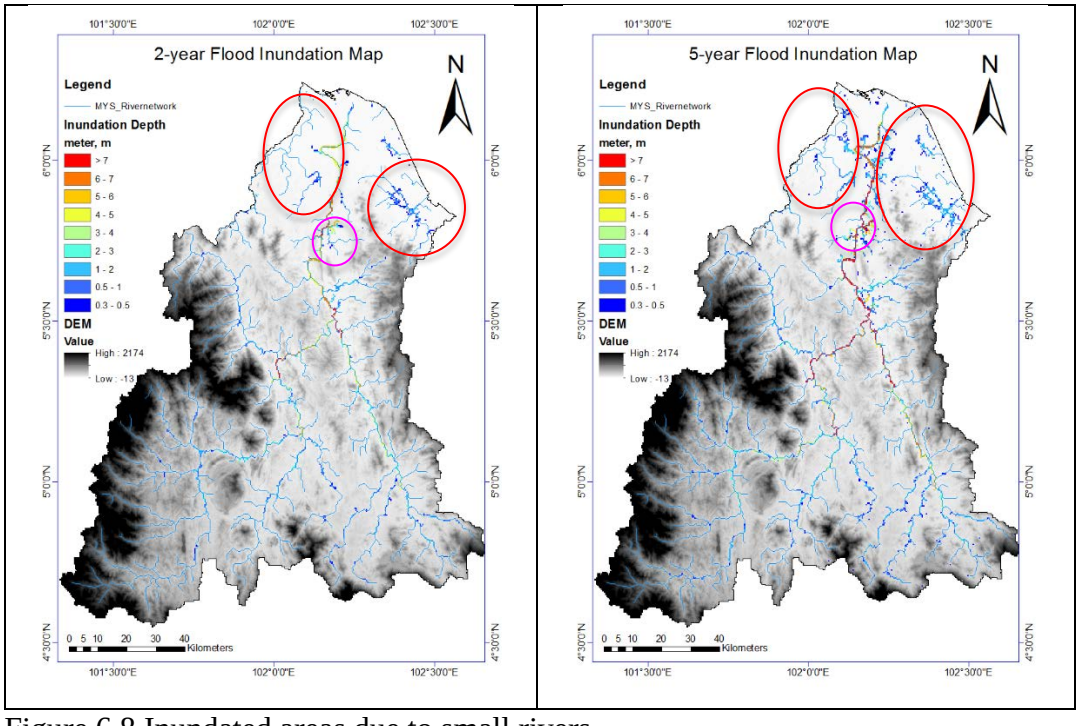

Figure 6.8 Inundated areas due to small rivers.

The inundation area from the main channel of the Kelantan River started to expand from 10-years flood. The flood will inundate the northern Machang area up to >7 m, Kuala Krai area up to >7 m and the largest inundation area is in Pasir Mas area up to 4 m (Figure 6.9). There are some inundation spots can be detected in the upstream region. In the 10-years flood, the inundated area caused by the small rivers is not so much different than the 2 and 5-year floods.

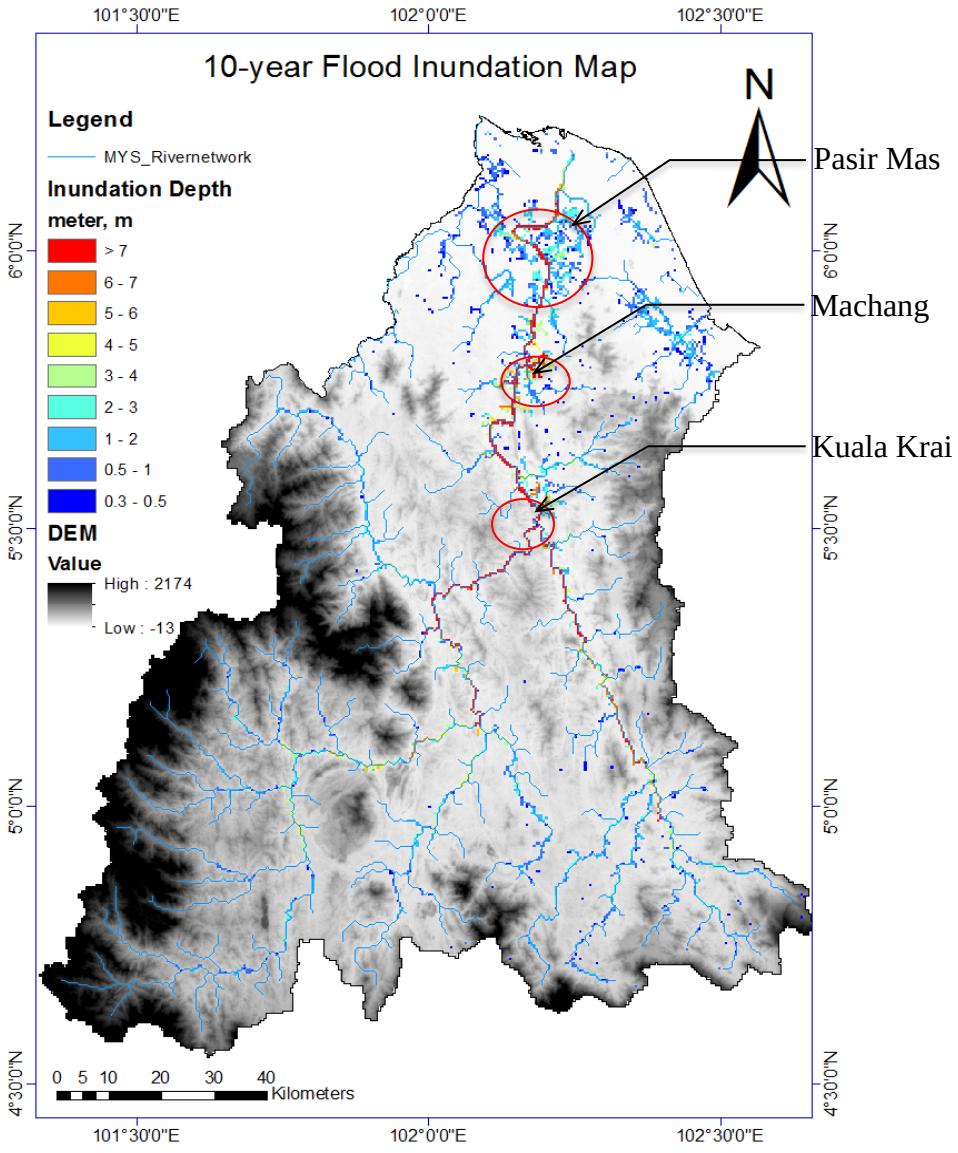

Figure 6.9 High inundation areas in 10-year flood.

In the 50-year flood, Kota Bharu, the capital of the Kelantan State starts to be inundated up to 3 m high (Figure 6.10). This area is highly populated with a lot of public infrastructures such as stadium, hospital and airport. The location of stadium is just less than 1 km from the Kelantan River. The low land areas are mostly covered by water with depth up to 5 m high and along the river channel (0.5-1.5 km), the inundated areas are more than 7 m high. The situation in the upstream area is more or less the same as the 10-year flood.

The inundations because of the small rivers are also increasing in depth and inundation area. However, these areas are mostly agricultural areas. The small rivers start to flood Rantau Panjang, a populated area just in the border of Malaysia and Thailand. This populated area in Thailand side is called Sungai Kolok, a town which usually share the same flood experience with Rantau Panjang due to overflowing of Golok River.

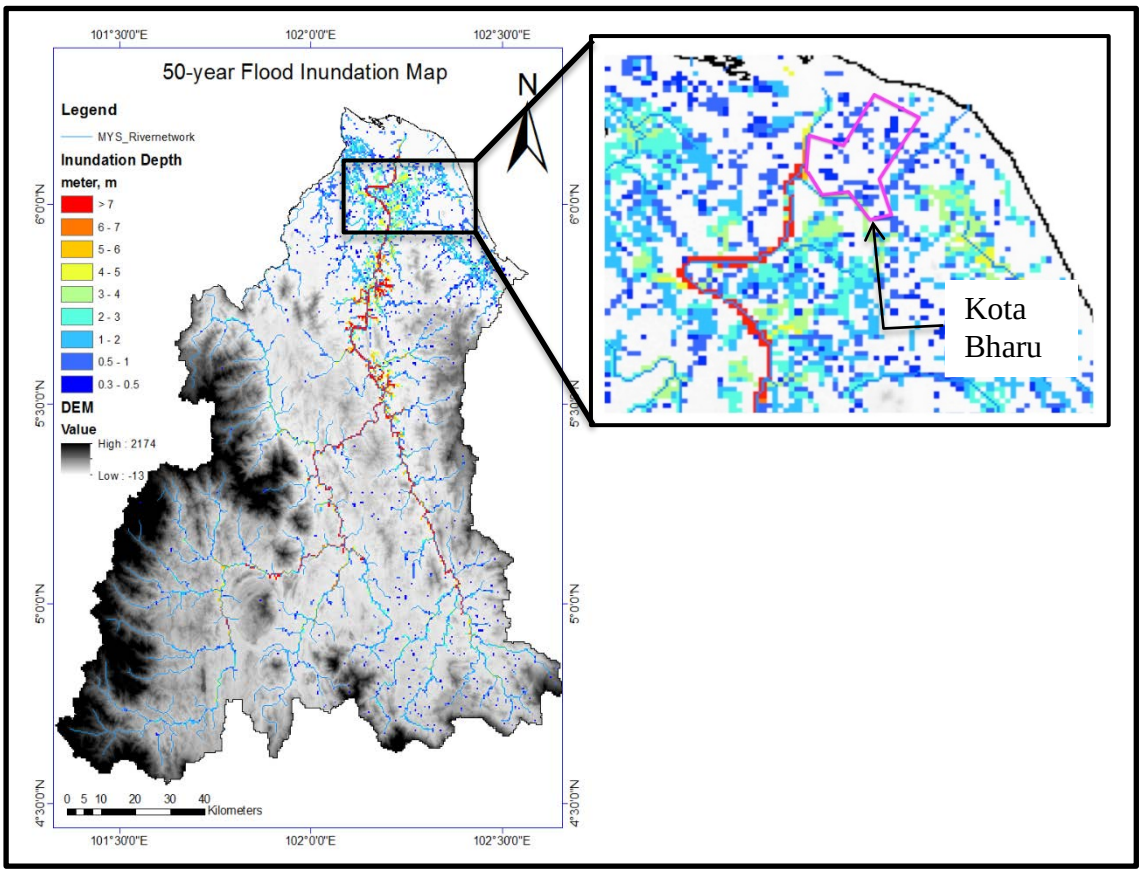

Figure 6.10 Inundation in Kota Bharu from 50-year flood.

In the 200-year flood, the populated area such as Kota Bharu, Machang, Tanah Merah, and Kuala Krai are severely flooded. The inundation depth in Kota Bharu is up to 3 m, in Machang is more than 7 m, in Tanah Merah is up to 7 m, and in Kuala Krai is more than 7 m. (Figure 6.11). In 200-year flood, most of the areas are inundated, thus it is important to place evacuation points based on this inundation map, particularly in areas close by the inundated populated areas. It is important to place facilities close by these evacuation points, in particular clean water facilities in emergency situation.

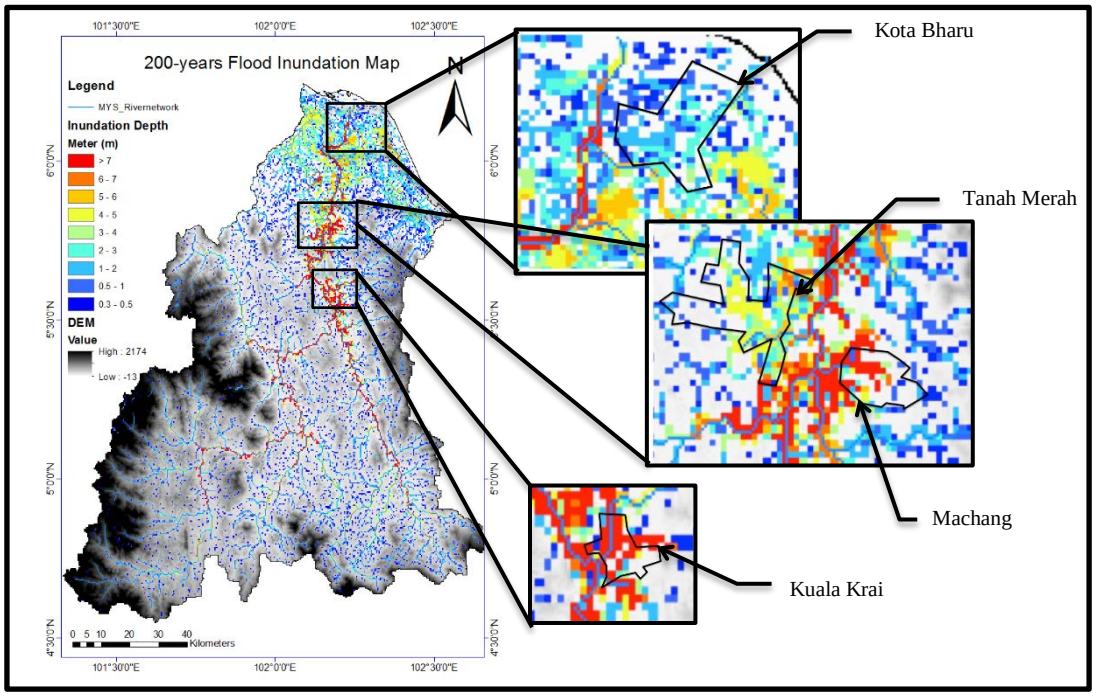

Figure 6.11 Inundation in populated areas from 200-year flood.

The overall increasing trend in most of the area in Kelantan River Catchment will worsen the flood situation in the future. It is likely that the floods with higher magnitude will have higher probability. As such the 2-year flood may have more inundation area and/or depth (Figure 6.12).

The inundated area from the small rivers (flows to the sea or linked with Golok River) in the low land areas may be increased due to the increasing trend of rainfall from already high average of rainfall near the Rantau Panjang, Pasir Mas area (border with Thailand) and in Pasir Putih area (coastal northwest side). The increasing trend of high average rainfall can be seen also in the upstream area, in particular in Gunung Gagau Station which is a mountainous area. Area with relatively low average rainfall such as in GOB Station is

likely to increase, as such the contribution from the upstream regime to the downstream flow will likely to increase too, in particular contribution from the Lebir River (from southwest side) and the Nenggili River (from southeast side). Thus, precautions should be placed in the meeting point of this river, the Kuala Krai area.

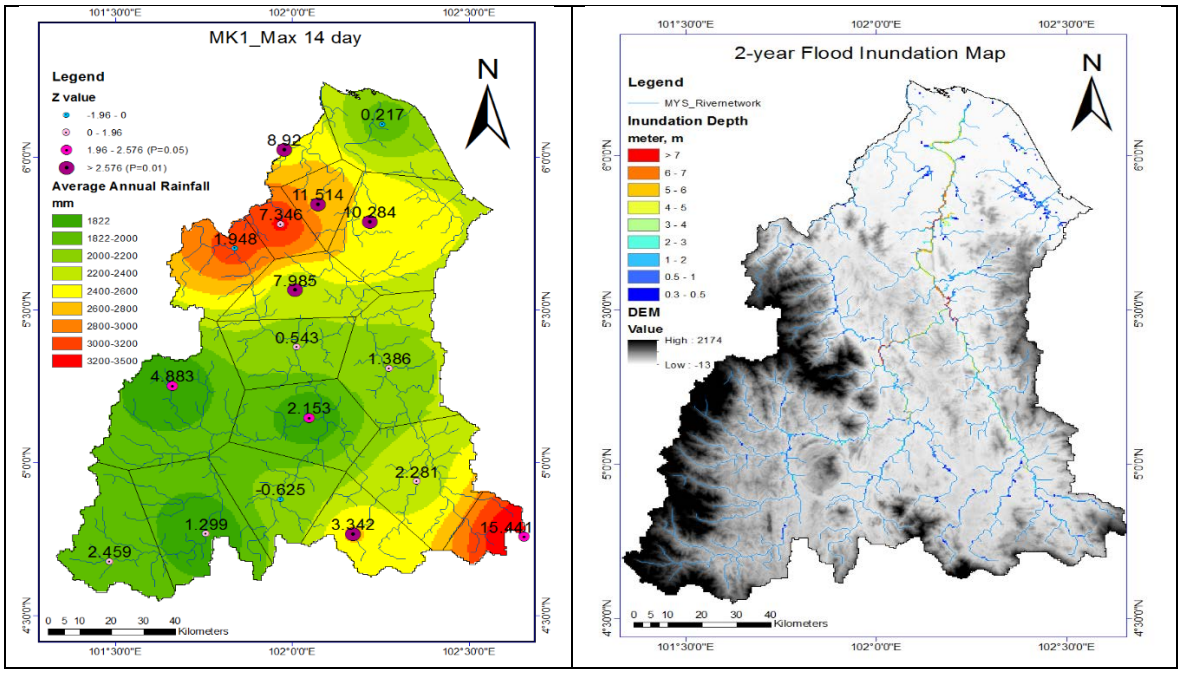

Figure 6.12 Comparison between the trend analysis and inundation map.

6.5 SUMMARY

The hazard maps show increasing inundation area and depth with the increasing magnitude of floods. The hazard maps also show that the contribution of small rivers in the northeast and northwest area are significant and should not be excluded to produce the hazard map in Kelantan Area. The inclusion of these rivers will produce more integrated results in the inundation area in particular for the lowland areas.

The inundation maps can give information for populated area on the magnitude of flood the area will be inundated and how deep the inundation will take place. These maps show that floods in Pasir Mas and Pasir Putih areas start to be inundated in 2-year flood area with the maximum inundation depth of 3 m in 2-year flood and 6 m in 200-year flood. The Rantau Panjang area start to be inundated in 50-year flood with inundation depth up to 3 m in 50-year flood and 5 m in 200-year flood. The most populated Kota Bharu area

(located a bit away from the river) start to be inundated in 50-year flood with maximum inundation depth of 3 m and the worst is with inundation depth of 4 m for 200-year flood. Machang and Kuala Krai starts to be inundated in 10-year flood with more than 7 m inundation depth. Particularly for Kuara Krai area, the 200-year flood inundates more than half of the populated area with more than 7 m inundation depth. The Tanah Merah area starts to be inundated in 200-year flood with inundation depth up to 7 m only in a few spots and mostly inundated in 5 m depth.

The overall increasing trend in rainfall in all Kelantan River Catchment may increase the probability of higher magnitude of flood. The trend analysis compared with the inundation maps suggests particular attention should be placed on the contribution of inundations by smaller rivers in the northeast and northwest area due to the likelihood of rainfall increase with the high level of confidence. The trend analysis also suggests placing emphasize in the change of rainfall in the Gunung Gagau and GOB stations, its contribution to the discharge in the Lebir and the Nenggili Rivers. These rivers may increase the already vulnerable area at the meeting point of the rivers, the Kuala Krai area.

Finally, the information from these inundation maps can be utilized to place both structural and non-structural flood mitigation measures, in particular for populated areas. As an example, the high magnitude of flood inundation map can be used to place evacuation points with identified clean water facilities reliable during emergency periods.

CHAPTER 7 CONCLUSIONS AND RECOMMENDATIONS

7.1 CONCLUSIONS

Malaysia is one of the countries that are regularly receiving floods and Kelantan State is one of the states in Malaysia which was severely affected by floods. This research focuses on Kelantan River as the only main river in Kelantan State which contributed to floods in the region. This study attempted to increase the efficiency of flood early warning system and reducing the impact of the flood to the community and country's economy aiming at three specific objectives. This research used RRI Model for rainfall-runoff-inundation simulation in the area. The research can be furthermore compared to other researches in the same area in order to improve the policy making and decision taking for flood management. The main conclusions are summarized as follows:

a) Objective 1: To propose an equation for calculating the time of concentration, T_c with a diffusive wave, *DW* approximation for river channel with considering the effect of inundation extent. The new equation may help to increase the early warning.
   In the conclusion of Chapter 4, T_c estimation method improve by considering diffusive wave and inundation extent. According to the results of analysis, the proposed estimation method with DW approximation with flood inundation showed closer estimations of T_c by the other two methods (simulation and empirical). Therefore, it is important to consider diffusive wave and inundation extent in flat topography. These findings are important and can be used for the authorized party such as Department of Drainage and Irrigation (DID) or Kelantan State Government for future development.

b) Objective 2: To understand the long-term trend of rainfall and frequency analysis of rainfall to predict future trends.
   The results of this study are hoped to be able to contribute to researches in order to better understand the the frequency of occurrence and pattern of the extreme rainfall.

Based on the empirical analysis in Chapter 4, MK1 and MK3 conducted to understand the trend of precipitation in Kelantan River Catchment. In conclusion, MK1 and MK3 explain good agreement in increasing and decreasing trend. Station located at upstream (Gunung Gagau, Upper Chiku, Brook, and Blau) tends to bring more precipitation from analysis results. The increasing trend will increase more surface flow if the land use changes are not well preserved. The increasing of surface flow may trigger more debris flow from upstream to downstream. Station located at downstream (Ulu Sekor, JPS Machang, Bendang Nyior, Rumah Kastam, and Kg. Durian Daun) show increasing trend for annual, maximum and seasonal precipitation. Downstream station with increase trend tends to cause a severe flood and large flood extent. These can be a high-risk area for future development. Therefore, future concerns need to be considered by the policy maker.

c) To develop the flood hazard map for different return period and different rainfall intensity for evacuation centre relocation and to identify high risk and low-risk area.
This research uses the GEV frequency analyses and Rainfall-Runoff-Inundation (RRI) model to visualize the inundated areas of floods with different return periods. This research benefits from the momentum of the unprecedented flood in 2014 in a view to proposing an updated inundation maps. The inundation maps were developed using different methods and hydrological models, as such it is essential to compare results of the various types of hazard maps using different methods to improve the existing flood management practices.

7.2 LIMITATIONS

Several limitations of the study need to be presented. This is due to many factors such as specific climate conditions of the study area (i.e. monsoon catchment, heterogeneous land use types), limitations in data used (i.e. streamflow, precipitation, remotely-sensed images), limitations in climate change factors (i.e. not including temperature, evapotranspiration, ENSO phenomena). Many studies indicate that stream flows trends need to be studied for time series analysis in order to understand more about potential floods that have occurred or may happen in the future (Frei et al., 2000; Buchele et al., 2006). The limitations for hydrological modelling while develop hazard mapping are high

resolution of DEM data, updated and high –scale or detailed soil and land use map. This study applied low spatial resolution DEM data of SRTM with 15 arc-second in RRI model.

7.3 RECOMMENDATIONS

- In this study, types of land use only divided into three types which are urban, agriculture and forest. Detailed agriculture land may be good to be apply as different types of agriculture activities will contribute to different hydrological process.
- Further research using a long term simulations instead of event based may be provide better understanding. Evaporation changes better to be included.
- Time series analysis studies can be carried out to explore the linkage between precipitation trends to stream flow and ENSO conditions. This will provide a comprehensive understanding in the study area.

REFERENCES

CHAPTER 1

Ali Khan, M. M., Shaari, N. A., Achmad Bahar, A. M., Baten, M. A., & Nazaruddin, D. A. (2014). Flood impact assessment in Kota Bharu, Malaysia: a statistical analysis. *World Applied Sciences Journal, 32*(4), 626-634. doi:10.5829/idosi.wasj.2014.32.04.422

Ang, K. H. (2015). *Adaptation and mitigation towards monsoon floods in Kota Bharu, Kelantan.* Lulu.com.

Chahinian, N., Moussa, R., Andrieux, P., & Voltz, M. (2005). Comparison of infiltration models to simulate flood events at the field scale. *Journal of Hydrology, 306*(1), 191-214. doi:10.1016/j.jhydrol.2004.09.009

Chan, N. W. (1995). Flood disaster management in Malaysia: An evaluation of the effectiveness of government resettlement schemes. *Disaster Prevention and Management: An International Journal, 4*(4), 22-29. doi:10.1108/09653569510093405

Chan, N. W. (1997). Institutional arrangements for flood hazard management in Malaysia: An evaluation using the criteria approach. *Disasters, 21*(3), 206-222. doi:10.1111/1467-7717.00057

Chan, N. W. (2002). *Reducing flood hazards exposure and vulnerability in Peninsular Malaysia flood.* London: Taylor & Francis Publisher.

Chan, N. W., & Parker, D. J. (1996). Response to dynamic flood hazard factors in Peninsular Malaysia. *The Geographical Journal, 162*(3), 313-325. doi:10.2307/3059653

Chow, V. T. (1956). Hydrologic studies of floods in the United States. *International Association of Scientific Hydrology, 42*, 134-170.

De, U. S., Dube, R. K., & Prakasa Rao, G. S. (2005). Extreme weather events over India in the last 100 years. *Journal of The Indian Geophysical Union, 9*(3), 173-187.

DID. Drainage and Irrigation Department. (2004). *Annual flood report of DID for Peninsular Malaysia.* Kuala Lumpur: Unpublished report.

DID. Drainage and Irrigation Department. (2008). *Annual flood of DID for Peninsular Malaysia.* Kuala Lumpur: Unpublished report.

Foody, G. M., Ghoneim, E. M., & Arnell, N. W. (2004). Predicting locations sensitive to flash flooding in an arid environment. *Journal of Hydrology, 292*(1-4), 48-58. doi:10.1016/j.jhydrol.2003.12.045

Geis, D. &. (1980). Flood hazards. *Journal of Architectural Education, 33*(4), 28-31.

Grothmann, T., & Reusswig, F. (2006). People at risk of flooding: Why some residents take precautionary action while others do not. *Natural Hazards, 38*(1), 101-120. doi:10.1007/s11069-005-8604-6

Guo, Q., Ma, K., Yang, L., & He, K. (2010). Testing a dynamic complex hypothesis in the analysis of land use impact on lake water quality. *Water Resources Management, 24*(7), 1313-1332. doi:10.1007/s11269-009-9498-y

Hassan, A. (2004). *Growth, structural change and regional inequality in Malaysia.* Ashgate Publishing Ltd.

Hamzah, H. (2005). *Roadmap toward effective flood hazard mapping in Malaysia.* Concluding Report, JICA region focused training course on flood hazard mapping.

Islam, M. M., & Sado, K. (2000). Development of flood hazard maps of Bangladesh using

NOAA-AVHRR images with GIS. *Hydrological Sciences Journal, 45*(3), 337-355. doi:10.1080/02626660009492334

Jaafar, J. (2004). Emerging trends of urbanisation in Malaysia. *Journal of the Department of Statistics, Malaysia, 1*(1), 43-54.

Jonkman, S. N., & Kelman, I. (2005, February 18). An Analysis of the Causes and Circumstances of Flood Disaster Deaths. *Disasters, 29*(1), 75-97. doi:10.1111/j.0361-3666.2005.00275.x

Junk, W. J. (1997). *The central amazon floodplain: ecology of a pulsing system.* Springer.

Kundzewicz, Z. W., & Takeuchi, K. (1999). Flood protection and management: quo vadimus? *Hydrological Sciences Journal, 44*(3), 417-432. doi:10.1080/02626669909492237

Mays, L. W. (2004). *Stormwater collection systems design handbook.* New York: McGraw-Hill.

Milly, P., Wetherald, R. T., Dunne, K. A., & Delworth, T. L. (2002). Increasing risk of great floods in a changing climate. *Nature, 415*, 514-517.

MMD. Malaysian Meteorological Department. (2007). *Report on heavy rainfall that caused floods in Kelantan and Terengganu.* Kuala Lumpur: Malaysian Meteorological Department.

Mustafa, Y. M., Amin, M., Lee, T. S., & Shariff, A. (2005). Evaluation of land development impact on a tropical watershed hydrology using remote sensing and GIS. *Journal of Spatial Hydrology, 5*(2), 16-30.

Nawaz, F., & Shafique, M. (2003). Data integration for flood risk analysis by using GIS/RS as tools. *Map Asia Conference 2003.*

Niehoff, D., Fritsch, U., & Bronstert, A. (2002). Land-use impacts on storm-runoff generation: scenarios of land-use change and simulation of hydrological response in a meso-scale catchment in SW-Germany. *Journal of Hydrology, 267*(1), 80-93. doi:10.1016/S0022-1694(02)00142-7

Nyarko, B. K. (2002). Application of a rational model in GIS for flood risk assessment in Accra, Ghana. *Journal of Spatial Hydrology, 2*(1).

Pinter, N., van der Ploeg, R. K., Schweigert, P., & Hoefer, G. (2006). Flood magnification on the River Rhine. *Hydrological Processes, 20*(1), 147-164. doi:10.1002/hyp.5908

Rostvedt, J. O. (1968). *Summary of floods in the United States during 1962.* Washington: United States Government Printing Office.

Shafiee, M., Ahmad, A., Hassan, F., Yaakub, M. A., Low, K. S., Fatt, C. S., . . . Mat Amin, M. Z. (2004). Development of an operational monsoon flood management system. *Third National Microwave Remote Sensing Seminar*.

Sooryanarayana, V. (1988). Flood in Malaysia. *The working group on tropical climatology and human settlements, the 26th Congress of The International Geographical Union.* New South Wales.

Tapsell, S. M., Penning-Rowsell, E. C., Tunstall, S. M., & Wilson, T. L. (2002, May 24). Vulnerability to flooding: health and social dimensions. *Philosophical Transactions of The Royal Society London Series A: Mathematical, Physical and Engineering sciences, 360*(1796), 1511-1525.

Wan Ismail, W. F. (1996). Urban growth determinants for the state of Kelantan of the state's policy makers. *Buletin Ukur, 7*(3), 176-189.

Wang, S., Kang, S., Zhang, L., & Li, F. (2008). Modelling hydrological response to different land-use and climate change scenarios in the Zamu River basin of northwest China. *Hydrological Processes, 22*(14), 2502-2510. doi:10.1002/hyp.6846

Wilson, M. D. (2004). *Evaluating the effect of data and data uncertainty on predictions of flood inundation.* Southampton: University of Southampton.

Wohl, E. E. (2000). *Inland flood hazards: human, riparian and aquatic communities.*

Cambridge University Press.
Wooldridge, S., Kalma, J. D., & Kuczera, G. (2001). Parameterisation of a simple semi-distributed model for assessing the impact of land-use on hydrologic response. *Journal of Hydrology, 254*(1), 16-32.
Zehe, E., Singh, A. K., & Bardossy, A. (2006, October 30). Modelling of monsoon rainfall for a mesoscale catchment in North-West India II: stochastic rainfall simulations. *Hydrology and Earth System Sciences, 10*(6), 807-815.
Zhang, X., Yu, X., Wu, S., Zhang, M., & Li, J. (2007). Response of land use/coverage change to hydrological dynamics at watershed scale in the Loess Plateau of China. *Acta Ecologica Sinica, 27*(2), 414-421. doi:10.1016/S1872-2032(07)60013-4

CHAPTER 2

Awadalla, S., & Noor, I. M. (1991). Induced climate change on surface runoff in Kelantan Malaysia. *International Journal of Water Resources Development, 7*(1), 53-59. doi:10.1080/07900629108722492
Chan, N. W. (1995). Flood disaster management in Malaysia: An evaluation of the effectiveness of government resettlement schemes. *Disaster Prevention and Management: An International Journal, 4*(4), 22-29. doi:10.1108/09653569510093405
Chan, N. W. (2002). *Reducing flood hazards exposure and vulnerability in Peninsular Malaysia flood.* London: Taylor & Francis Publisher.
DID. Drainage and Irrigation Department. (2004). *Annual flood report of DID for Peninsular Malaysia.* Kuala Lumpur: Unpublished report.
Garbrecht, J., & Martz, L. W. (2000). *Digital elevation model issues in water resources modeling. Hydrologic and hydraulic modeling support with Geographic Information Systems.* Redlands CA, USA: ESRI Inc.
Grothmann, T., & Reusswig, F. (2006). People at risk of flooding: Why some residents take precautionary action while others do not. *Natural Hazards, 38*(1), 101-120. doi:10.1007/s11069-005-8604-6
Hassan, A. (2004). *Growth, structural change and regional inequality in Malaysia.* Ashgate Publishing Ltd.
Ibbitt, R., Takara, K., Mohd Desa, M., & Pawitan, H. (2002). *Catalogue of river for Southeast Asia and the Pacific Volume IV.* Jakarta, Indonesia: UNESCO-IHP.
Jonkman, S. N., & Kelman, I. (2005, February 18). An Analysis of the Causes and Circumstances of Flood Disaster Deaths. *Disasters, 29*(1), 75-97. doi:10.1111/j.0361-3666.2005.00275.x
KFD. Kelantan Forest Department. (2006). *Ringkasan awam untuk rancangan pengurusan hutan 2006-2015 bagi negeri Kelantan Darul Naim.* Kelantan: Unpublished report.
Sayama, T., Ozawa, G., Kawakami, T., Nabesaka, S., & Fukami, K. (2012). Rainfall-runoff-inundation analysis of the 2010 Pakistan flood in the Kabul River basin. *Hydrological Sciences Journal, 57*(2), 298-312. doi:10.1080/02626667.2011.644245
Syed Hussain, T., & Ismail, H. (2013). Flood frequency analysis of Kelantan River Basin, Malaysia. *World Applied Sciences Journal, 28*(12), 1989-1995.
Tangang, F. T., Juneng, L., & Ahmad, S. (2007). Trend and interannual variability of temperature in Malaysia: 1961-2002. *Theoretical and Applied Climatology, 89*, 127-141.
Tapsell, S. M., Penning-Rowsell, E. C., Tunstall, S. M., & Wilson, T. L. (2002, May 24). Vulnerability to flooding: health and social dimensions. *Philosophical Transactions of The Royal Society London Series A: Mathematical, Physical and Engineering Sciences,*

360(1796), 1511-1525.
Zakaria, A. S. (1975). The geomorphology of Kelantan delta (Malaysia). *CATENA, 2*, 37-350.

CHAPTER 3

Lehner, B., Verdin, K., & Jarvis, A. (2008). New global hydrography derived from space borne elevation data. *EOS, Transactions, American Geophysical Union, 89*(10), 93-94. doi:10.1029/eost2008EO10
Sayama, T., Ozawa, G., Kawakami, T., Nabesaka, S., & Fukami, K. (2012). Rainfall-runoff-inundation analysis of the 2010 Pakistan flood in the Kabul River basin. *Hydrological Sciences Journal, 57*(2), 298-312. doi:10.1080/02626667.2011.644245
Strömqvist, J., Arheimer, B., Dahné , J., Donnelly, C., & Lindström, G. (2012). Water and nutrient predictions in ungauged basins: set-up and evaluation of a model at the national scale. *Hydrological Sciences Journal, 57*(2), 229-247.

CHAPTER 4

Corps of Engineers. (1954). *Airfield drainage investigation.* Washington D.C.: U.S. Army, Los Angeles District for the Office of the Chief of Engineers, Airfield Branch Engineering Division, Military Construction.
DID. (2000). *Urban storm water management manual for Malaysia.* Kuala Lumpur: Percetakan Nasional Malaysia Berhad.
Ibbitt, R., Takara, K., Mohd. Desa, M., & Pawitan, H. (2002). *Catalogue of River for Southeast Asia and the Pacific-Volume IV.* Jakarta, Indonesia: UNESCO-IHP.
Ishihara, T., & Takasao, T. (1959). Fundamental researches on the unit hydrograph method and its application. *Transactions of the Japan Society of Civil engineers, No. 60*, Extra Paper (3-3).
Izzard, C. F. (1943). Overland flow tests - tabulated hydrograph. *Bureau of Public Roads*.
Jonkman, S. N., & Kelman, I. (2005). An analysis of the cause and circumstances of flood disaster deaths. *Disasters, 29*(1), 75-97.
Kibler, D. F., & Aron, G. (1983). Evaluation of Tc methods for urban watersheds. *Frontiers in Hydraulic Engineering: Proc. Cambridge Conf.* (pp. 553-558). New York: ASCE.
Lehner, B., Verdin, K., & Jarvis, A. (2008). New global hydrography derived from space borne elevation data. *EOS, Transactions, American Geophysical Union, 89*(10), 93-94. doi:10.1029/eost2008EO10
Machmeier, R. E., & Larson, C. L. (1968). Runoff hydrographs for mathematical watershed model. *Journal of the Hydraulics Division, 94*(6), 1453-1474.
Saghafian, B., & Julien, P. Y. (1995). Time to equilibrium for spatially variable watersheds. *Journal of Hydrology, 172*(1-4), 231-245.
Sayama, T., Ozawa, G., Kawakami, T., Nabesaka, S., & Fukami, K. (2012). Rainfall-runoff-inundation analysis of the 2010 Pakistan flood in the Kabul River basin. *Hydrological Sciences Journal, 57*(2), 298-312. doi:10.1080/02626667.2011.644245
Singh, V. P. (1976). Derivation of time of concentration. *Journal of Hydrology, 30*, 147-165.
Su, D., & Fang, X. (2004). Estimating traveling time of flat terrain by 2-dimensional overland flow model. In H. J. Gerhard, & S. U. Wim (Eds.), *Shallow Flows* (pp. 629-636). London: Taylor & Francis. doi:10.1201/9780203027325.ch79
Syed Hussain, T., & Ismail, H. (2013). Flood frequency analysis of Kelantan River Basin, Malaysia. *World Applied Sciences Journal, 28*(12), 1989-1995.

Takasao, T., & Shiba, M. (1978). Lumping of the basin model and constants in the kinematic wave method. *Disaster Prevention Research Institute Annuals, No. 21B-2*, 207-217.
Wong, T. S. (2008). Effect of channel shape on time of travel and equilibrium detention storage in channel. *Journal of Hydrologic Engineering, 13*(3), 189-196.
Yen, B. C. (1982). Some measures for evaaluation and comparison of simulated models. *Proc. 2nd Int. Conf. on Urban Storm Drainage* (pp. 341-349). Littleton, Colorado: Water Resources.
Zakeri, M. N., Saghafian, B., Golian, S., Moramarco, T., & Shamsai, A. (2012). Derivation of travel time based on diffusive wave approximation for the time-area hydrograph simulation. *Journal of Hydrologic Engineering, 17*(1), 85-91. doi:10.1061/ (ASCE) HE.1943-5584.0000399

CHAPTER 5

Abdulkareem, J. H., & Sulaiman, W. N. (2016). Trend analysis of precipitation data in flood source areas of Kelantan River Basin. *Jurnal Teknologi, 78*(9-4), 115-127.
Alias, N. E. (2014). *Improving extreme precipitation estimates considering regional frequency analysis.* Kyoto University.
Alias, N. E., Mohamad, H., Chin, W. Y., & Yusop, Z. (2016). Rainfall analysis on the Kelantan Big Yellow Flood 2014. *Jurnal Teknologi, 78*(9-4), 83-90.
Barredo, J. I. (2007). Major flood disasters in Europe: 1950–2005. *Natural Hazards, 42*, 125-148. doi:10.1007/s11069-006-9065-2
Brakenridge, G. R. (2017, May 15). *Global Active Archive of Large Flood Events*. Retrieved from Darthmouth Flood Observatory, University of Colorado: http://floodobservatory.colorado.edu/Archives/index.html
Burn, D. H., & Hag Elnur, M. A. (2002). Detection of hydrologic trends and variability. *Journal of Hydrology, 255*, 107-122.
Castillo, E., Hadi, A. S., Balakrishnan, N., & Sarabia, J. M. (2005). *Extreme value and related models with applications in engineering and science.* A John Wiley & Sons, Inc.
Changnoon, S., & Demissie, M. (1996). Detection of change in streamflow and floods resulting from climate fluctuations and land use drainage changes. *Journal of Climate Change, 32*, 411-421.
Chow, V. T. (1964). *Manual of Applied Hydrology.* McGraw Hill.
Conover, W. J. (1980). *Practical nonparametric statistics.* New York: John Wiley.
DID. (2000). *Urban storm water management manual for Malaysia.* Kuala Lumpur: Percetakan Nasional Malaysia Berhad.
Fathian, F., Dehghan, Z., Bazrkar, M. H., & Eslamian, S. (2016). Trends in hydrological and climatic variables affected by four variations of the Mann-Kendall approach in Urmia Lake basin, Iran. *Hydrological Sciences Journal, 61*(5), 892-904.
Hamed, K. H. (2009). Exact distribution of the Mann–Kendall trend test statistic for persistent data. *Journal of Hydrology, 365*, 86-94.
Hamed, K. H., & Rao, R. (1998). A modified Mann-Kendall trend test for auto-correlated data. *Journal of Hydrology, 204*, 182-196.
Hosking, J. R., & Wallis, J. R. (2005). *Regional frequency analysis: an approach based on L-moments.* Cambridge University Press.
Hu, M., Sayama, T., Duan, W., Takara, K., He, B., & Luo, P. (2017). Assessment of hydrologic extremes in the Kamo River Basin, Japan. *Hydrological Sciences Journal*. doi:10.1080/02626667.2017.1319063
Kendall, M. G. (1975). *Rank Correlation Methods.* London: Griffin.

Lehner, B., Doll, P., Alcamo, J., Henrichs, T., & Kaspar, F. (2006). Estimating the impact of global change on flood and drought risks in Europe: A continental, integrated analysis. *Climatic Change, 75*(3), 273-299. doi:10.1007/s10584-006-6338-4

Mann, H. B. (1945). Nonparametric tests against trend. *Econometrica: Journal of the Econometric Society*, 245-259.

Pradhan, B. (2009). Flood susceptible mapping and risk area delineation using logistic regression, GIS and remote sensing. *Journal of Spatial Hydrology, 9*(2), 1-18.

Prevention Web. (2014, December 15). *UNISDR*. Retrieved from Prevention Web: http://www.preventionweb.net/countries/mys/data/

Rajczak, J., Pall, P., & Schar, C. (2013). Projections of extreme precipitation events in regional climatesimulations for Europe and the Alpine Region. *Journal of Geophysical Research: Atmospheres, 118*, 3610-3626. doi:10.1002/jgrd.50297

Salmi, T. (2002). Trend analysis of air quality monitoring data using Mann-Kendall tests. Retrieved from http://www.nilu.no/projects/ccc/tfmm/geneva3/reports/TSalmi.ppt

Sen, P. K. (1968). Estimates of the regression coefficient based on Kendall's tau. *Journal of the American Statistical Association, 63*, 1379-1389.

Stephens, M. A. (1986). Tests based on EDF statistics. *Goodness of fit Techniques 68*, 97-193.

Tabari, H., & Talaee, P. H. (2011). Recent trends of mean maximum and minimum air temperatures in the western half of Iran. *Meteorology and Atmospheric Physics, 11*(3-4), 121-131.

Takara, K. (2009). Frequency analysis of hydrological extreme events and how to consider climate change. *Water Resources and Water-Related Disasters under Climate Change,- Prediction, Impact Assessment and Adaptation, 19th UNESCO-IHP Training Course.* Kyoto University.

Takara, K., & Stedinger, J. (1994). Recent Japanese contributions to frequency analysis and quantile lower bound estimators. *Stochastic and Statistical Methods in Hydrology and Environmental Engineering*, 217-234.

Takara, K., & Takasao, T. (1988). Criteria for evaluating probability distribution models in hydrologic frequency analysis. *Journal of Japan Society of Civil Engineering 393*, 151-160.

Takara, K., & Tosa, K. (1999). Storm and flood frequency analysis using PMP/PMF estimates. *Proceedings of the Proc. International symposium on Floods and Droughts*, (pp. 7-17). Nanjing, China.

Takasao, T., Takara, K., & Shimizu, A. (1986). A basic study on frequency analysis of hydrologic data in the Lake Biwa basin. *Annual of Disaster Prevention Research Institute Kyoto University 29*, 157-171.

Tanaka, S., & Takara, K. (1999). Goodness-of-fit and stability assessment in flood frequency analysis. *Journal of Japan Society of Civil Engineering 43*, 127-132.

Yevjevich, V. (1972). *Probability and statistics in hydrology.* Fort Collins, Colorado, USA: Water Resources Publication.

Yu, Y. S., Zou, S. M., & Whittemore, D. (1993). Nonparametric trend analysis of water-quality data of rivers in Kansas. *Journal of Hydrology, 150*, 61-80.

Yue, S., Pilon, P. J., Phinney, B., & Cavadias, G. (2002). The influence of autocorrelation on the ability to detect. *Hydrological Processess, 16*, 1807-1829.

CHAPTER 6

Alaghmand, S., Abdullah, R., Abustan, I., & Vosoogh, B. (2010). GIS-based River Flood Hazard Mapping in Urban Area (A Case Study in Kayu Ara River Basin, Malaysia). *International Journal of Engineering and Technology, 2*(6), 488-500.

Alexander, D. (1993). *Natural Disasters.* New York, USA: Chapman & Hall.

Andjelkovic, I. (2001). *Guidelines on non-structural measures in urban flood management.* Paris: UNESCO.

Chan, N. W. (1995). *A contextual analysis of flood hazard management in Peninsular Malaysia.* London: Middlesex University.

Chan, N. W. (2009). Environmental humanities initiative: concept and actualisation in Universiti Sains Malaysia as a niche area. *Workshop on Establishing an Environmental Humanities, Cluster at the Social Transformation Research Platform.* USAINS.

Chan, N. W. (2011). Addressing flood hazards via environmental humanities in Malaysia. *Malaysian Flood Hazards via Environmental Humanities in Malaysia, 12*(2), 11-22.

Feldman, A. D., & Owen, H. J. (1997). *Communication of Flood-risk Information: Hydrology and Hydraulic Workshop on Risk Based Analysis for Flood Damage Reduction Studies.* California, USA: USACE.

Islam, R., Kamaruddin, R., Ahmad, S. A., Soon, J. J., & Anuar, A. R. (2016). A review on mechanism of flood disaster management in Asia. *International Review of Management and Marketing, 6*(1), 29-52. Retrieved from ADRC.

Kundzewiez, Z. W. (2002). Non-structural Flood Protection and Sustainability. *International Water Resources Association, 27*(1), 3-13.

Levy, J. K., Gopalakrishnan, C., & Lin, Z. (2005). Advances in decision support systems for flood disaster management: Challenges and opportunities. *International Journal of Water Resources Development, 21*(4), 593-612. doi:10.1080/07900620500258117

Pradhan, B. (2009). Flood susceptible mapping and risk area delineation using logistic regression, GIS and remote sensing. *Journal of Spatial Hydrology, 9*(2), 1-18.

Prevention Web. (2014, December 15). *UNISDR*. Retrieved from Prevention Web: http://www.preventionweb.net/countries/mys/data/

Smith, K. (1996). *Environmental Hazards: Assessing Risk and Reducing Disaster*. London, England: Routledge.

Udono, T., & Sah, A. K. (2002). Hazard mapping and vulnerability assessment. *Regional Workshop on Total Disaster Risk Management.* Japan: PASCO.

Vari, A. (2002). Public involvement in flood risk management in Hungary. *Journal of Risk Research, 5*(3), 211-224. doi:10.1080/13669870110042606

CHAPTER 7

Buchele, B., Kreibich, H., Kron, A., Ihringer, J., Oberle, P., Merz, B., & Nestmann, F. (2006). Flood-risk mapping: contributions towards an enhanced assessment of extreme events and associated risks. *Natural Hazards and Earth System Sciences, 6,* 485-503.

Frei, C., Davies, H. C., Gurtz, J., & Schar, C. (2000). Climate dynamics and extreme precipitation and flood events in Central Europe. *Integrated Assessment, 1*(4), 281-300.